Marine Organisms as Markers in the Site Formation Processes of a Shipwreck from the 7th Century BCE

L-Università ta' Malta

UM | Maritime Archaeology Programme
Research Project

Author:
Anton Motivans

Supervisors:
Prof. Timmy Gambin
Dr. Julian Evans

Thesis submitted in partial fulfillment of the requirements for the degree of Master of Arts in Global Maritime Archaeology

Word Count: 24,206

Department of Classics and Archaeology
University of Malta

April, 2024

ABSTRACT

The ceramic cargo of the *Phoenician* shipwreck (Gozo) is covered by encrusted marine organisms that have accumulated over ~2 700 years. This research identifies and characterizes these benthic communities and presents a new method that advances their role as records of spatial and environmental data, which is subsequently used to inform site formation processes and supplement archaeological interpretation.

Four amphorae (A18, A24, A06, and A40) were selected from different positions across the site and the variation in their associated biological communities was quantified using 92 different 10x10cm test squares. A total of 4,121 individual organisms representing 28 unique species were recorded. These included Anthozoa, Bryozoa, Foraminifera, Mollusca – Bivalvia, and Mollusca – Vermetidae. The organisms were found to be un-evenly distributed across the artifact surfaces and could be divided into five visually and compositionally distinct growth phases. This biological data was then linked with its spatial context. Artifacts were laser scanned with coded markers on their surface and integrated into a composite 3D model of the site derived from multiple years' worth of photogrammetric models.

This method contextualized the distinct growth phases and allowed for the interpretation of artifact movement. A18, A24, and A06 were found to have been very stable over time. Their growth phases run mostly parallel to each other and to the seabed. Abrasion from neighboring artifacts is localized and indicative of consistency in orientation. A40 was not consistent with the others and likely represents a case of major post-depositional movement. It was found to be located in a channel bisecting the wreck and in proximity to other artifacts (notably A97) where movement was also identified.

By identifying different types of movement through the study of marine benthos, this dissertation has demonstrated the effectiveness of a new method for the study of site formation processes and underwater archaeological interpretation.

Keywords: wreck site formation processes, benthic encrusting organisms, *Phoenician* shipwreck, 3D modeling, post-depositional artifact movement

ACKNOWLEDGMENTS

This research was made possible by the guidance, support, and feedback of Prof. Timmy Gambin and Dr. Julian Evans. It was immeasurably enhanced by the input and assistance of Alberto Bravo-Morata Rodríguez (laser scanning, 3D modelling, discussion, and workspace sharing) and similarly benefitted greatly from the contributions of Elena Motivans (R, data analysis and visualization), Dr. Jasmine Ferrario (bryozoan identification), and John Wood (sediment modelling).

I would like to extend my thanks to the Department of Classics & Archaeology for providing me with access to collections, facilities, and equipment; to the team involved in the excavation of the *Phoenician* wreck, without whom none of this research could have been possible; and to the Superintendence of Cultural Heritage for accommodating me on a reduced hour schedule while completing this dissertation.

Importantly, I would like to also thank my family and friends for their unending support. I am truly grateful to have all of you in my life.

TABLE OF CONTENTS

LIST OF FIGURES

1. INTRODUCTION

The shipwreck that an archaeologist sees often appears very different than how it would have been at the time of its sinking. The marine environment and the passage of time work together through a number of biological, physical, and chemical processes to remove, add, and disorganize what exists at a site. This can be observed in the case of the *Phoenician* shipwreck that was identified at a depth of 110m outside of Xlendi Bay, Gozo. The goal of this dissertation is to focus on the biological processes interacting with the *Phoenician* wreck in order to better understand some of these changes. More specifically, it is the benthic organisms encrusting the ceramic cargo of the wreck that will be examined. In the past, encrustations were often removed as part of the conservation process for underwater finds. It is only more recently that their potential is being realized. Recent studies like that of Ricci et al. (2019), Gravina et al. (2021), and Secci et al. (2021) have highlighted this research potential.

These three studies approach the topic with different aims. Ricci et al. (2019) uses encrusted benthos and signs of bio-erosion to infer the position of artifacts from a site where excavation notes are lacking; Gravina et al. (2021) explores the life traits and ecological affinities of organisms encrusted to an artifact, discussing how the communities reflect surrounding habitats; and Secci et al. (2021) uses encrusted benthos and the discoloration of artifacts to model sediment accretion at a wreck site. These studies effectively demonstrate how benthic organisms can be used to inform site formation processes and supplement archaeological interpretation. They offer a range of applications and highlight the value in studying these specific biological processes. At the same time, they represent new developments in an emerging sub-field. The work of Secci et al. (2021), in particular, demonstrates how recent advances in 3D modeling and site recording can be used to answer new and more complicated questions.

The topic of post-depositional movement has been referenced by these authors but has not received any in-depth discussion. This dissertation addresses that research gap. Being able to identify the movement of artifacts is valuable because it would enhance the interpretation of a

site. It could be used to differentiate between areas of stability and re-organization, to provide insights into the size/shape of a ship and how it broke apart, and could be used to identify major anthropogenic or natural impacts to a site. Encrusted organisms represent the perfect opportunity to interpret this movement because their locations on the artifacts remain unchanged. Consequently, they serve as records of which parts of an artifact were exposed to what environmental conditions at different points in the object's life-history. By looking to benthic organisms as records of artifact movement, this dissertation is addressing a research gap and proposing a new direction for the archaeological interpretation of these organisms.

Two aims guide the research along this path. The first aim of this dissertation is to identify and characterize the benthic organisms encrusted to amphorae from the P*hoenician* shipwreck and the second is to use this information to develop and evaluate the effectiveness of a new method for interpreting the movement of underwater archaeological objects. Because these aims differ from those of previous studies, new and altered methods were employed. Four amphorae (A18, A24, A06, and A40) were chosen from around the site to serve as proxies for the biological processes of their respective locations. Their surfaces were examined and a list of unique organisms was compiled. Counts and sizes of these organisms were collected through the use of a grid system and 10x10cm test squares. This standardization facilitated the comparison of data both within and across amphorae and led to the delineation of five visually and compositionally distinct growth phases. In order to contextualize these growth phases, 3D models of the artifacts, along with their grid systems, were made using a handheld laser scanner. These were subsequently integrated into a composite 3D model of the site that had been built on photogrammetric models made throughout the excavation process. This meant that biological data from each test square could now be linked with its precise recovery position at the site. It also contextualized the orientation of growth phases and the relationships of the four amphorae to their neighboring artifacts.

Through these methods, this dissertation was able to successfully use encrusted benthic organisms to identify artifacts that had undergone movement. Further still, it allowed for the differentiation between two different types of movement and was effective at evaluating areas of long-term stability and major post-depositional re-organization.

2. SITE BACKGROUND

2.1 Geographical and Historical Context

The Maltese archipelago is situated in the central Mediterranean and comprises the three inhabited islands of Malta, Gozo, and Comino (see fig. 1). Although once connected to Sicily when sea levels were much lower during the last glacial maximum (up until around 13 000 years ago), it has essentially existed in close to its current form throughout the Holocene (Foglini et al., 2016, p. 15). It is within this context that the Stentinello culture, Phoenicians, Carthaginians, Romans, Byzantines, Arabs, Normans, Knights Hospitaller of St John, French, and British forces came to exert and fight for influence and control (Cassar, 2000). Because of its location and the fact that it is an archipelago with many protected anchorages, Malta's history is one intrinsically linked with maritime activity. This is evidenced from the arrival of the earliest known humans to the island by boat around 7000 years ago to the strategically vital role the islands played as a British naval base during World War II (Cassar, 2000, p. 47; Gambin, 2020, p. 341; Short, 2000, p. 1). Beginning with the earliest inhabitants and continuing on to the present day, maritime networks and the movement of people and goods by sea has played a crucial role in shaping life on the Maltese islands.

This is certainly true of the Phoenician period. Maritime trade was the driving force of economic and political power for the Phoenicians. Their homeland was a narrow coastal territory that aligns roughly with the border of modern-day Lebanon. Bound geographically by mountains and powerful neighbours, the Mediterranean Sea represented their main opportunity for expansion (Aubet, 2001, p. 17). The Phoenicians capitalized on this prospect and ultimately achieved naval supremacy, coming to weigh heavily on the international politics and power struggles of the time (Aubet, 2001, p. 17). It is within this context of expansion that colonies like that of Malta were established during the 8th century BCE (Bonanno, 2005, p. 22).

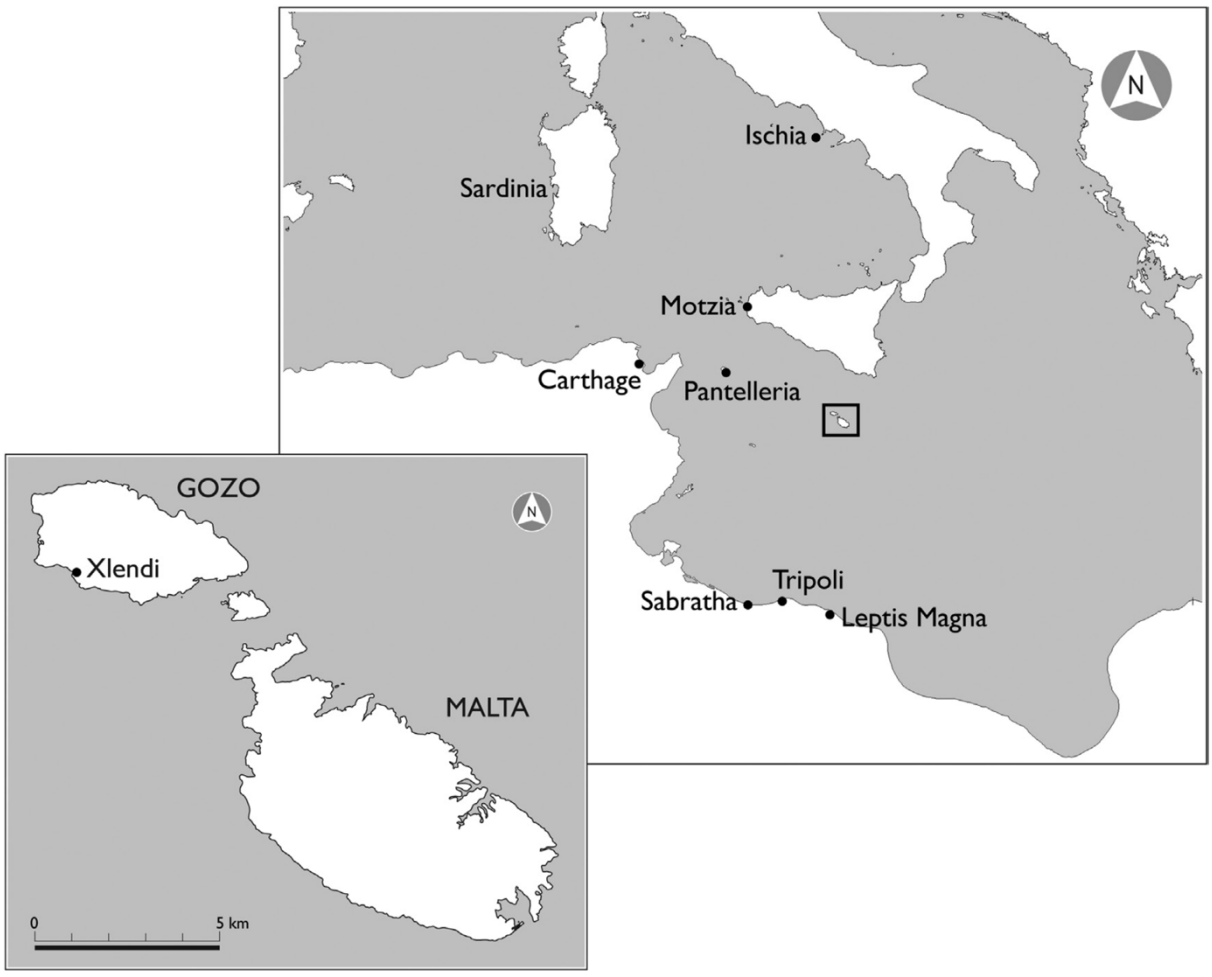

Figure 1 Map showing the location of the Maltese archipelago with reference to relevant locations during the Phoenician Period (Gambin et al., 2018, p. 72).

At this time, the rival Greeks were already becoming more established along the coast of eastern Sicily. The Phoenicians, in order to bolster their westward expansion, needed ports of call of their own in the central Mediterranean (González, 1999, p. 26). Malta represented an ideal place in that it was in the open sea away from the Greeks, had many protected anchorages, and could be integrated easily into established trade routes out of Crete going west (González, 1999, p. 26). During this time, the Phoenicians took up permanent residence in Malta and benefitted from the traffic and trade passing through it. As a result, Malta was integrated into a developing network that economically and socially linked the different regions of the Mediterranean basin for the first time (Aubet, 2001, p. 355).

The Phoenician colony in Malta served primarily in support of shipping and acted as a transit base. It was characterized by a relatively scattered and limited population that never developed to the extent of other nearby colonies in Tunisia, western Sicily, or Sardinia. This is, in part, a result of the well-established indigenous population with whom the Phoenicians shared the island (Aubet, 2001, p. 234-235). As Carthage came to replace Tyre as the Phoenician administrative and economic center in the mid-6th century BCE, Malta became an increasingly marginal colony and remained so until falling under Roman rule after the second Punic War (González, 1999, p. 28; Aubet, 2001, p. 235).

2.2 Archaeological Context

The Phoenicians are evidenced archaeologically in Malta by, among other sites, the temple to Astarte at Tas-Silġ and the distribution of tombs towards the interior and west of the island in areas like Rabat and Mdina (Bonanno, 2005, p.46-49; Vella, 2005, p. 444-445). Artifacts recovered from these sites reinforce the trade networks that the islands were a part of. Examples of carved ivory objects and stone religious furniture point to Syro-Palestinian origins, limestone sculptural elements to Cyprus, and silver jewelry to Spain (Bonanno, 2005, p. 57).

The temple to Astarte located at Tas-Silġ is an important site because of the role it played in the maritime cultural landscape of the time. Integrating elements of the Megalithic temple that already stood there, the re-purposed site sat at a key vantage point overlooking Marsaxlokk harbour. From there, it served as a landmark to mariners, a place where they could practice their beliefs and rituals, and a legitimization of Malta as an extension of the Phoenician homeland (González, 1999, p. 27; Vella, 2005, p. 446). Other sites like the shrines at Ras ir-Raheb and Ras il-Wardija served similar purposes. They were located on prominent headlands and would have served as navigational aids for maritime activity (Gambin, 2005, p. 21; Vella, 2005, p. 445-446,). The sanctuary at Ras Il-Wardija is particularly important here because of its location just over one kilometer north of Xlendi Bay.

Xlendi Bay, along with Marsalforn, would have been the main harbours in Gozo throughout the Phoenician period and antiquity (Gambin, 2005, p. 21). It is important to note that the size and shape of these bays has changed drastically since then. Sedimentation has reduced their size and subsequently limited the amount of protection they can offer. The ancient shorelines are evidenced by the presence of marine deposits and signs of wave action and coastal erosion nearly 200 meters inland from the current coastline (fig. 2-3)(Gambin, 2005, p. 22). This means that, for the Phoenicians, Xlendi and Marsalforn Bay would have been significantly bigger and safer harbours than they are today. As the first place of refuge available to mariners travelling from Carthage or Pantelleria, this would have been strategically significant (Gambin, 2005, p. 21).

Xlendi is an area of significant archaeological interest both in terms of a Maltese context and within the wider Mediterranean. Originally identified as a site by divers of the *HMS Falcon* in 1961, the area has been continually re-visited and studied by a number of subsequent organizations (Azzopardi, 2013, p. 287). The site consists of hundreds of artifacts scattered across an area of 67 000m^2 and down to a depth of 105m. The artifacts which comprise the site are highly varied and indicative of the prolonged use of Xlendi Bay as a center for maritime activity. Recovered material ranges from between 2500-1500 BCE (Tarxien Cemetery sherd) and 900-1200 CE (Islamic jug) (Azzopardi, 2013, p. 289). The majority of artifacts, however, appear to date from 400 BCE to 400 CE (see fig. 4). Because of the scattered nature of the site and the wide range of typologies that were identified, many questions about the site persist. At this point, even the

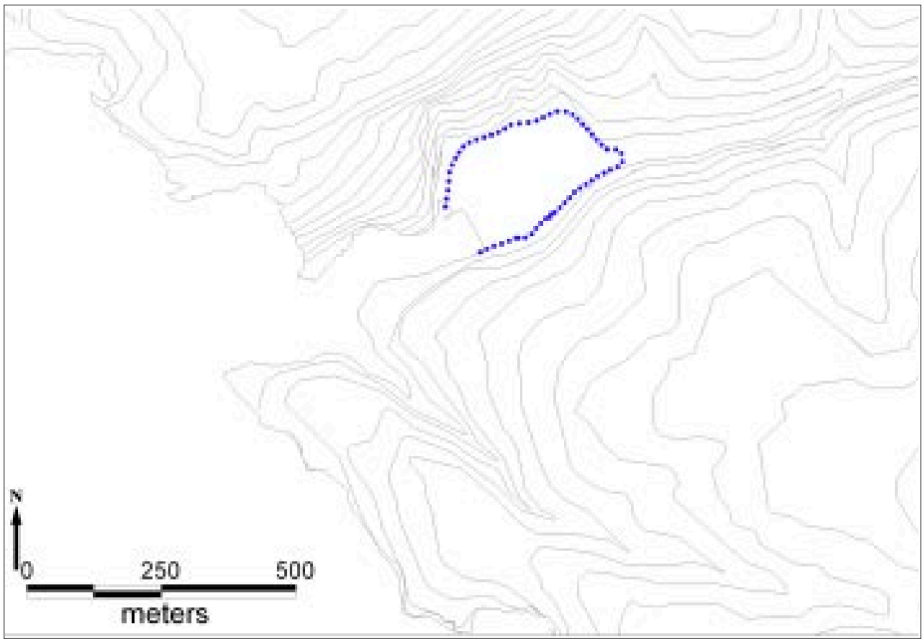

Figure 2 Contour map of Xlendi. The dotted line delineates the extent of the ancient harbour (Gambin, 2005, p. 23).

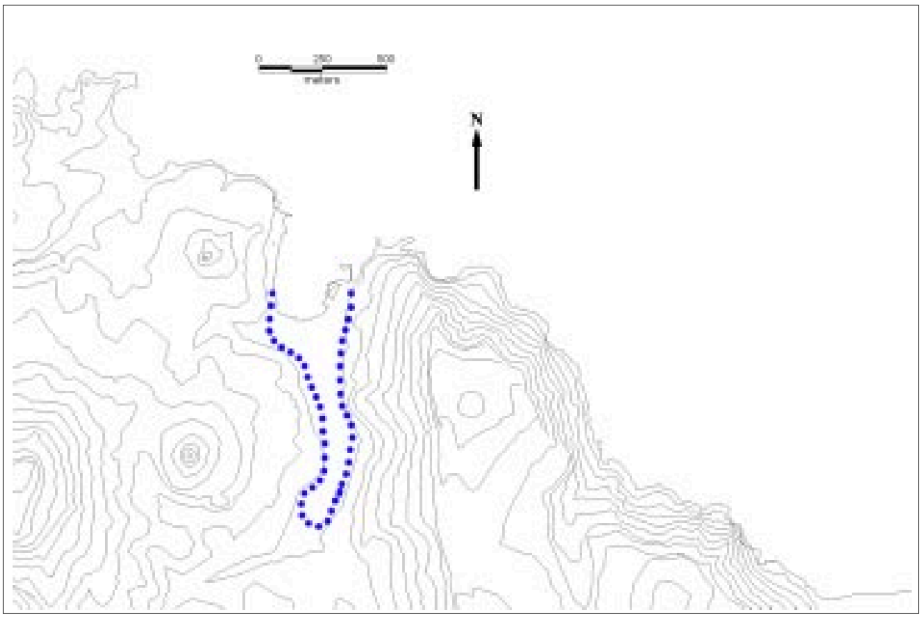

Figure 3 Contour map of Marsalforn. The dotted line delineates the extent of the ancient harbour (Gambin, 2005, p. 24).

Identifying no.	Type	Approximate date	Place of production	Quantity	Assemblage
Xlendi 1	Tarxien Cemetery	2500–1500 BC	Malta	1	1
Xlendi 2	Ramon 2.1.1.2	End 7th century BC	Sardinia, Sicily, Tunis	1	2
Xlendi 3	Ramon 2.2.1.2	4th century BC	Malta, Sicily, Tunisia	At least 3	3
Xlendi 4	Sagona urn 3–4:III	410–300 BC	Malta	1, more in deep water	3–4
Xlendi 5	Sagona urn 3–4:IV	410–300 BC	Malta, Ibiza, Carthage	3, more in deep water	3–4
Xlendi 6	Ramon 3.2.1.2	3rd century–146 BC	Carthage, Sicily, Malta	3, lots in deep water	4
Xlendi 7	Cintas 176 jug	3rd century BC	Unknown	1	4
Xlendi 10	Ramon 7.3.1.1	End 3rd–mid 2nd century BC	Northern Tunisia	1	5
Xlendi 11	Ramon 7.4.2.1	Mid 2nd century BC	Carthage	1	5
Xlendi 13	Flat-bottomed amphora	End 2nd century BC	Unknown	1	5
Xlendi 14	Graeco-Italic amphora	Mid 2nd century BC	Sicily, Tyrrhenian Italy	2, more in deep water	5
Xlendi 15	Bruno Malta type 1	End 2nd–end 1st century BC	Malta	10 more in deep water	5
Xlendi 16	Dressel 1A	2nd–1st century BC	Tyrrhenian Italy	4, more in deep water	5
Xlendi 17	Lamboglia 2	End 2nd–end 1st century BC	Northern Italy, Dalmatia, Albania	2	5
Xlendi 19	Dressel 2–4	1st century BC	Italy, France, Spain	7, more in deep water	6
Xlendi 20	AC3	1st century BC–2nd century AD	Crete	4	7
Xlendi 21	Bruno Malta type 2	1st and 2nd century AD	Unknown, possibly Malta	1	7
Xlendi 22	K 109 amphora	3rd–4th century AD	Aegean	1	7
Xlendi 23	K 107 lid	3rd century AD	Aegean	1	7
Xlendi 24	Tripolitana III	3rd century AD	Tripolitania	1	7
Xlendi 25	Keay V	End 2nd–end 3rd century AD	Tunisia	1	7
Xlendi 26	Africana II variant	3rd century AD	Tunisia	1	7
Xlendi 27	Keay XXVI	5th century AD	North Africa, Carthage	3	8
Xlendi 28	Keay XXXVB	5th century AD	Tunisia	1	8
Xlendi 29	Keay XXXII	4th–5th century AD	Tunisia	1	8
Xlendi 30	Keay IIIA	4th–5th century/ 7th century AD	Tunisia	3	9
Xlendi 31	Islamic jug	10th–13th century AD	Unknown	1	10

Figure 4 Catalogue of artifacts recovered from Xlendi Bay (Azzopardi, 2013, p. 289).

nature of deposits is uncertain. While the site likely comprises several shipwrecks, other processes like loss overboard or goods being washed out to sea likely contributed to the assemblage (Azzopardi, 2013, p. 293). Site formation processes have also undoubtedly re-organized the site and further complicated its interpretation.

2.3 The *Phoenician* Shipwreck

2.3.1 From Discovery to Excavation

It is within the context of Xlendi that, in 2007, the *Phoenician* shipwreck was identified. The wreck was first captured on side-scan by the Malta Shipwreck Project. An ongoing effort by the University of Malta and the Superintendence of Cultural Heritage aimed at surveying the entirety of Malta's territorial waters. Following the discovery, additional remote sensing campaigns were launched to better understand the site. These included an additional pass with side-scan sonar (done at a higher frequency for improved resolution), a sub-bottom profiler survey, and an ROV survey. Together, these campaigns yielded more information about the nature and composition of the wreck through the collection of still images, videos, and geological data. The results were used to better plan future campaigns on the site (Gambin, 2018, p. 71).

It was ultimately in 2014 that researchers first saw the site with their own eyes from the cabin of the *Remora 2000* (a two-person manned submersible). The submarine was brought on as part of the GROPLAN project and was used to produce a very high-resolution 3D model of the entire site (fig. 5). This 3D model was then further elaborated upon through the integration of individual artifact models. The results, visible in fig. 6, show how idealized amphorae forms were aligned with their corresponding theoretical positions. This hybrid model allows for a better spatial understanding of the site and was used to answer specific research questions as well as inform future campaigns.

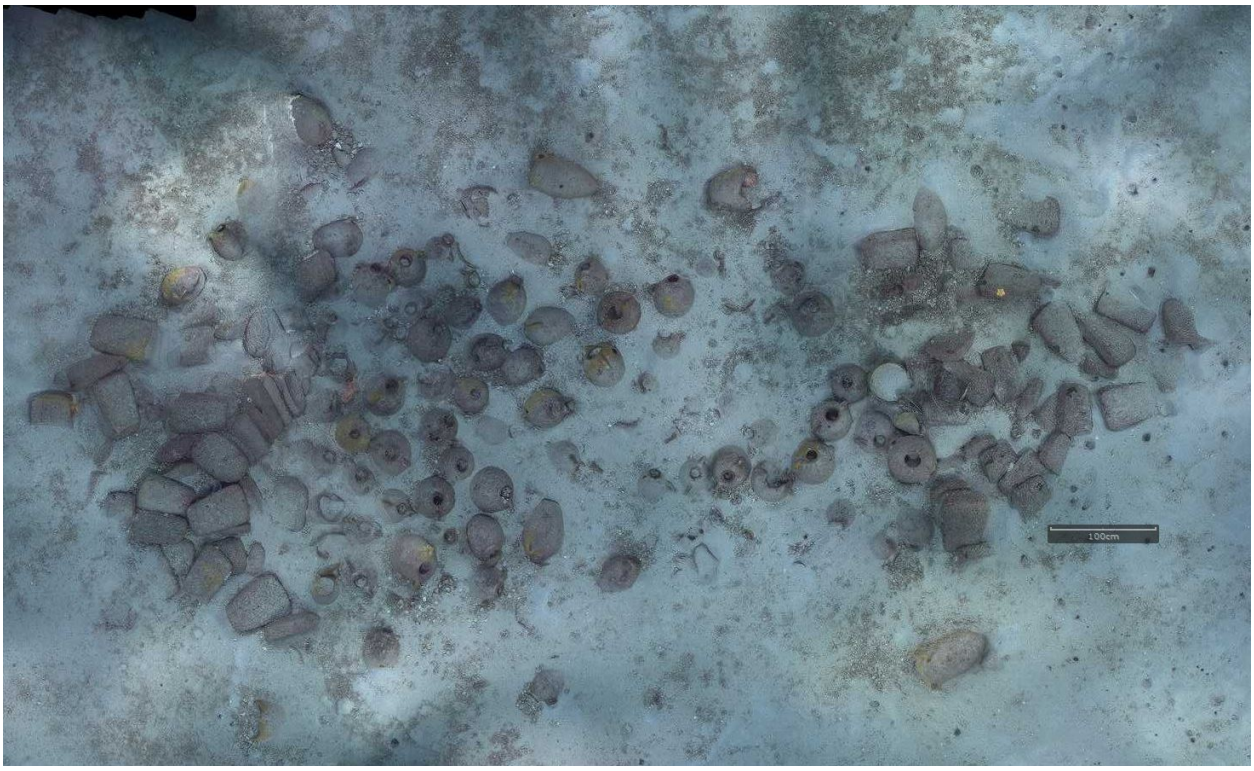

Figure 5 The first 3D model created of the site in 2014. It shows the wreck of the *Phoenician* prior to any archaeological disturbance (Courtesy of the Department of Classics & Archaeology, University of Malta).

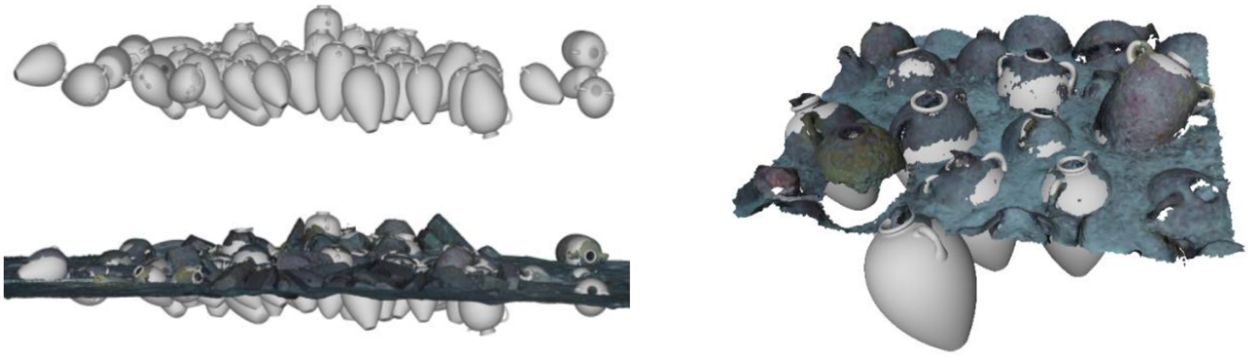

Figure 6 The first composite model of the site. Created using manual recognition of amphora typology (Drap et al. 2015, p. 30378).

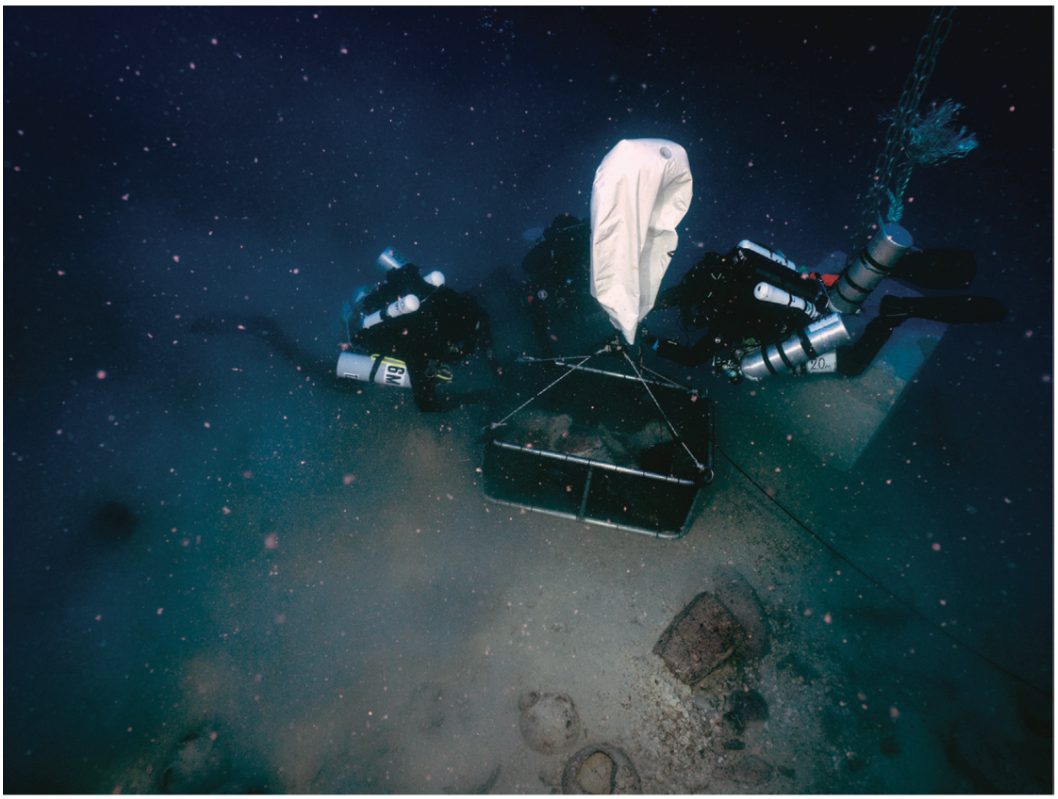

Figure 7 Rebreather divers lifting artifacts from the site (D. Gration, Courtesy of the Department of Classics & Archaeology, University of Malta).

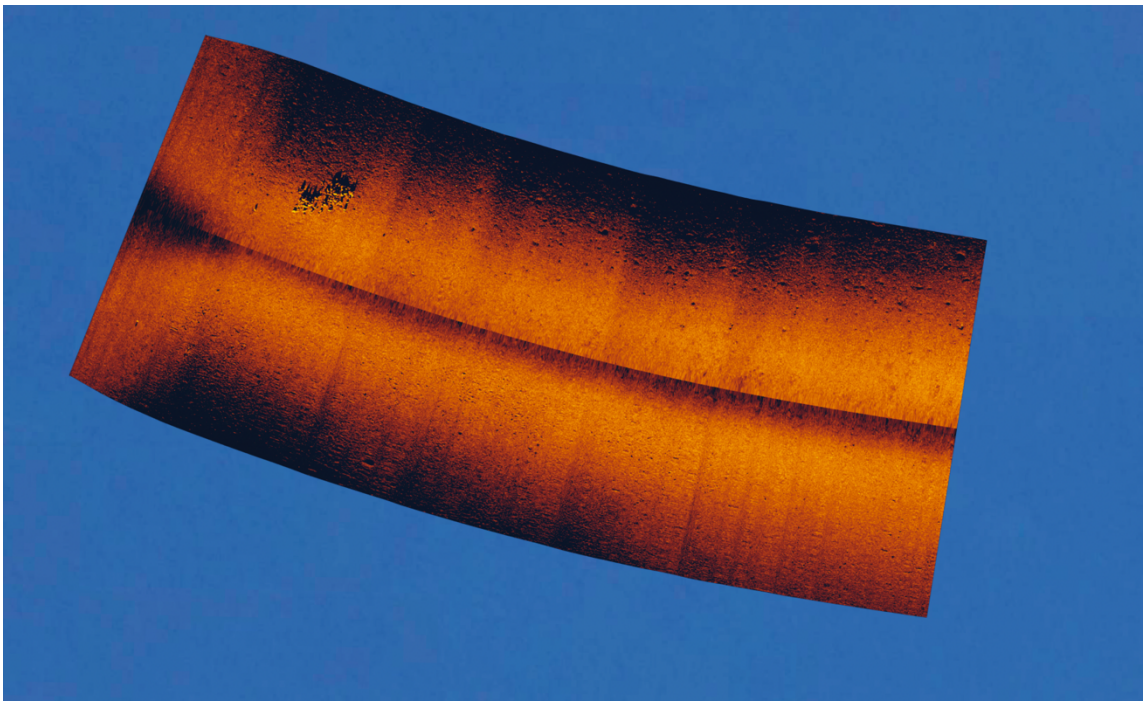

Figure 8 Side-scan image of the Phoenician wreck and its immediate surroundings (Courtesy of the Department of Classics & Archaeology, University of Malta).

In addition to the model, the submarine was also used to raise several artifacts. These included a saddle quern base, an ovoid amphora, a flat-bottomed amphora, and an urn (Gambin, 2018, p. 79). Over the following campaigns of 2016 to 2021, closed-circuit rebreather divers took over the work of systematic recoveries, excavation, and documentation (fig. 7). The challenges posed by the extreme depth were significant. As the deepest underwater archaeological excavation carried out by mixed gas divers, many safety concerns and logistical challenges had to be reconciled. For instance, due to decompression requirements, divers were limited to only twelve minutes of bottom time for dives that lasted a total of 160 minutes (Gambin, 2018, p. 84). It was within these challenging and limiting conditions that the excavation of the site was carried out. Although difficult, the importance and rarity of the site warranted such action (Gambin, 2018, p. 84).

2.3.4 Environmental Conditions at the Site

The *Phoenician* shipwreck rests at a depth of 110 m. The surrounding sediment is a coarse-muddy-sand and there are no geological features in the immediate vicinity of the wreck (fig. 8). There is a slight slope across the site as the end closer to the block (visible in fig. 7) is 0.65 m deeper than the other end. This means that there is a change of 65 cm over a distance of 12 m. Water temperature around the wreck is always a steady 14-15^{o}C while currents, on the other hand, are variable. They can be strong on the surface but are rare at 110 m. When current is observed at depth, it is not negligible. In general, the site is dark, relatively cold, and for the most part stable.[1]

[1] Gambin, T. (2024) Email to Anton Motivans, 28 March.

2.3.2 Cargo

The cargo was divided into three main sections. One section comprising a variety of ceramic containers and two others on either end of it made up of saddle querns and rubbing stones. Based on the elements of the cargo that were visible, it was determined that a minimum count of 66 saddle querns, 7 rubbing stones, 99 amphorae, and 2 vases made up the ship's cargo (Gambin, Sourisseau & Anastasi, 2021, p. 4). The estimated weight of this cargo was calculated to be roughly 6.5 metric tonnes with the ship itself likely measuring 15 m by 4 m (Gambin, Sourisseau & Anastasi, 2021, p. 4).

The saddle querns and rubbing stones show no signs of use and make up a significant percentage of the ship's cargo (Gambin, Sourisseau & Anastasi, 2021, p. 5, 6). The querns are large (approx. 30 x 45 cm), mostly uniform, and trapezoidal in shape. When used, these querns would have remained in a fixed position while the smaller and more oblong/elliptical rubbing stones were worked back and forth across their surface. This way of processing grains and preparing other foodstuffs is typical of as far back as the late Paleolithic and runs up until the 5th century BCE (Gambin, Sourisseau & Anastasi, 2021, p. 6). Although, naturally, the size and shape of these types of querns varied both temporally and geographically (Yatoo, 2016; Fronteau, 2020; Avshalom-Gorni, Frankel, and Getzov, 2004). Petrographic and chemical analyses of the major and trace elements of the querns from Xlendi revealed that they originated from the island of Pantelleria (Renzulli et al., 2019, p. 347). As part of the same study, samples of a millstone recovered from 6th century BCE levels at a site in Cádiz, Spain were also examined. It was determined that they too originated from Pantelleria. This works to show the importance of the island for the procurement of basaltic millstones in Archaic Phoenician trade, the range over which the goods were distributed (over 1500 km), and their broader distribution across other known sites in the Central-Western Mediterranean (Sicily, Tunisia, and Mallorca) (Renzulli et al., 2019, p. 347). Crucially, the study also provides a broader context for the *Phoenician* shipwreck of Xlendi Bay and the trade it was engaged in.

The ceramic section of the cargo consists of a variety of objects including amphorae, urns, jugs, bowls, and plates. It similarly plays an important role in interpreting the site. Of the visible

cargo, three main groups of amphorae can be distinguished (Gambin, Sourisseau & Anastasi, 2021, p. 6). The first group, which itself comprises two sub groups, is characterized by several key elements. These include a flat base, vertical strap handles positioned on the shoulder, and an overall rounded and squat shape (Gambin, Sourisseau & Anastasi, 2021, p. 7). The neck and handles, which are circular in section, play the most important part in differentiating between the two sub-groups. With one having a more pronounced neck and handles which join it to the shoulder of the amphora. This difference, along with examples from other groups, can be seen in fig. 9. There are some slight variations in the size of amphorae within this grouping. These differences are, however, only minor and the result of a less standardized production. Both shapes have been recorded on other sites from the Archaic central Mediterranean. Notably in Pithecusae, at the necropolis of San Montano (Gambin, Sourisseau & Anastasi, 2021, p. 8). Petrographic analysis of the fabric of this group revealed a local Maltese production (Anastasi et al., 2021, p. 6). This is interesting because it speaks to the diffusion of Phoenician and Greek influence and exchange at a time when both cultures were expanding westward (Anastasi et al., 2021, p. 6).

The next group of amphorae is made up of examples that are different both in terms of style and origin. They are ovoid in shape, have a tapered and somewhat pointed base, and a high rounded shoulder that culminates in a narrow neck-less opening (Gambin, Sourisseau & Anastasi, 2021, p. 8). The handles are, similar to the first group, rounded and vertical. Typologically, they are consistent with Ramón's T-2.1.1.1 and T-3.1.1.2 types and point to a western origin (Gambin, Sourisseau & Anastasi, 2021, p. 8). This is corroborated by a petrographic study which found amphorae from this group to be of a Carthaginian production (Anastasi et al., 2021, p. 6). Existing research on this type reveals that they have been found throughout the central Mediterranean and can be securely dated to between 720 and 680 BCE (Gambin, Sourisseau & Anastasi, 2021, p. 10).

The third and final group, like the first, comprises two sub-groups. They are globular ollas with flat bases and two horizontal handles located towards the middle of the container's body (Gambin, Sourisseau & Anastasi, 2021, p. 10). The main element differentiating between the two sub-groups of ollas is the neck. One has a wider and more open neck while the other is higher,

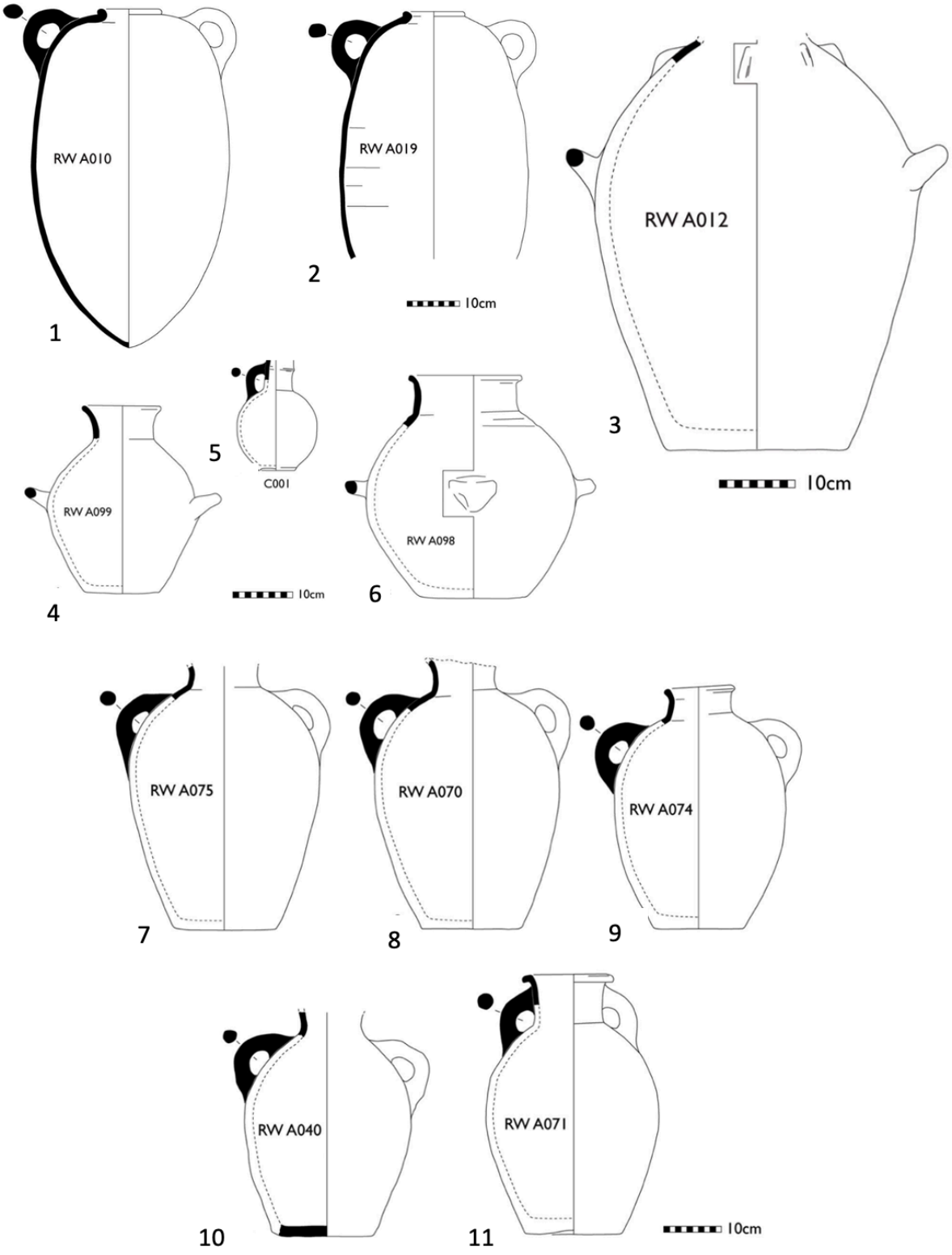

Figure 9 Illustrations of amphorae from group 1A (7-10), 1B (11), 2 (1&2), 3 (3&4), a Phoenician round-mouthed jug (5), and an isolated container recovered a distance from the wreck (6) (Gambin, Sourisseau & Anastasi, 2021, p. 7-12)

narrower, and more cylindrical. Examples from the first sub-group vary significantly in size and range from 32 to 53cm in height (Gambin, Sourisseau & Anastasi, 2021, p. 10). Because of this, they are difficult to place. While some similarities exist between forms from Pithecusae and Lazio, petrographic study of the fabric of the first sub-group suggest a Maltese origin (Gambin, Sourisseau & Anastasi, 2021, p. 10). The second sub-group belonging to this category is, at this point, even more difficult to trace. There are some similarities to a tradition in Mozia and a local Maltese production is also possible but, since no artifacts from this sub-group have been raised from the seabed, conclusions remain speculative for the moment (Gambin, Sourisseau & Anastasi, 2021, p. 13, 14).

2.3.3 Other Studies

On top of petrographic analyses, other studies have also been carried out on the cargo recovered from the wreck. Among these is a palynological assessment of the sediment contained within one of the raised amphorae. The research identified 500 different terrestrial pollen grains belonging to 39 different taxa (Mifsud, 2019, p. 69). Of these, two are not local to Malta and can potentially be seen as evidence for the previous journeys made by the ship. Still other studies have been aimed at identifying the original contents of the amphorae. Residue analysis has been conducted on several samples and has returned high lipid levels. These results, however, are only partial and belong to a work that has yet to be published.

The original contents of the amphorae had been replaced over time by sediment and biological inclusions. Research has also been carried out on these inclusions. They were found to contain the remains of 54 different species of mollusk and represent a range of substrate preferences. The majority prefer soft substrates (silts to sands) but others are associated with hard substrates, coral, or seagrass. One pelagic species was also identified. All live in the continental shelf and can be found to depths of 200 m.[2] (Giaime, 2023).

[2] Giaime, M. (2023). Email to Anton Motivans, 15 April.

The documentation and partial excavation of the site has opened the door to these further studies. They allow for a better understanding of the wreck and its context. This dissertation seeks to build on and expand this body of knowledge by examining site formation processes. An aspect which has, until now, received little attention.

3. LITERATURE REVIEW

3.1 Introduction to Literature Review

This study, which focuses on the marine benthos associated with the *Phoenician* shipwreck, is rooted firmly in research centered around site formation processes. One of the purposes of the following section is to discuss how the study of site formation processes (hereafter referred to as simply SFPs) arose and developed. Doing this will work to show both the theoretical and methodological range of the field while also situating this particular research within it. It is important to also remember that the processes which transform archaeological sites can vary substantially and are the result of a multitude of factors. Because of this, the study of them often requires an inter-disciplinary approach that draws on the fields of geology, biology, and chemistry. This is certainly the case for this study. Central to the goals of this paper is the idea that marine biology can be used to interpret a wreck site and answer archaeological questions. With all this in mind, what follows is an examination of SFPs and a discussion of the theoretical and methodological approaches to the multi-disciplinary study of them.

3.2 Site Formation Processes

3.2.1 Origins of the Field

It is necessary to begin a discussion of SFPs by acknowledging the work of Michael B. Schiffer. Although the major concepts discussed in his 1987 seminal work *Formation Processes of the Archaeological Record* were being employed prior to the book's publication, the work serves as a crucial review of scholarship at the time. It also worked to catapult the relatively niche topic

into the mainstream of archaeological thought. Central to what Schiffer (1987) puts forward is the categorization of SFPs into two distinct types. Under this framework, all processes acting on archaeological sites can be understood as either cultural or environmental (i.e., natural). In outlining cultural formation processes, Schiffer discusses reuse, cultural deposition, reclamation, and disturbance processes (Schiffer, 1987). He then further fleshes out these processes with examples by talking about how human actions like salvage, refuse disposal, plowing, etc. can come to affect what exists in the archaeological record and in what condition. In contrast to this, the category of environmental formation processes is defined by things like decay, erosion, glaciation, alluvial processes, etc. Schiffer examines these natural processes' effect on the archaeological record at three scales; impacts on individual artifacts, entire sites, and the broader regions within which they exist.

Schiffer's work, however, is focused almost exclusively on terrestrial sites and fails to examine the unique processes (both cultural and environmental) that act on their underwater counterparts. This duty is instead taken up by Keith Muckelroy (1978). In his book *Maritime Archaeology*, he is forthright with the importance of studying SFPs. He writes that the "validity of any conclusions reached in maritime archaeology depends fundamentally on the understanding of these processes" and that "their study must occupy a central place in the sub-discipline" (Muckelroy, 1978, p. 157). What the archaeologist finds on the seabed, more often than not, exists in a vastly different and deeply altered form. This is illustrated well by looking at ancient shipwrecks in the Mediterranean. In many of these cases, the archaeologist will be left primarily with only a mound of amphorae (see Demesticha, 2011; Greene, Leidwanger, Özdas, 2011; Kazianes, Simossi, Haniotes, 1990; Delaporta, Jasinski, Søreide, 2006; Royal, 2006; Sakellariou et al., 2007). It is from this mound that they seek to understand the size and build of the ancient ship and the "highly organized" and "dynamic" form it took under operation prior to its wrecking (Muckelroy, 1978, p. 157). If the goal is to grasp the latter by studying what is available in the former, a well-grounded understanding of why and how things have changed is imperative. It is through the study of SFPs that the transformations enacted on a shipwreck site can be quantified for the purpose of decoding and contextualizing what material evidence remains. In some ways,

these processes can then be theoretically reversed to build a more complete picture of what has existed in the past.

Like Schiffer, Muckelroy makes sense of these processes by organizing them into two main categories. His categories of “extracting filters” and “scrambling devices” account for transformations enacted on shipwrecks that result in a loss or disorganization of archaeological evidence (Muckelroy, 1978, pp. 160-175). Material floating away during the process of wrecking, later salvage operations, and the disintegration of materials are all considered to be extracting filters insofar as they contribute to the removal of archaeological evidence (Muckelroy, 1978, p. 165). Scrambling devices, on the other hand, refer to processes which re-organize evidence as the ship breaks apart, settles on the seabed, and interacts with currents and sediments (Muckelroy, 1978, pp. 169-182). A generic model for these processes is represented by Muckelroy’s flowchart in fig. 10. It traces the transformations undergone by a ship from the process of its wrecking to the seabed distribution observed by the marine archaeologist.

3.2.2 Cultural Processes

Since its publication in 1978, Muckelroy’s work has been continually revised and expanded. This shows how fundamental his work was, how relevant it is today, and how the sub-field has developed since. While often continually referenced, few engage with his work as explicitly as Gibbs (2006). In the article, Gibbs examines the legacy of Muckelroy’s work 30 years on with a particular focus on the cultural side of SFPs. An aspect, he believes, to have been inadequately covered. Muckelroy’s model really only discusses cultural processes in terms of salvage operations. Even as he describes the process of wrecking, more emphasis is placed on the buoyancy of materials than on the actions of the crew. Gibbs (2006) fills this gap by creating his own model (fig. 11) that outlines the impacts cultural processes can have during the process of wrecking. This model sees these processes as playing out over five unique phases; the pre-impact threat phase, pre-impact warning phase, impact, recoil, and the rescue and post-disaster phase (Gibbs, 2006, p. 9). At the impact stage, for example, the crew is forced to choose whether to remain onboard or abandon their vessel (Gibbs, 2006, p. 9). The resulting assemblage could look

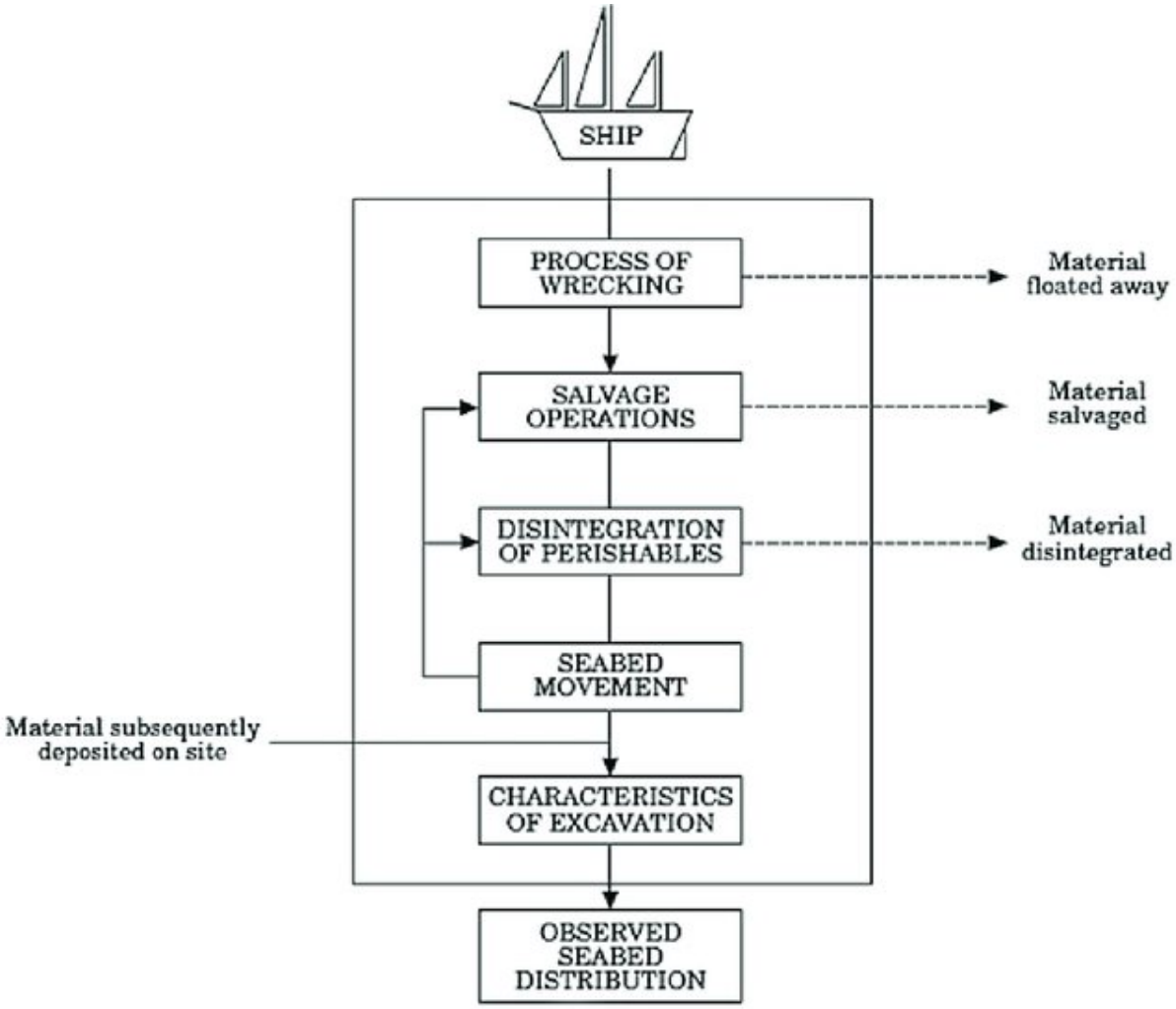

Figure 10 Muckelroy's flowchart detailing wreck site formation processes. It traces the transformations undergone by a ship from the process of its wrecking to its distribution on the seabed at the time of archaeological intervention (Muckelroy, 1976, p. 282).

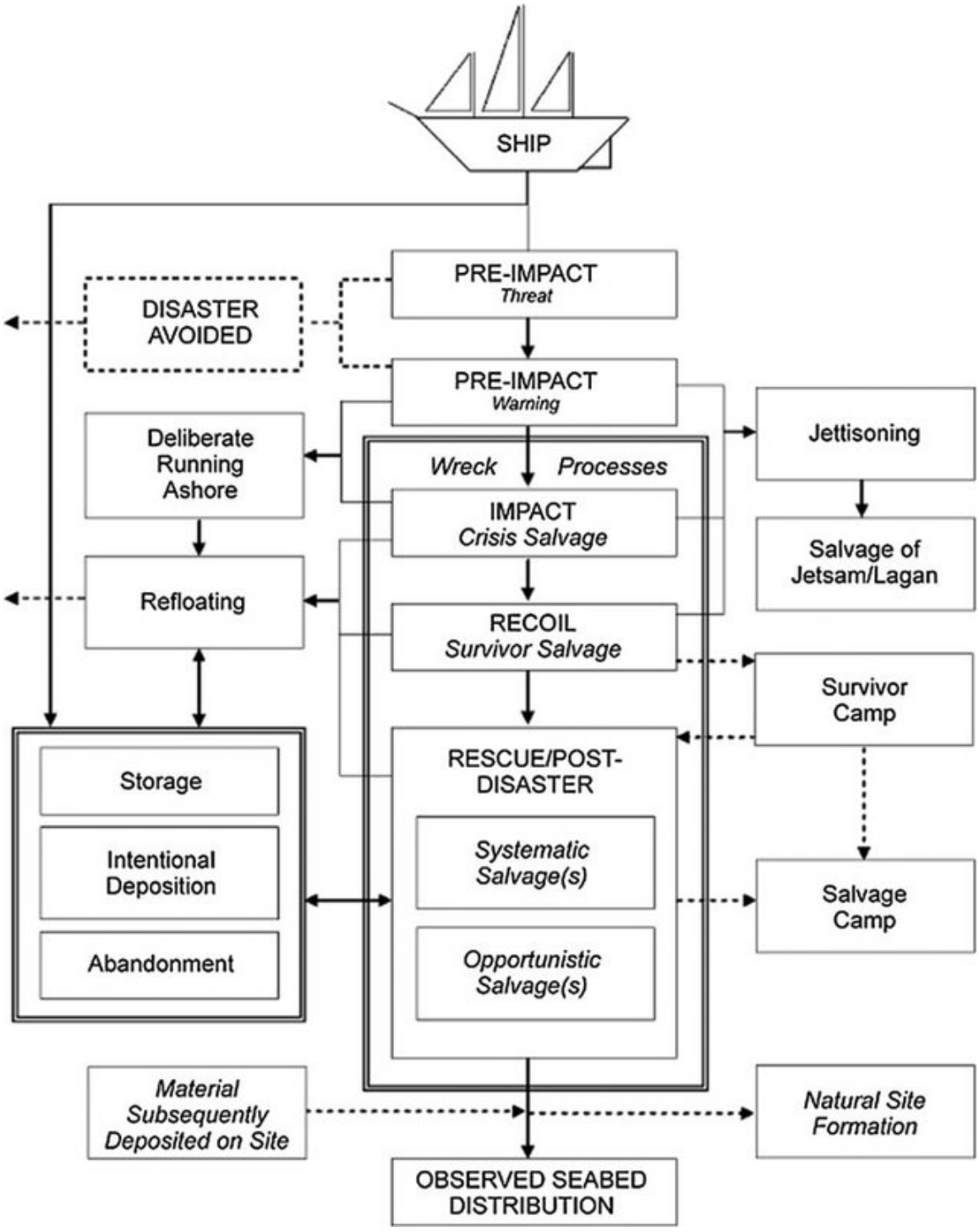

Figure 11 Gibbs' flowchart outlines the significance and nuance of cultural/anthropogenic factors when determining a wreck's observed seabed distribution. It was designed in response to Muckelroy's flowchart which only listed a single anthropogenic factor as contributing to this process (Gibbs, 2006, p. 16).

quite different as a result of this decision. If they remain onboard, they might try deploying an anchor, jettisoning heavier items, or patching leaks (Gibbs, 2006, p. 9). On the other hand, they might deploy lifeboats and carry out crisis salvage if they decide to abandon ship (Gibbs, 2006, p. 9). What is ultimately deposited as part of an archaeological wreck site will depend on these decisions and their success or failure. In this way, Gibbs (2006) argues that cultural processes play an important role in the wider formation processes of a site. Especially at the wrecking stage.

While Gibbs (2006) is successful in arguing the importance of cultural processes in wreck SFPs, the scope of his research is narrower than the full breadth of these processes. His model falls short, in fact it fails to address cultural impacts beyond what he calls the "rescue/post-disaster" phase (Gibbs, 2006, p. 16). Instead, he is proposing that only freshly deposited material and natural processes shape the wreck past this phase. He then does not account for the multiple long-term human impacts that can continue to alter a site. These impacts come mainly in the form of trawling, dropped or dragged anchors, fishing gear, looting (when possible), and marine litter.

The long-term impacts of trawling in particular is the focus of a study by Brennan et al. (2016). The project focused on a deep-water ancient wreck in a heavily trawled area off the coast of Ereğli, Turkey. By producing micro-bathymetric maps of the site in 2011 and 2012, the team was able to quantify the effects of trawling over the course of a year. From this data, it was determined that in the area of their survey (roughly 184 m^2), there was a net volumetric loss of about 15 m^3 worth of sediments (Brennan et al., 2016, p. 87). The repetitive trawling over the site was the dominant process in sediment distribution and inhibited the natural processes whereby the wreck would act as a sediment trap (Brennan et al., 2016, p. 87). In this way, trawling has both a continued scrambling and extracting effect on the wreck. When a trawl cuts through a wreck site, it can re-arrange archaeological material as well as collect it. Additionally, the removal of sediments can re-expose timbers and other organic material to a marine environment that is hostile to their survival. At which point natural processes once again come to play an increasingly important role.

3.2.3 Natural Processes

Muckelroy recognized that the natural world and environmental processes are central to the understanding of underwater wreck SFPs. In a study focusing on better understanding this relationship, he compared the preservation and environmental attributes of twenty different wrecks scattered across British waters (Muckelroy, 1978, pp. 160-165). For this study, the attributes looked at were:

1. Maximum offshore fetch, within 30° of the perpendicular to the coast.
2. Sea horizon from the site; i.e., sector within which there is more than 10 kilometers of open water.
3. Percentage of hours during which there are winds of Force 7 or more from directions within the sea horizon.
4. Maximum speed of tidal streams across site.
5. Minimum depth of site.
6. Maximum depth of site.
7. Depth of principal deposit on site.
8. Average slope of the sea-bed over the whole site.
9. Underwater topography: the proportion of the site over which the sea-bed consists of geologically recent sedimentary deposits.
10. Nature of the coarsest material within these deposits.
11. Nature of the finest material within them.

By attributing quantitative values to each attribute and examining their relationship to the state of preservation for each wreck, the study could determine which factors had the greatest observable impact on underwater wreck sites (Muckelroy, 1978, pp. 162-163). It was concluded that, while all eleven attributes had their effects, the ones with the strongest correlation were underwater topography and the nature of the coarsest and finest deposits (i.e., attributes 9, 10, and 11) (Muckelroy, 1978, pp. 162-163). This study is important because it represents one of the

first projects aimed directly at the scientific evaluation of environmental impacts on wreck SFPs. While there was earlier interest in this topic, it was largely limited to broad and general characterizations (e.g., Dumas, 1962). In this way, the project set the stage for the more scientific and empirical work that followed. Work which would build on this approach in order to identify and evaluate a more complete range of environmental impacts.

What stands out about Muckelroy's research now is that all eleven attributes deal only with what could be considered the physical conditions of the wreck site environment. Fast forward to studies like that of Bethencourt et al. (2018) and what is being looked at also includes chemical and biological conditions. This is the product of both the progress made within the discipline and the technological advances that facilitate the identification and measurement of new indicators.

In the Bethencourt et al. (2018) study, the team investigated two wrecks off the coast of Cadiz, Spain. Since both wrecks are associated with the Battle of Trafalgar (1805), they serve as an ideal real-world laboratory for studying the varying outcomes that result from different environmental conditions over the same period of time (Bethencourt et al., 2018, pp. 100-101). The team went about this by carrying out studies which measured properties of the water, sediments, and living organisms affecting the sites. In assessing the impact of physical processes on the wrecks, the team evaluated sediments and morpho-dynamics by looking at grain size, sediment mobility, geomorphological changes, positional data, and accretion/erosion models. The physical properties of water at the sites were instead evaluated in terms of wave parameters (height, strength, and frequency) and current velocity. For the chemical characterization of the wreck site environment, they carried out sediment coring across the site to determine the pH, oxidation-reduction potential (ORP), and total organic carbon (TOC) in different areas and at different depths. Salinity, temperature, pH, ORP, and dissolved oxygen readings were, similarly, taken at different intervals in the water column across both sites. Finally, when characterizing the biological impacts to the site, the study performed a quantitative analysis of sessile communities on both natural rocky bottoms and artificial substrates.

As a result of carrying out these studies into the physical, chemical, and biological impacts of the marine environment on the two wreck sites, Bethencourt et al. (2018) was able to explain

the differences in preservation and composition at the two sites. Some of these findings are summarized in the following excerpt;

> "[…] in Fougueux shipwreck large iron objects are corroding at a higher rate (between 0.180 and 0.246 mmpy) due to high sediment remobilization and transport induced by waves at this site, causing damage by direct mechanical effect on metallic material and by removing the layer of corrosion products developed on the artefacts. Meanwhile artillery on Bucentaure site, covered with thick layers of biological concretion, is well preserved, with lower corrosion rates (0.073 to 0.126 mmpy), and archaeological information is guaranteed." (Bethencourt et al., 2018, p. 99)

These conclusions highlight the inter-connected nature of physical, biological, and chemical processes and the importance of their joint study when examining the range of natural processes acting on underwater shipwreck sites. While a fuller understanding of wreck SFPs necessitates such an all-encompassing approach, the specialized knowledge each individual process often requires means that the majority of scholarship tends to tackle one at a time. So as Bethencourt et al. (2018) serves as a synthesis of several studies, most of these more focused individual studies will center on either physical (e.g.; Quinn & Smyth, 2018, Fernández-Montblanc et al., 2018, Smyth & Quinn, 2014, Quinn & Boland, 2010, Quinn et al., 2007), chemical (e.g; Moore, 2015, Horn, 2014, MacLeod & Steyne, 2011, Foecke et al., 2010), or biological processes (e.g; Gravina et al., 2021, Secci et al., 2021, Ricci et al., 2019, González-Duarte et al., 2018). It is among these specialized studies that this particular thesis situates itself. While it does take into account the range of processes acting on the *Phoenician* wreck off the coast of Xlendi, this thesis is nevertheless concerned foremost with the study of a biological process. Specifically, the benthic communities associated with the ship's cargo.

3.2.4 Biological Processes

Biological processes and the methods used to study them can vary substantially and can answer a wide range of research questions. In some cases, these biological processes may be

scrambling evidence (e.g., octopus' "gardens" as a collection of re-organized material) while, in others, they may be extracting it altogether (e.g., *Teredo navalis* eating away at ship timbers). There are also cases of biological growth protecting archaeological materials. This can be seen in the Bethencourt et al. (2018) example from earlier as well as in a case from the Xlendi project itself. Fig. 12 shows the painted decoration on a jug that was revealed after the biological accretion that was protecting it fell off during excavation.

In addition to their direct impact on archaeological remains, biological processes also offer valuable environmental insight. This information, derived with the help of geo-archaeological methods, can be used to better situate sites within a changing landscape. A pertinent example of this type of study is that of Marriner et al. (2012). As part of this project, core samples were taken from around the Burmarrad ria, Malta. This area represents an estuary environment where the lower portion of a valley meets the sea. The core samples were then analyzed by stratigraphically characterizing the different sediments, pollen, and mollusk shell inclusions. Because the different assemblages could be grouped into environmental categorizes like "upper estuarine", "lower estuarine", "marine", "marsh", and "fluvial", the researchers were able to use this biological data to re-construct the impact of rising sea-levels and increased sedimentation on the landscape (Marriner et al., 2012, pp. 61-64). This approach would explain how harbour structures might come to be found much further inland from the present-day coastline.

These examples highlight some of the ways that biological data can be used to better understand artifacts and the wider environments within which they are found. It is important to remember that both artifacts and environments undergo changes over time and that biological processes serve both as agents of change and records of it. This concept is one of the main anchors of the research presented in this thesis.

Biological processes are the result of both motile and sessile organisms but this research focuses exclusively on those that are sessile. The main reason for this is that the recovered amphorae from the Phoenician shipwreck still boast an impressive collection of encrusted marine organisms. Although often-times removed as part of the cleaning process, these organisms have here been left in place in order to facilitate research into SFPs and the characterization of benthic communities associated with the site. There are studies which focus on the motile organisms

Figure 12 Photographs taken of a small jug (C10) recovered from the *Phoenician* wreck. The images show how decorative painted elements were preserved underneath encrusted bivalves (author).

associated with shipwrecks (see Paxton et al., 2022) but these tend to be less targeted at answering archaeological questions. They contribute primarily to assessments made regarding the current biological conditions of a wreck and its effectiveness as an artificial reef (see also Jimenez et al., 2017). In this way, they are more helpful when it comes to developing and implementing management strategies for underwater cultural sites rather than interpreting them archaeologically. Because sessile organisms are, on the other hand, encrusted to the surfaces of submerged artifacts, they lend a more direct hand in the spatial interpretation of a site.

A good example of this is the work of Ricci et al. (2019). As part of the study, researchers examined twenty-six statues recovered from the *Antikythera* shipwreck that are now in the collection of the National Archaeological Museum of Athens. Because the artifacts were raised over 100 years ago and excavation records are so limited, little is known about the original distribution of artifacts on the sea-floor (Ricci et al., 2019, p. 92). In order to address this gap in knowledge, the team turned to evidence left behind from the biological colonization of these artifacts (fig. 13). They found their surfaces to be dominated by serpulids, bryozoans, brachiopods, red algae, and calcareous demosponges (Ricci et al., 2019, p. 81). By mapping the location of these organisms and associated bio-erosion on the artifacts, spatial relationships could be interpreted. Statues which had elements void of any biological growth and boasting good preservation would have been covered quickly in those areas by sandy or silty sediments which prevented colonization by marine biota. Other statues which did not have any of these unspoiled areas would have had all of their surfaces exposed for a period of at least three months (Ricci et al., 2019, p. 98). However, not necessarily all surfaces were exposed at once. Rather, different parts of the artifacts could have been exposed at different times as the result of movement across the site. Artifacts displaying this kind of biological colonization, the researchers determined, would have been resting on rockier and conglomerated sediments and would have shifted as a result of seismic activity and the breaking apart of the ship's hull (Ricci et al., 2019, p. 98). The behaviors and characteristics of these marine encrusting organisms also play a significant role in the spatial interpretation of the site. For example, as they are filter feeders, a concentration of brachiopods on one side of an artifact would suggest a greater exposure to currents (Ricci et al.,

2019, p. 100). Similarly, growth rates and the observed size of encrusted organisms can play a role in hypothesizing the duration of exposure in a particular area (Ricci et al., 2019, p. 100).

The study by Ricci et al. (2019) is instrumental in framing the research comprised in this thesis. It offers a solid framework for approaching this type of study as well as valuable insight into how data can be collected and interpreted. The statues recovered from the *Antikythera* wreck represent a biological assemblage from a depth of 50-64 m (Ricci et al., 2019, p. 81). As such, some of the species identified have also been found on amphorae from the *Phoenician* wreck (which itself rests at a depth of roughly 110 m). The study by Ricci et al. (2019) then serves as an interesting point of comparison for wreck sites within the context of the wider Mediterranean basin. A discussion can be had about differences in the colonization of marble and ceramic artifacts and the effects of different depths and sediments.

Without records pertaining to the distribution of artifacts on the seabed, the goal of Ricci et al. (2019) was to fill this gap. However, since detailed records for this already exist in the case of the *Phoenician* wreck, different research questions can be pursued. Principally the establishing of a vertical record of the changes in benthic community composition. This can be used to identify major episodes of sedimentation onsite, identify areas of the site characterized by prolonged relative stability, and track the movement of artifacts over time.

In this way, the thesis comes to draw more from the study of Secci et al. (2021). The project centers on the 4th century BCE *Mazotos* shipwreck. It rests in 45m of water and sits roughly 1.5 nm off the southern coast of Cyprus (Secci et al., 2021, p. 2). Equipped with 3D photogrammetric models of the site and each of its individual amphorae, the team sought to reconstruct environmental and sedimentation processes. This was accomplished by modeling sediment horizons onto the photogrammetric models of each individual artifact (discernable by discoloration and obvious changes in organism distribution). These were, in turn, aligned and overlaid with elements that were visible in the model of the entire site. The result is a composite model made up of a number of individual 3D objects as can be seen in fig. 14 (Secci et al., 2021, pp. 6-7). This method was successful in identifying and reconstructing two different seafloors. One of them represents the seafloor at the time of excavation and works to prove the legitimacy of the method while the other represents an older level (Secci et al., 2021, p. 9). This relic seafloor,

Figure 13 Marble statues recovered from the *Antikythera* wreck displaying encrusting organisms and signs of bio-erosion (Ricci et al., 2019, p. 99).

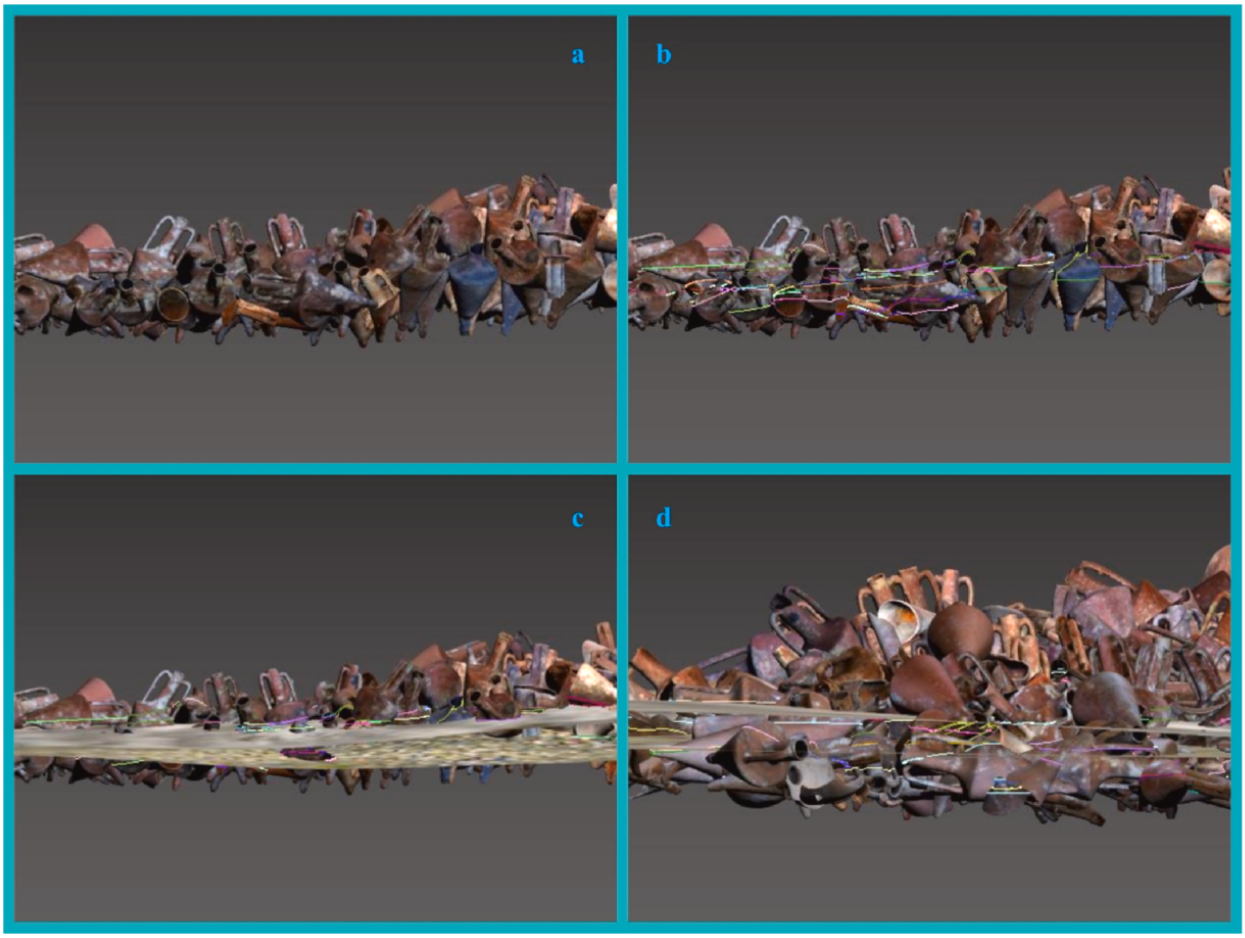

Figure 14 Screengrabs from the model produced of the *Mazatos* shipwreck. Highlighting a) alignment, b) identification of sediment horizons, c) and d) seafloor reconstructions (Secci et al., 2021, p. 9).

visible through redox staining and encrusting organisms, sheds light on sediment accumulation at the site. In turn, contributing to the study of natural processes acting on the site.

When collecting biological data, the team photographed each recovered amphora immediately after it was raised. The entirety of the artifact was captured to create a photogrammetric model and additional photos were also taken along transects laid the length of the amphorae with a tape measure. In their methods they describe how, “the digital camera is hand-held at the same distance from the object, to ensure that a similar area (ca. 13 cm x 19 cm) is photographed” (Secci et al., 2021, p. 7). The images were, in turn, analyzed using the software photoQuad. Resulting in percent coverage values for the seven categories established by the team. These categories being; “coral, macro algae, calcareous algae, sponges, bryozoans, other organisms (e.g., polychaetes, foraminifera, bivalves), […] [and] free or uncolonized substrate (e.g., clay, marine aggregates)” (Secci et al., 2021, p. 7). The concentrations of organisms were then related to their precise locations on the artifacts and any notable features like holes, cracks, or other irregularities.

Unfortunately, the project is still underway. The article by Secci et al. (2021) discusses preliminary results but, to date, nothing has been published about the actual integration of biological data into the photogrammetric model of the site. Their initial findings stem solely from sedimentological modeling. While this means that it does not provide comparable results or a framework for analyzing biological data, the study is nevertheless essential in informing the research done for this thesis. It serves as a conceptual model by guiding research design and data acquisition strategies. Importantly, it is also a testament to the potential of visualizing and analyzing data spatially through photogrammetric models. A similar approach can be implemented in the case of the *Phoenician* wreck because equivalent models already exist. High resolution photogrammetric models of the site were made pre-disturbance and regularly throughout the excavations (Gambin et al., 2018, pp. 80-82). Additionally, 3D renderings of the individual raised amphorae, produced using a laser scanner (the Artec Leo with an accuracy of up to 0.1mm and a resolution of up to 0.2mm), also already exist.

Since both the *Mazotos* and *Phoenician* are categorized as coherent sites and characterized by the typical tumulus shape, similar approaches can be adopted in both cases.

These approaches can also be used to answer different questions. The primary goal of Secci et al. (2021) is to "attempt a reconstruction of the environment and sedimentation processes at the site" (Secci et al., 2021, p. 1). And, while they do briefly mention the potential for looking at the "dislocation" of artifacts, it is a topic that goes mostly un-explored (Secci et al., 2021, p. 1). The goal of this thesis is similarly, to reconstruct the environment and sedimentation processes of the *Phoenician* shipwreck. However, a greater emphasis is placed on doing this through the lens of movement.

The work done on the *Mazatos* also serves as an important reference point for this thesis because of the similarities in site composition. By examining the biological colonization of a ceramic cargo, the study is more similar to the *Phoenician* and its amphorae than Ricci et al. (2019) and the marble statues of *Antikythera*. This is not to say that the study by Ricci et al. (2019) is of any less value. To the contrary, it serves as an important analytical framework and an interesting point of comparison from a materials perspective. This is also true of the article published by Gravina et al. (2021). The study is centered around the benthic community of a Carthaginian bronze naval ram lost in battle as part of the First Punic War in 241 BCE (Gravina et al., 2021, p. 2). Recovered off the coast of western Sicily in the Aegadian islands, it also represents the closest project geographically. The ram was also recovered from a depth quite similar to that of the *Phoenician*. Between 75m and 95m compared to the *Phoenician*'s 110m (Gravina et al., 2021, p. 2).

The study differs from those already discussed in that it focuses on the benthic community of a single artifact. Because of this, the discussion revolves less around SFPs and instead on examining species composition and the traits of dominant organisms (Gravina et al., 2021, p. 1). The findings were compared to similar datasets from surrounding habitats in order to examine possible colonization patterns and better understand the bronze ram as a proxy of marine biodiversity (Gravina et al., 2021, p. 1). What they found was that the ram had a high level of species richness and, "showed strong similarity with coralligenous reefs and detritic circalittoral habitats, with *Posidonia* beds and photophilic rocky bottoms, and to a lesser degree with the deeper bathyal habitats and caves" (Gravina et al., 2021, p. 14). This means that the Carthaginian ram's organism assemblage serves as a record of the existence of these surrounding

environments over the course of the two millennia it sat on the seabed. In this way, the article also differs from those already discussed in that, at its core, it is rooted in the use of archaeological material to answer biological questions. Just as the benthic communities of submerged artifacts can be used to understand processes of archaeological site formation, they can also be used to understand marine biodiversity. While the work of Gravina et al. (2021) is limited in what it can contribute to this research in terms of archaeological interpretation, it is crucial for what it contributes from this biological perspective.

The study be Gravina et al. (2021) acts as a guide for how biological data recovered from a submerged artifact can be analyzed and interpreted. Using nMDS ordination plots, cluster analysis, and species count graphs, the data that was gathered can be interpreted to show what ecological affinities/habitats are represented and to what degree (Gravina et al., 2021, p. 12). Similarly, statistical forms of analysis like SIMPER were used to calculate percentages of dissimilarity between samples (Gravina et al., 2021, p. 13). Similar, albeit adapted, methods are employed by this dissertation.

3.3 Conclusion to Literature Review

Few studies have met at this particular intersection of underwater archaeology and marine biology. While this literature review has included research into SFPs from over the past fifty years, there are only a small number of these which center around an in-depth analysis of biological processes. Of these, many will fall into one of two categories. They commonly tend to either focus on assessing the impact of marine organisms on the preservation of a site (e.g., *Teredo Navalis* and exposed wood) or they look at a site's impact on local marine life (e.g., modern wrecks as artificial reefs). Few have looked to encrusted marine benthos for how they can inform the study of SFPs and be used as a tool for archaeological interpretation.

Of these, the most important studies are those done by Ricci et al. (2019), Secci et al. (2021), and Gravina et al. (2021). Looking at the benthic communities of, respectively, marble statues from *Antikythera*, amphorae from *Mazotos*, and a bronze ram from the Aegadian islands,

they lay the ground work for benthic studies in an underwater cultural heritage context. They represent an underwater archaeology that is increasingly multi-disciplinary. One that works closely with the field of marine biology in order to study the spatial relationships of artifacts, different phases of sedimentation, and colonization phases of organisms representing different habitat affinities. This dissertation draws on the work of all three authors as it adds to this discourse and pursues the new objective of identifying and interpreting artifact movement.

4. Methods

4.1 Brief Overview

The main aims of this dissertation are; 1. to identify and characterize the benthic organisms encrusted to amphorae from the P*hoenician* shipwreck and 2. to use this information to develop and evaluate the effectiveness of a new method for interpreting the movement of underwater archaeological objects. This has been done by quantifying the organisms of four key amphorae using a standardized sampling method. This type of method was adopted to facilitate the comparison of biological data across artifacts and the site. Each sample represented a surface area of 100cm^2 and all marine life observed within it was identified, counted, and measured. These counts were then statistically compared and used to discern distribution patterns. This, along with the other data that was collected, characterized the benthic communities of the *Phoenician*. In order to interpret the movement of artifacts, this biological data was integrated into a composite 3D model of the site. The resulting context allowed for the interpretation of spatial relationships and the identification of post-depositional artifact movement.

4.2 Amphora Selection

The artifacts that were available for study were either recovered from the excavation squares D7 and E7 (fig. 15) or from various scattered position across the site. Those from outside the excavation squares were targeted for recovery based on their typologies and represent the diversity of the ship's cargo. Out of these, only artifacts that were structurally sound, had completed de-salination, and were visible in early photogrammetric models of the site were considered. The four that were selected include A18, A24, A06, and A40. By focusing on these amphorae, this research examines the benthic communities of the *Phoenician* shipwreck through

four key proxies. These amphorae were selected on the basis of the variety of comparable data they would generate. They span the width of the wreck, reach out both fore and aft, extend both out of the seabed and under it, represent a variety of orientations, and exhibit properties suggestive of both movement and stability. Their locations relative to each other and the wider wreck can be seen in fig. 16.

For the research that was carried out, these four amphorae were deemed sufficient. While it is undoubtedly true that including additional artifacts would contribute to a more comprehensive understanding of the site, this was beyond the scope of the research presented here. The process for each amphora is lengthy and the method is, in some aspects, experimental. It was decided that, at this stage, these four amphorae would serve as an adequate test of the method and would produce sufficient results. In the event that additional data should be required, replicability will be possible as all necessary information is being included.

4.2.1 A18 and A24

Both A18 and A24 are mostly intact, fully desalinated, and have key elements (mouth, rim, handle, etc.) visible in pre-disturbance models. Importantly, they are also beneficial to this research from a spatial analysis perspective because they were located next to each other at the site. As a result, they shed light on the dynamics of neighboring artifacts. Amphora A24 was positioned such that just enough of its distinctive elements are visible in photogrammetric models. This meant that a 3D scan of the artifact could be aligned with confidence while also ensuring a substantial amount of sub-surface data. This is complemented by A18 because more of its surface was exposed. Which means that it serves as a better record of benthic organisms from the seabed up. Together, they provided a vertical record of ecological succession and a platform for examining the consistency/dissimilarity of biological processes playing out on neighboring artifacts.

Figure 15 The location of the excavation trench (squares D7 and E7) (Courtesy of the Department of Classics & Archaeology, University of Malta).

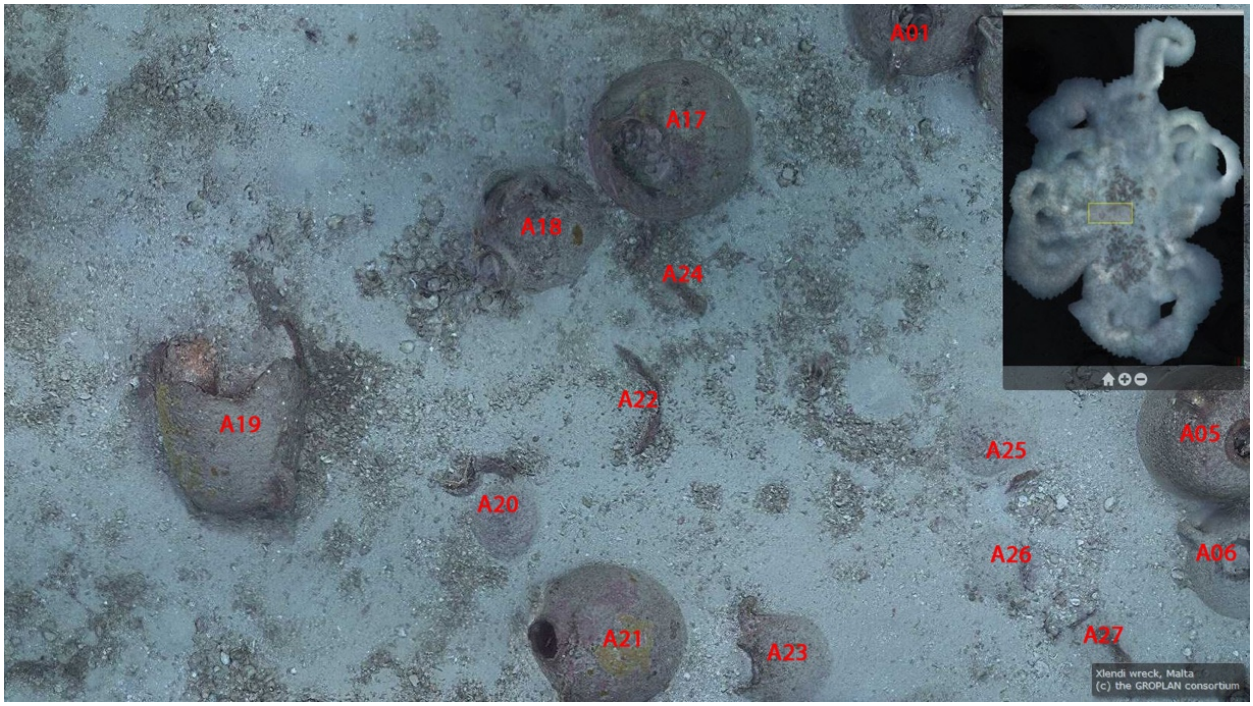

Figure 16 The locations of A18 and A24 shown in photos from 2014 (Courtesy of the Department of Classics & Archaeology, University of Malta).

4.2.2 A06

The amphora A06 was selected because it was recovered from the opposite side of the trench from A18 and A24. As such, it represented a good opportunity to investigate how biological composition differed across the width of the wreck. The amphora was similarly structurally sound, fully desalinated, and easily aligned with photogrammetric models. A06 was also selected because it appears upright in photos of the site whereas A18 and A24 look slanted. In order to investigate how these different orientations relate to movement across the site, it was included in the research.

4.2.3 A40

The amphora A40 was a targeted recovery and it did not come from the excavation trench. It was recovered from an area on the other end of the amphora pile. As a result, it was included in this research to investigate the variability of benthic communities running the length of the ceramic cargo. While A18 and A24 were slanted at the time of recovery and A06 was upright, A40 was entirely on its side. By selecting it to be included in this research, the relationship between orientation and possible movement was also further investigated. As with the others, A40 was fully intact, desalinated, and visible in early models of the site.

4.3 Identification and Characterization of Benthic Communities

The type of data collected and the way it was collected drew on established principles utilized in biological research. Throughout the process, Anastasios Eleftheriou's *Methods for the Study of Marine Benthos* (2013) was consulted and adhered to. Drawing on this source, the methods used for this research were designed to investigate three key indicators. These were species composition, relative abundances, and spatial patterning (Eleftheriou, 2013, p. 16). In

addition to Eleftheriou (2013), the methods developed for data collection were also influenced by the studies of Gravina et al. (2021), Secci et al. (2021), and Ricci et al. (2019).

4.3.1 Building an Identification Sheet

The organisms encrusted to the amphorae were thoroughly examined using hand-held magnification. This was done in order to distinguish as many individual species as were present. As each new organism was encountered, it was photographed using a macro lens and described. Organisms that appeared to share the same characteristics were photographed and grouped together in order to bolster a species category. Entirely new categories were created for morphologically distinct organisms. At this point, eight broader categories were established. These were; 1. Bivalves, 2. Bryozoans, 3. Corals, 4. Foraminifera, 5. Serpulids, 6. Spirorbids, 7. Verimetids, and 8. Others. Examples of organisms making up these categories are pictured in fig. 17.

As these identifications are predominantly at the phylum or class level, they served as broader categories into which species could be grouped. It was the next step to then build lists of the distinct species which fell into these groupings. In an effort to minimize the effects of bias or subjectivity, this was done independently by two individuals (the author and Dr. Julian Evans). Each observer organized all the photos of individual organisms belonging to a given category (e.g., Bryozoans) into groups, with each group representing a particular species, thus creating a species list. The lists created by the two individuals were then compared against one another and only minor differences were observed. After these were reconciled, the result was an identification sheet that comprised one species of bivalve, twelve bryozoans, two corals, one foraminifer, seven serpulids, two spirorbids, one vermetid, and a category for “others”. While this list was expected to grow slightly over the course of data collection, it served as a more than adequate launching point.

A file was then created for each identified unique species. This included several photos (full organism, detailed close ups, different examples, etc.) and a description of identifying

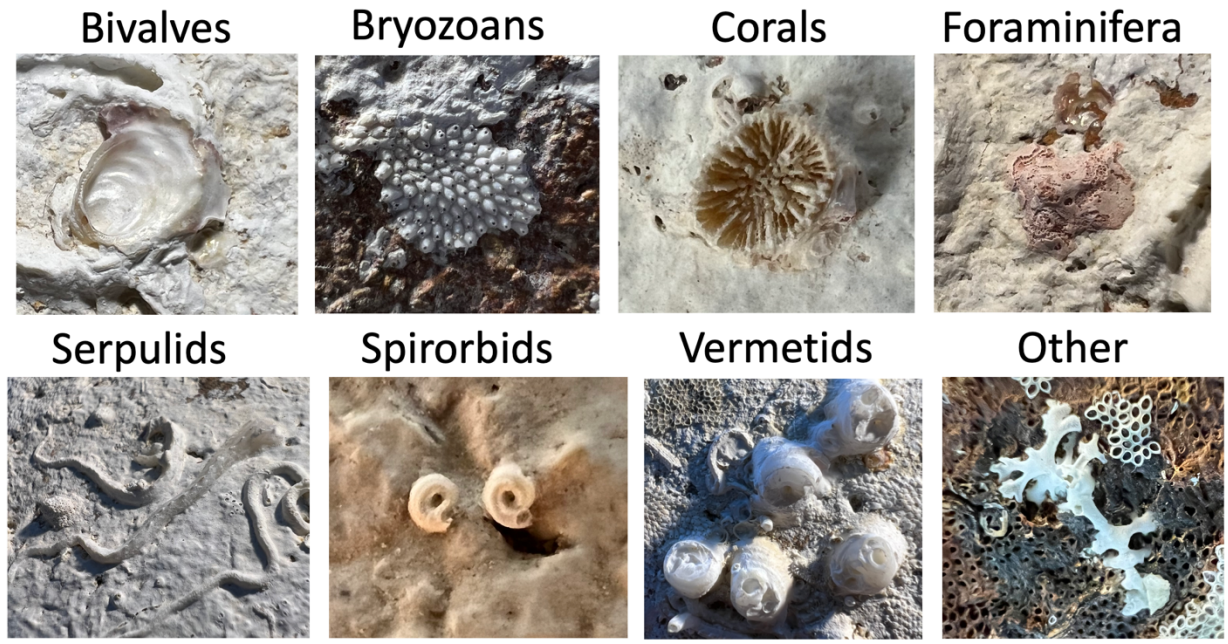

Figure 17 Examples of organisms from each of the eight broad categories that were defined (Dr. Julian Evans and author).

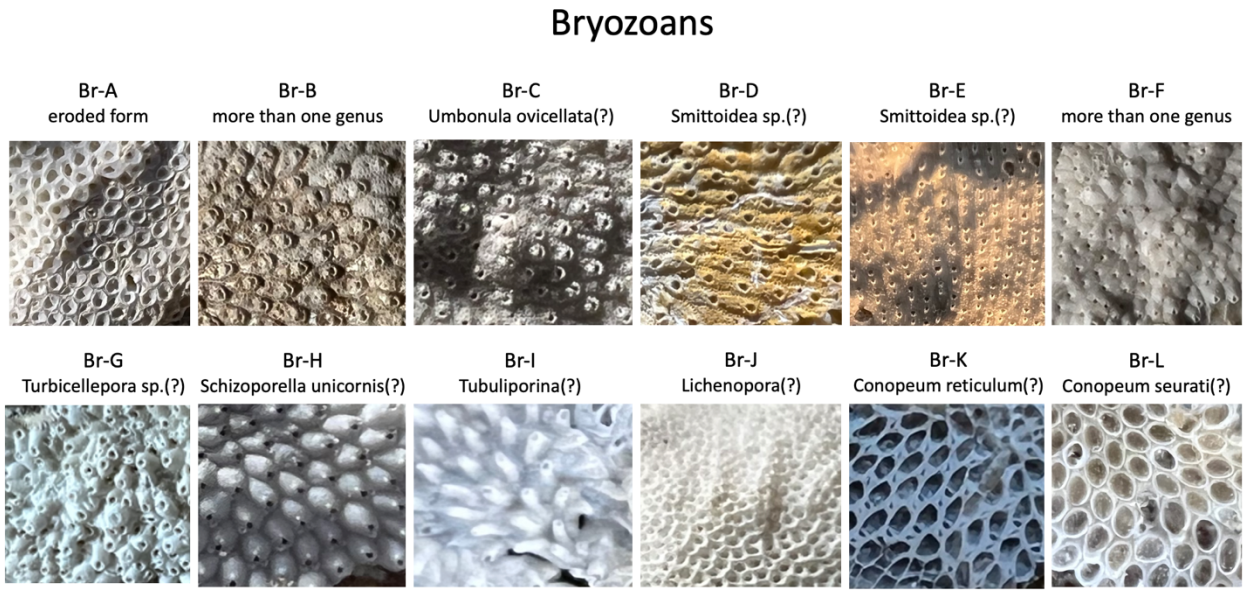

Figure 18 Examples of different bryozoan species that were encountered. With tentative identifications (Dr. Julian Evans, Dr. Jasmine Ferrario, and author).

attributes (e.g.; “individual zooids not clearly defined but appear more as openings in one uniform fabric”, etc.). Each species was assigned a code (e.g., “Br-A”, “Br-B”) to facilitate subsequent data collection while the images/descriptions were sent to experts for specialist identification. An example of the resulting IDs can be seen in fig. 18. The identification sheets were crucial in that they worked to define the scope of the research at this early stage. While not final, it provided a general understanding of how many species were present. This played a role in shaping later methods of data collection and research design. Having the identification sheets as a reference throughout the process of data collection was crucial.

4.3.2 Data Collection

With the amphorae selected and a list of already identified species compiled, the process of data collection began. It was known from earlier research that the methods employed by Secci et al. (2021) would be the most applicable at this stage. This was because of the similarities in the materials and aims of both studies. Much in the same fashion, the amphorae were photographed along transects running their length. The camera was held at the same distance from the objects so that roughly the same amount of area was covered in each image (Secci et al., 2021, p. 7). To visualize the entirety of the transect, the images were then stitched together using the software *Panorama Stitcher* and *Hugin*.

The results, however, were less than desirable. The product was often a picture which was distorted and lacking in detail. While it was clear that the stitched images could not be used, it was also determined that the individual photographs themselves presented their own problems. While different categories of organisms could be easily distinguished from looking at the photos (e.g.; bryozoans, coral, etc.), the resolution was not high enough to distinguish between different species within these categories (e.g.; *Conopeum reticulum* vs. *Conopeum seurati*). This wasn’t an issue in the study of Secci et al. (2021) because they were only grouping organisms into broader categories to determine percent coverage. It was, however, an issue for this research. One that was significant enough to require the development of new methods.

It was decided that square sampling units would be more effective than transects. Especially in terms of producing standardized and workable datasets. To do this, a tape measure was used to lay a baseline along the length of each amphora and small stickers were placed at 10cm intervals along this baseline. Originating at each point along the baseline, additional stickers were then placed at 10 cm intervals around the circumference of the amphorae and running perpendicular to the baseline. Stickers of two colours were used in order to distinguish between the baseline (blue) and these other points (red). An example of this can be seen with A18 in fig. 19. Care was also taken to ensure that the stickers were not overly adhesive. This ensured that no damage was done to the artifacts and minimized their impact on biological accretions. Each sticker was assigned a name that linked it to its position relative to the baseline and circumference. Points on the baseline were each given an alphabetical signature (e.g.; A0, B0, C0, etc.) and numbers were assigned to differentiate those along the circumference (e.g..; A1, A2, A3, etc.). Because of the irregular shapes of the amphorae, this in itself did not produce a workable grid. This is to say that, for example, the points A4 and A5 did not make a perfect 10x10cm square when joined with the points B4 and B5.

The devised solution was a flexible frame. A 10x10 cm square cut into a piece of paper. The top corners of the square were aligned with two points along the grid (e.g.; A1 and A2) and taped in place using minimally adhesive tape. This flexible test square could bend with the curvature of the artifacts but would always represent a 10x10 cm square. This is shown in fig. 20. Some distortion did still occur that had a minor impact on the area represented but this was accepted as a tolerable level of error. Data was collected from each square while this paper frame was still in place. It offered a clear boundary of what should and should not be counted.

With the frame in place, handheld magnification (Gowlland Folding Magnifier with 10x Magnification) was used to assist in the process of manual data collection. Magnification was used to visually scan the entire surface of each square and identify the presence/absence of each distinct species. As a result of this process, several new species were identified, photographed, and added to the identification sheets. Even species that had already been identified and described were re-photographed if exceptionally good, clear, and intact individuals were encountered. Beyond recording presence/absence, the number of individuals of each unique

Figure 19 Amphora A18 with the grid system in place (Author).

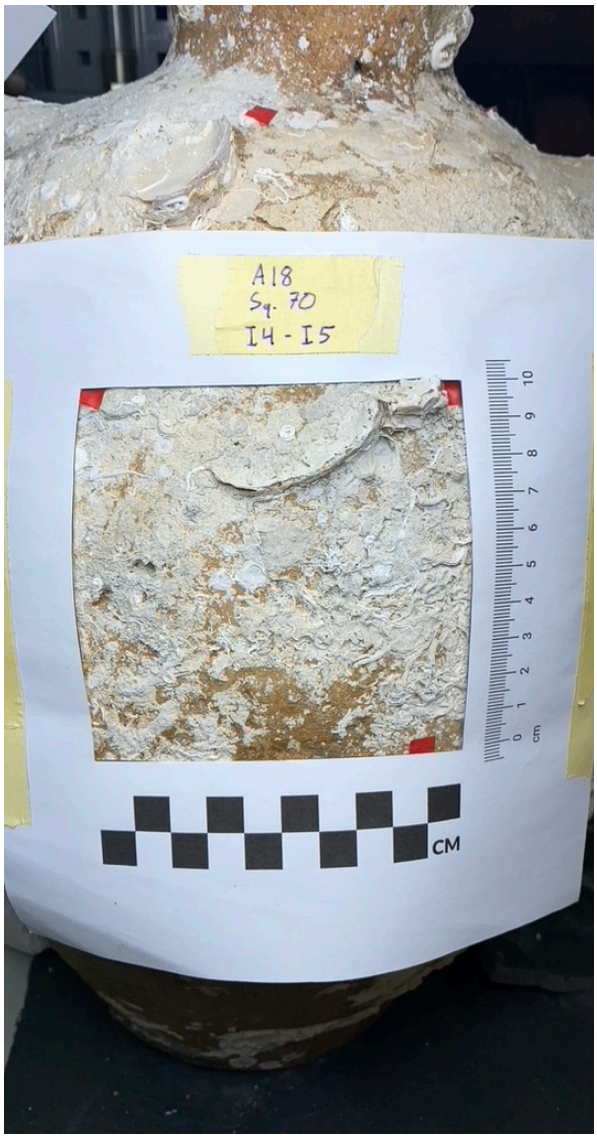

Figure 20 The flexible frame being used to delineate a sample square on A18 (Author).

Amphora	Square	Organism	Species	Present	Count	Size (cm)	Covered	Covered By	Covering	Covering What	Notes	Notes General
A06	89	Bivalve	A									Mostly un-colonized surface. Signs of abrasion and loss of some organisms. Likely buried quicky? Nothing on base. Original intact slip?
			B									
		Bryozoan	A	yes	3	2x1	yes	bryozoan, serpulid, spirorbid	yes	bryozoan, coral		
			B									
			C									
			D									
			E									
			F	yes	3	0.75x0.5	yes	bryozoan, serpulid	no	N/A		
			G									
			H	yes	4	0.75x0.25	yes	bryozoan, serpulid	no	N/A		
			I	yes	1	0.5x0.25	yes	bryozoan, serpulid	no	N/A		
			J									
			K									
			L	yes	4	1x1	yes	serpulid, spirorbid	no	N/A		
			M									
			N	yes	1	0.5x0.25	yes	bryozoan	yes	bryozoan		
			O	yes	2	0.25x0.25	yes	serpulid, spirorbid	no	N/A		
			P									
		Coral	A	yes	2	<0.5	yes	bryozoan	no	N/A		
			B									
		Feraminafor	A	yes	2	<0.5	no	N/A	no	N/A		
		Serpulid	A									
			B	yes	1	>0.75	yes	bryozoan	no	N/A		
			C									
			D									
			E									
			F									
			G	yes	1	>0.5	no	N/A	no	N/A		
			H	yes	1	>0.75	no	N/A	no	N/A		
			I									
			Unid.	yes	>10	<0.5	yes	serpulid	yes	bryozoan, serpulid		
		Spirorbid	A	yes	>10	<0.5	no	N/A	yes	bryozoan, serpulid		
			B									
		Verimetidae	A									
		Other										

Figure 21 A sample form showing how biological data was collected for each sample square. (Author)

species was also recorded. Because of this, it is known precisely how many of each species are present in any given square. Measurements were also taken. The length and width of the largest example of each species was recorded for every square along with other spatial notes regarding the superimposition of organisms. All of this data was compiled into excel spreadsheets organized like the one shown in fig. 21.

4.3.3 Data Analysis

Methods for analyzing the data were targeted at both qualitatively and quantitatively differentiating between distinct phases of biological growth. These distinct phases could be visually discerned and were noted throughout the process of data collection. However, conclusions based on visual interpretation alone would fail to account for the differences in species composition and distribution. In order to examine how biological growth differed between these phases, each square had to be assigned to a phase.

To do this, photographs were taken of the amphorae with their grid stickers in place. The program *Adobe Illustrator* was then used to manually delineate different growth phases visible on the artifacts. These phases represent areas that were both visually and compositionally distinct in terms of the organisms that were present. Differences in the composition, orientation, and spatial context of these phases, when characterized and quantitively compared, served as a record of biological processes acting on the wreck. In this way, they also lend themselves to the interpretation of site formation processes more broadly. Throughout the process of delineating these phases in *Adobe Illustrator*, the amphorae were nearby and continuously referred to. Borrowing and adapting methods used in the soil sciences, the horizons were labelled alphabetically with the upper-most phase being “A” (Zhan, Hartemink, and Huang, 2021). Phases “B”, “C”, “D”, and “X” were also identified. The reason for “X” being labelled non-sequentially is that it exhibited signs of abrasion and was characterized primarily by the loss, rather than the growth, of biological data.

Each sample square could now be assigned to its corresponding growth phase. In cases where a square straddled two phases, it was assigned to neither one and a new category was created (e.g. “A/B” or B/C”). With each sample square assigned to a phase, dissimilarity between phases could be quantified. This was done using the R package “vegan”. Values of dissimilarity for each test square were calculated and assigned a value between 0 and 1 using Bray-Curtis dissimilarity. This enabled test squares to be compared to one another quantitatively on the basis of species presence/absence and count. The output is a value between 0 and 1 (0 meaning the two squares are identical and 1 meaning they have nothing in common). To facilitate the interpretation of this data and summarize it visually, it was plotted using non-metric multi-dimensional scaling (nMDS). Two plots were generated. One where the sample squares were grouped by amphora and another where they were grouped by phase. Analyzing the data in this way meant that the differences in the composition and relative abundance of organisms in each square could be compared to characterize spatial patterning across artifacts and the site.

4.4 Interpreting the Movement of Artifacts

4.4.1 Integrating Data into the 3D Model

In order to better contextualize the data that was collected, it was integrated into a 3D model of the site. This added an important spatial element to the research because it allowed for the different phases of benthic colonization to be examined in relation to other artifacts and the wider wreck as a whole. As part of this process, a laser scanner (the Artec Leo with an accuracy of up to 0.1mm and a resolution of up to 0.2 mm) was used to create individual 3D scans of the amphorae A06, A18, A24, and A40. This was done with the baseline, grid, and test square stickers still in place. With these reference points integrated into the 3D model, the data for each square could easily be matched up with its real-world location on the amphora and within the wreck.

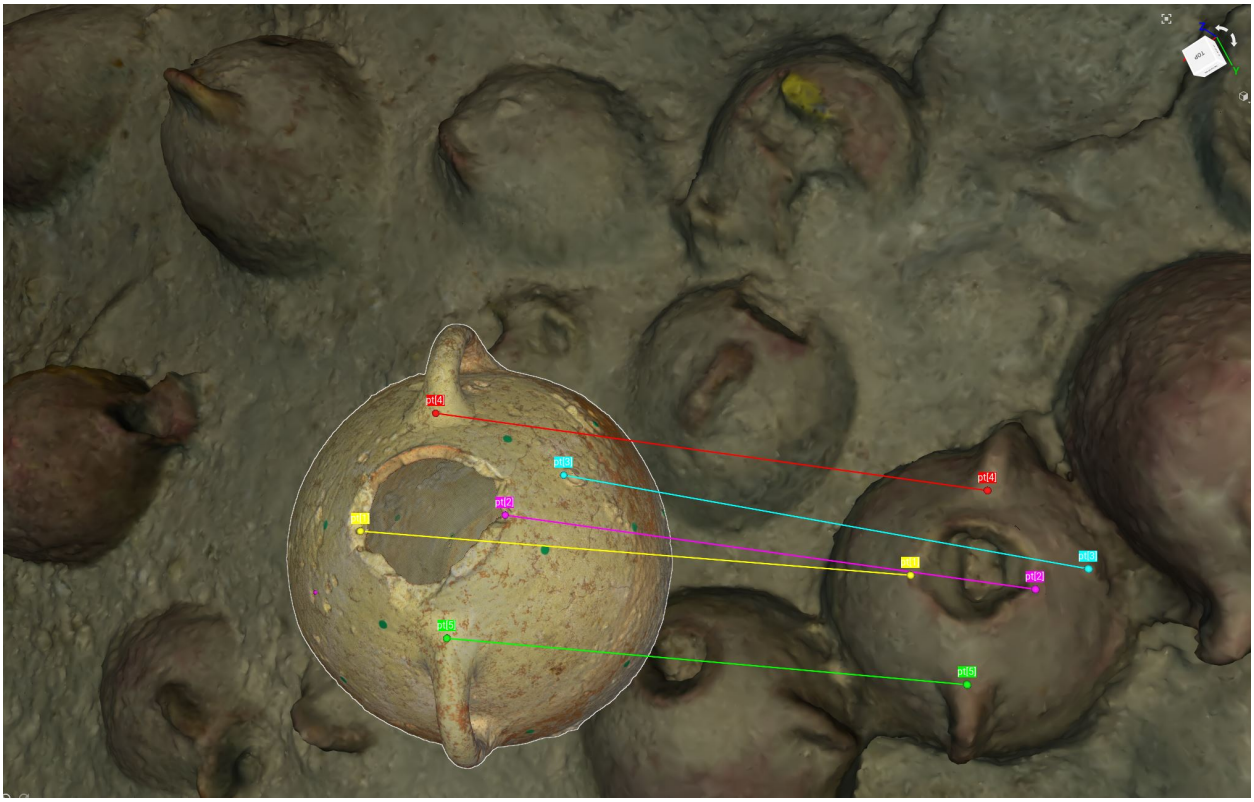

Figure 22 Screen grab showing part of the alignment process. Using the rim and handles to align artifact scans with the photogrammetric models of the site (A. Bravo-Morata Rodríguez and author).

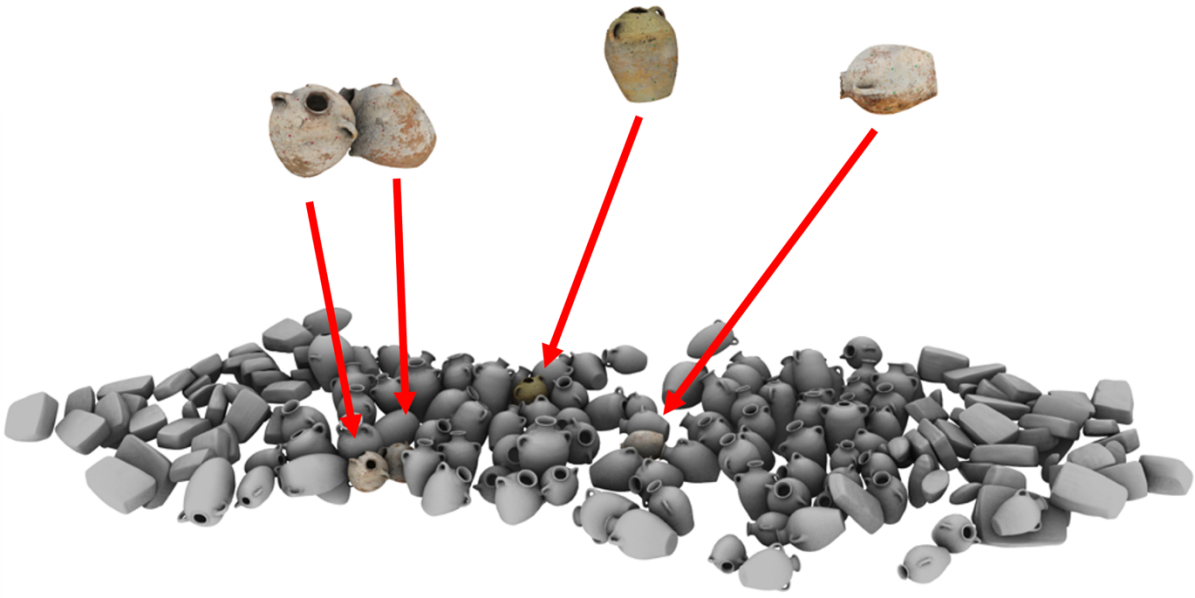

Figure 23 The positions of A18, A24, A06, and A40 (left to right) relative to the rest of the cargo (A. Bravo-Morata Rodríguez and author).

This is a new method for linking biological data to a 3D site model and was developed specifically for this research.

The laser scanner's proprietary software, *Artec Studio 17*, was used to align the models of individual artifact with their locations in the photogrammetric models of the site. Key points on the artifacts (e.g.; handles, rims, large encrustations, etc.) were aligned across both models and an example of this process can be seen in fig. 22. Both models were already to the same scale and, after this initial step had been made, only minor adjustments in orientation were required to achieve an accurate alignment. This process was carried out for each artifact included in this research. Alignments were also verified against the photogrammetric models produced over multiple seasons of excavation to ensure the highest possible accuracy.

A third layer was also incorporated into the workable model. The pre-existing layer features idealized models of each artifact typology already aligned with the photogrammetric models of the entire site. Together, these models of the individual artifacts and the wider wreck provide a crucial spatial element to the interpretation of the encrusted benthic organisms and, by extension, the biological processes and SFPs associated with the Phoenician shipwreck (fig. 23).

4.4.2 Using the Model to Interpret Movement

The 3D model allowed the artifacts to be examined in the positions and orientations they were recovered from. Knowing how they were positioned prior to recovery enhances how their biological encrustations can be studied for anomalies evocative of movement. The concept behind this is elaborated by the illustrations shown in fig. 24. This conceptual model presents several different examples of how the movement of artifacts over time can be recorded by the encrusted benthic organisms preserved on their exteriors. With this model in mind, the growth on the digitally in-situ artifacts was examined. Special attention was paid to the orientation of successive growth phases, how the same growth phases appeared on different artifacts, and how

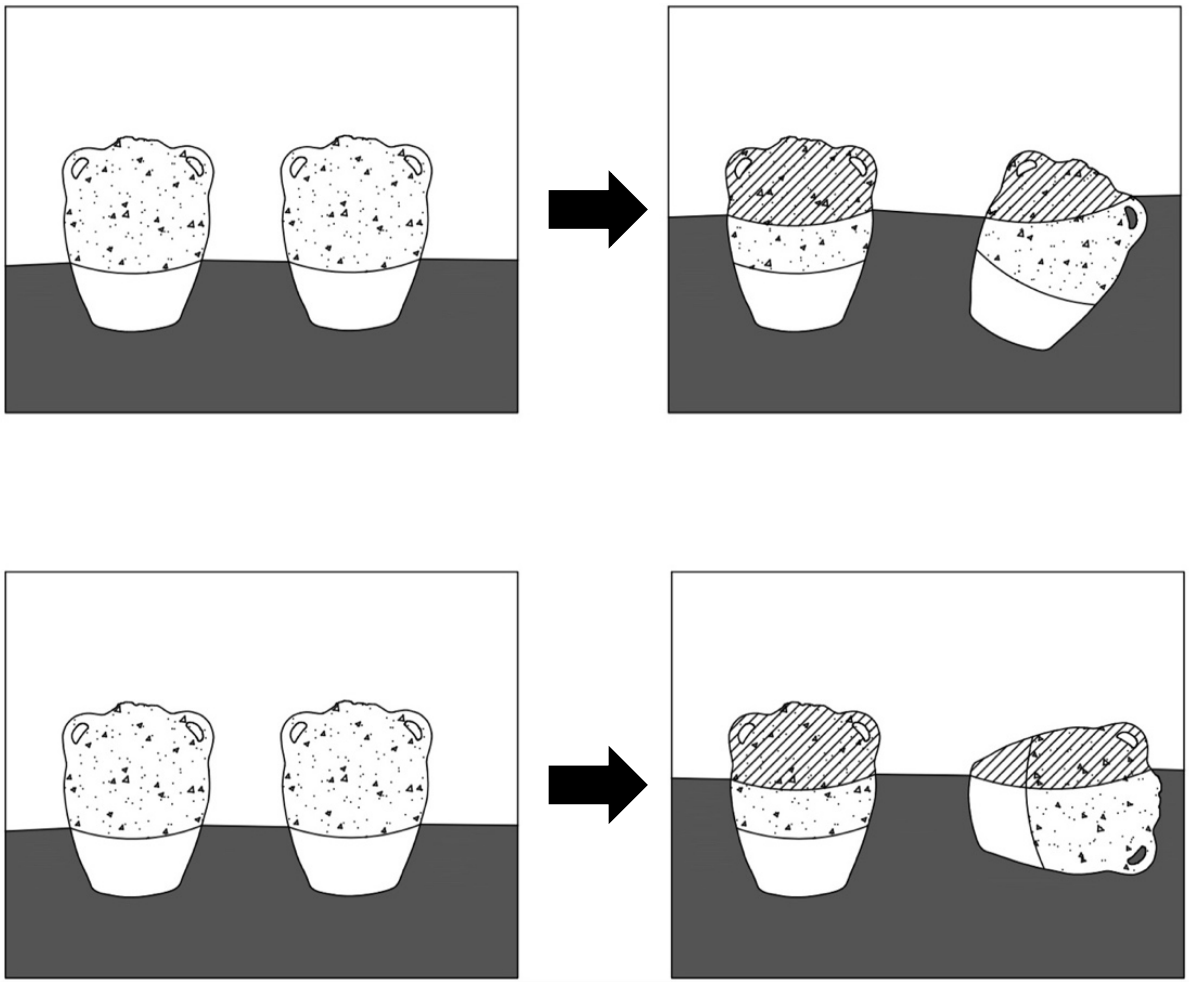

Figure 24 Conceptual model that illustrates how the movement of artifacts could be recorded by different phases of biological growth (Author).

artifacts interacted with their neighbors. This allowed for the identification and interpretation of two different kinds of movement.

4.5 Modelling Sediment Accretion

In assessing the biological growth on the recovered artifacts, it is important to remember that the phases of growth preserved on them are also linked to the sedimentation of the site. This is because processes of sediment accretion, in addition to artifact movement, impact what parts of an artifact are exposed to biological growth. In order to then supplement the analysis of biological processes acting on the site, sedimentation had to be considered. This was done by comparing photogrammetric models of the site made on the last day of excavation in 2017 and on the first day of excavation in 2018. These findings can be seen in fig. 25. It shows that new deposits of around 1-4 cm have accumulated in some areas between the amphorae. Another comparison (fig. 26) models both positive (red) and negative (blue) changes in the same area. Parameters were set to have a sharp threshold of 5%. This means that an area would only turn blue or red if more than a 5% change was detected. The results highlight the dynamic nature of these processes and further contextualize the first comparison. It shows that the areas where 1-4 cm have accumulated do not necessarily represent new deposits but rather the shifting of those already at the site. While it is possible that some of these changes could be the result of anthropogenic factors (fin kicks while conducting photogrammetry or slight alignment issues), the model is nevertheless effective at providing a general understanding of what natural processes of sedimentation look like over the period of a year. This provides valuable information that was used when interpreting the length of exposure for certain growth phases.

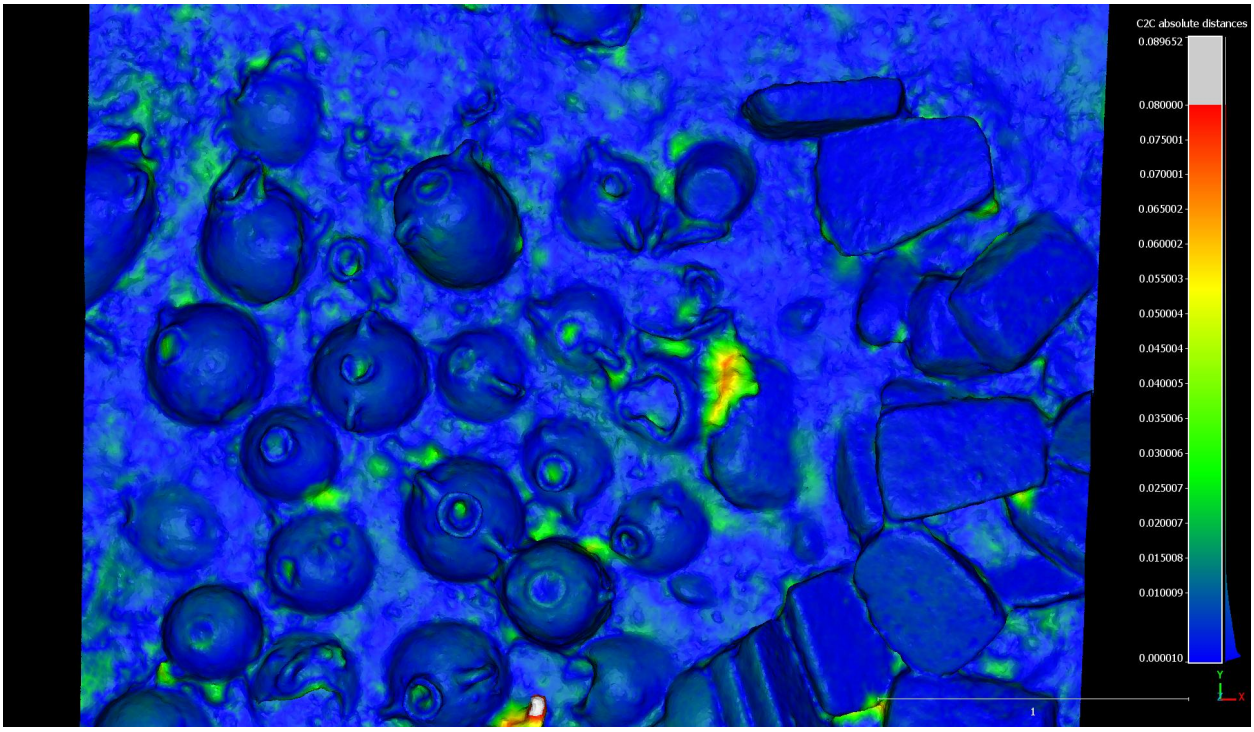

Figure 25 Comparison of photogrammetric models that illustrates the increase in sedimentation across a portion of the ceramic cargo over the period of one year (J. Wood).

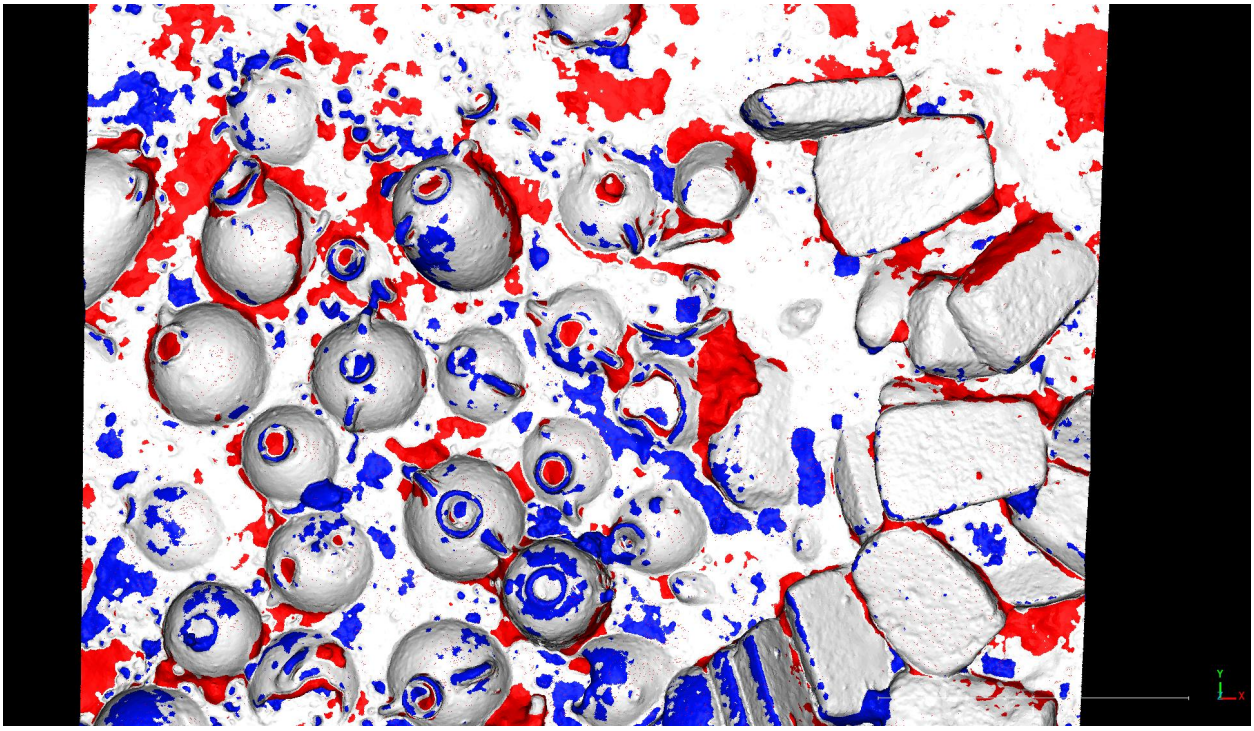

Figure 26 Comparison of photogrammetric models that illustrates where sediments have increased (red) and where they have been reduced (blue) (J. Wood).

5. Results

5.1 Organisms Present

As part of this research, a total of 4,121 individual organisms were recorded. Each of these could be categorized into one of six different major animal groups (with the exception of only 13 individuals). These major groups are: Anthozoa (stony corals), Bryozoa (false corals), Foraminifera (forams), Mollusca – Bivalvia (bivalves), and Mollusca – Vermetidae (vermetid snails). Each of these groups will be described to a general level in the following section. Examples of the organisms that were identified as belonging to each of these groups can be found in the appendix and are accompanied by photographs.

5.1.1 Bivalves

Bivalves are a class of mollusk that are characterized by a shell which is separated into two distinct valves joined together at a hinge. The majority of bivalves lead mostly sedentary lives, being cemented to rocky surfaces or burrowed within seabed sediments. Burrowing is achieved through extension of a locomotory foot from within the shell. Bivalves are suspension (filter) feeders or deposit feeders, having siphons that are used as intake and exhaust openings. Bivalves have a wide distribution and can be found at every latitude and depth. With over 15,000 species of bivalves inhabiting these diverse habitats, a significant degree of variation can be observed. This can be apparent especially when it comes to characteristics like size and complexity of eyes or other sensory organs. On the whole, bivalves are notable actors of bio-erosion. Some bore into rock, concrete, wood, corals, and plastic. Others, in search of hard surfaces and substrate come to foul ships and shipwrecks. (Britannica, 2024)

5.1.2 Bryozoans

A bryozoan is not a single organism but rather a colony of individual units referred to as zooids. Each individual zooid is, in itself, a complete animal that has the ability to share nutrients with its neighbours. These nutrients are pulled in from the water by a circle of ciliated tentacles that surround its mouth. As entirely sessile organisms, bryozoans are bound to a surface by the calcareous walls that surround each zooid and make up the rigid structure of the colony. Some fresh-water species can be less rigid in structure and are held together instead by more of a gelatinous membrane. On the whole, individual zooids rarely exceed 1 mm in size. While colonies of some species can grow up to 1 m in diameter, the majority of marine encrusting species typically grow to sizes of only a couple centimeters squared. Some species can grow un-attached on loose marine sediments, but most encrust rigid surfaces like rock, shells, pipes, marine litter, ships, and shipwrecks. (Britannica, n.d.)

5.1.3 Corals

Although mobile at the larval stage, coral polyps can only develop on a solid surface and, once they do, they transition to an entirely sessile existence. The polyp itself is hollow and cylindrical with one end anchoring the organism to a suitable surface and from the other end extending out an array of stinging tentacles. These tentacles are used to paralyze prey and move it towards the mouth of the animal. Depending on the species, stony corals can be solitary or colonial; in colonial species different polyp individuals live together with skeletons of adjacent individuals fused to form a single structure. Stony corals can reach sizes ranging from several millimeters in solitary species, up to several meters for colonies. Corals are widely distributed throughout all the world's oceans and can be found in both shallow waters and at depths approaching 6,000 m. (Britannica, 2024)

5.1.4 Foraminifera

Foraminifera are unicellular organisms. They consist of a cytoplasmic body surrounded by a type of shell referred to as a test. From within this test, they extend filament-like pseudopodia. These pseudopodia are temporary projections of the cell membrane itself and are used to both move or feed. Foraminifera are typically very small and most living species are less than 1 mm in diameter. They are distributed widely and can be found in almost all marine waters and at any depth. Since they are particularly sensitive to environmental factors like temperature, depth, oxygen, salinity, and pH, the organisms serve as important proxies for environmental reconstruction and can be used to determine the provenance of certain materials. They also play an important role in the development of seabed sediments. Dead foraminifera cover nearly 30% of the ocean floor as what is referred to as foraminiferal ooze. Additionally, the genus *Amphistegina*, for example, has been found to make up nearly 90% of certain locations' total sand biomass. (Britannica, n.d.; Guy-Haim et al., 2017)

5.1.5 Serpulids

Serpulids are marine worms (polychaetes) that are characterized by the calcareous tubes they form and their sessile nature. The tubes they inhabit are, for the vast majority of species, encrusted firmly to hard substrates. This can include natural substrates like rock and the calcareous encrustations of other organisms or cultural substrates like marine litter, harbour structures, ships, and shipwrecks. Serpulids tend to remain relatively small with tubes that typically do not exceed 15 cm in length and 1 cm in width. In some cases, dense clusters of these relatively small organisms can culminate in reef-like structures that total areas upward of 10 m^2. As completely sedentary organisms, serpulids feed using an array of retractable feather-like appendages. When retracted, they can seal the opening of their tube with a cartilaginous operculum or lid. (Montefalcone et al. 2022)

5.1.6 Vermetids

Vermetids are tube forming marine gastropod mollusks. Their calcareous tubes are irregularly coiled and firmly encrusted on suitably hard substrates. As such, they are sessile organisms and feed on particles suspended in the water. As they grow, the tube may come to grow away from the substrate and point outward in a freestanding manner. In responding to predation pressures, different vermetid species have developed an operculum or lid and long columellar muscles. These allow the organism to retract itself back quickly into the safety of its tube. Other species have instead developed aposematic colouring to ward off predators. Vermetids are associated primarily with warmer nearshore environments and play an important role in managing wave-induced coastal erosion and act as habitat engineers. (Sisma-Ventura et al., 2020; Bieler et al., 2023; Gordó-Vilaseca, Templado, and Coll, 2022)

5.1.7 Organisms Present but Intentionally Omitted from Counts

Data for three additional types of organisms was also collected but was deliberately omitted from the total organism counts. Because spirorbids are so small (in most cases 1 mm in diameter) and high in number (over 100 individuals recorded in some 10 cm x 10 cm test squares), the data collected for the group was not as accurate as for others and would skew results too heavily. In most cases an exact number of spirorbids could not be determined. Instead, values were typically recorded as ‘more than’ (>#). The same was done for a sub-group of serpulids that was characterized primarily by their small size (typically less than 5 mm long and less than 1 mm wide). With over 80 individuals in some test squares, they were omitted here for the same reason as spirorbids. Additionally, it was difficult to discern whether certain individuals in this category were not just juveniles of other serpulid sub-groups. For these reasons, the data for these very small serpulids and spirorbids were omitted from individual organism counts. Coralline algae was the third and final organism to be deliberately omitted from counts. This was because of difficulties in discerning the number of observed individuals. It was often unclear where one

individual stopped and another began. Because they occupy a large area (often exceeding a single sample square), it was decided that only noting presence/absence was the best way to collect data.

5.1.8 Major Animal Groups Sub-Divided by Individual Species

The six major animal groupings (bivalves, bryozoans, corals, foraminifera, serpulids, and vermetids) can be broken down further into 28 individual unique species. Over the course of data collection, 2 different bivalves, 15 different bryozoans, 1 coral, 1 foraminifer, 8 different serpulids, and 1 species of vermetid were identified. All 4,121 recorded organisms (except for 13 unidentified individuals) belong to one of these 28 unique species. Of the six major animal groups, bryozoans by far exhibited both the greatest numbers and diversity. They represent over half of all recorded individual organisms and account for 15 of the 28 encountered unique species. This is over twice the individuals of the next most populous group and just about twice the amount of diversity (15 unique species compared to 8). These results are visually summarized in figures 27 and 28 where both the number of individual organisms and the number of unique species have been graphed in relation to the major animal groups. Additionally, figure 29 shows the number of individuals belonging to each unique species. A full break down of these different unique species can be found in the appendix. The identification sheets included there contain photographs, descriptions, possible IDs, and other relevant information that is otherwise too lengthy to include here.

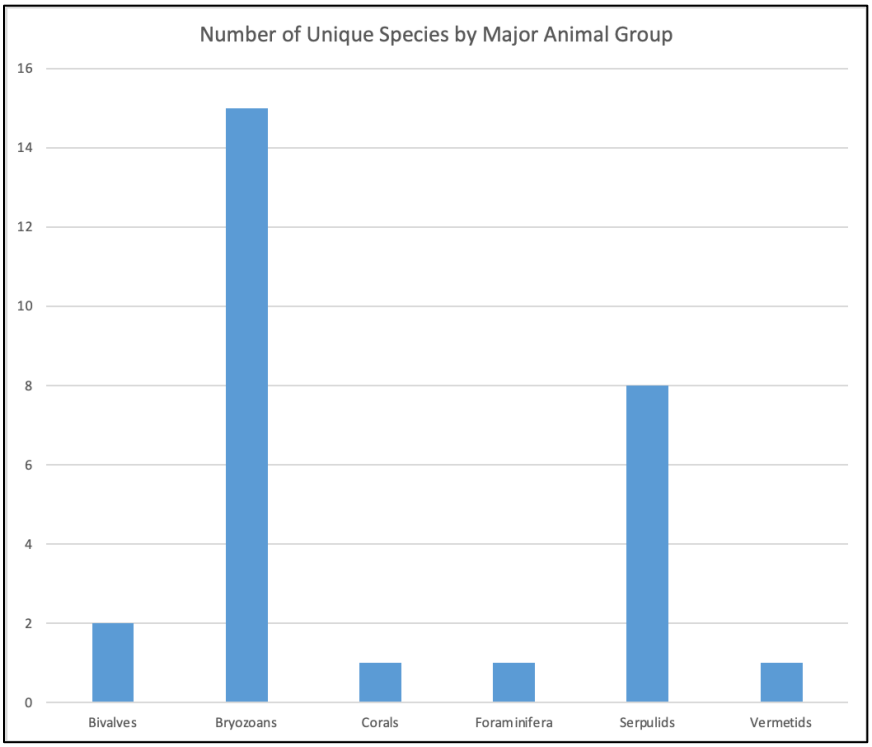

Figure 27 Graph showing the number of unique species identified for each major animal group (Author).

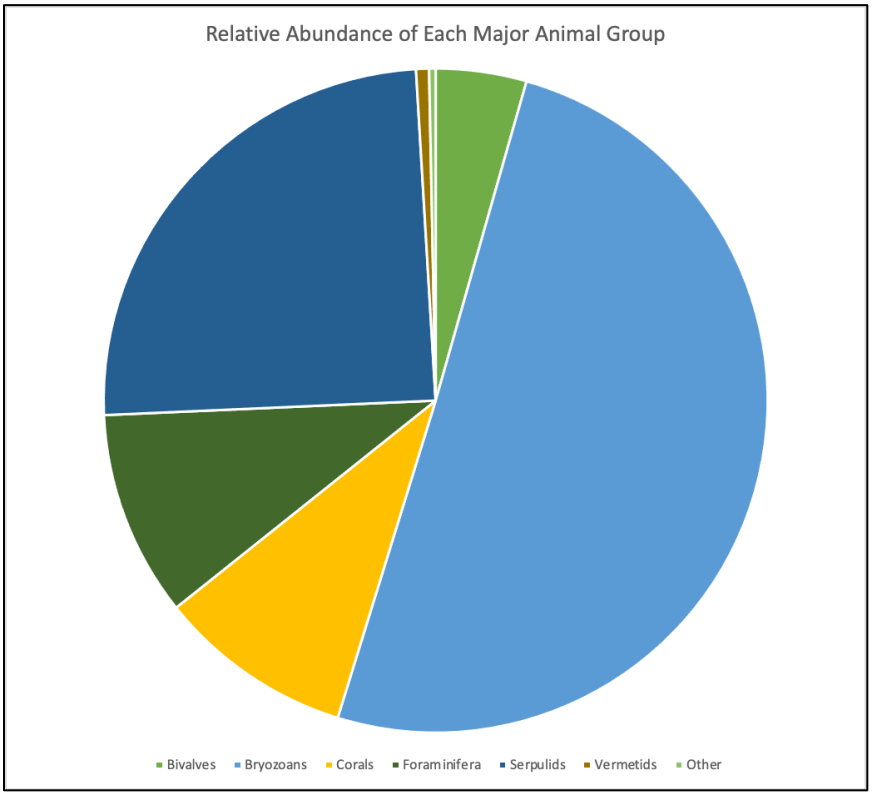

Figure 28 Pie chart showing the overall composition of studied individuals by major animal group (Author).

Total Individuals by Species	
Bi-A	180
Bi-B	2
Br-A	546
Br-B	55
Br-C	63
Br-D	24
Br-E	7
Br-F	171
Br-G	74
Br-H	160
Br-I	57
Br-J	27
Br-K	21
Br-L	539
Br-M	178
Br-N	89
Br-O	64
Co-A	392
Fe-A	413
Se-A	47
Se-B	403
Se-C	35
Se-D	46
Se-E	50
Se-F	104
Se-G	331
Se-H	4
Ve-A	26
Other	13
Total	4121

Figure 29 Number of individuals identified belonging to each species (Author).

5.2 How the Organisms are Distributed Across the Artifacts

5.2.1 Total Sampled Organisms by Artifact

Of the 4,121 individual organisms that were identified, the vast majority were from artifacts A18 and A24. They make up the bulk of the data with 1,846 and 1,457 individuals respectively. In comparison, 542 individuals are associated with amphora A06 and 276 individuals with A40. This disparity is the result of different sampling methods. In the case of A18 and A24, an overlapping grid system was used to ensure that all external organisms were mapped. For A06 and A40, test squares were placed strategically around the artifacts. The emphasis here was to collect data from each visually distinct phase of growth without having to map the entire object. This was done in order to evaluate the effectiveness of an alternative method that required significantly less time and labour.

Trends appear when looking at the counts of unique organisms divided by artifact. For the two amphorae that were mapped in their entirety, the top six organisms (in terms of number of individuals) are: Br-A, Br-L, Co-A, Fe-A, Se-B, and Se-G. Although not appearing in the same order (e.g.; A18 has more Br-A than Br-L while A24 has more Br-L than Br-A), the species making up the top six are the same for both. Amphora A06, which was only sampled strategically, yielded similar results. The top six organisms for A06 are the same ones as A18 and A24. This works to validate the effectiveness of the strategic sampling method in that it produces results that are comparable to the results obtained from full mapping. These results are visualized in fig. 30. They show that A06 fits the same overall species profile as A18 and A24.

The case is different for A40. The top six organisms (by number of individuals) are different than those of A18, A24, and A40. While having Fe-A, Br-L, and Se-G in the top six is consistent with the other amphorae, having Br-I, Ve-A, and Br-H is not. Especially in the observed quantities. More Br-I and Ve-A were found in the five test squares of A40 than the nine test squares of A06, the thirty-nine test squares of A18, or the thirty-nine test squares of A24. The biological landscape of A40 is also heavily dominated (in terms of the number of

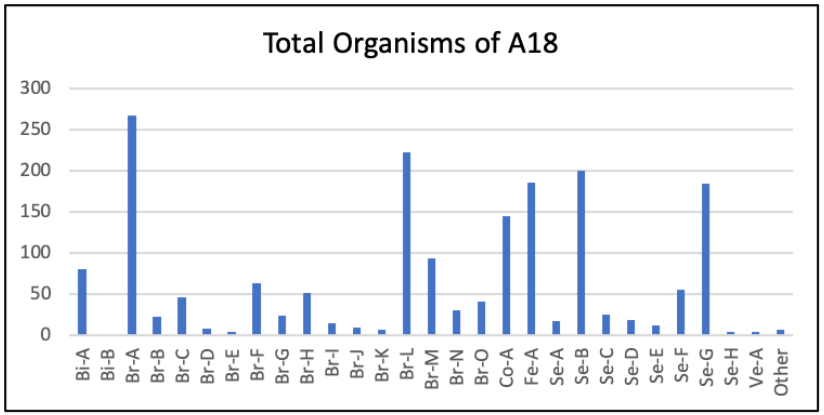

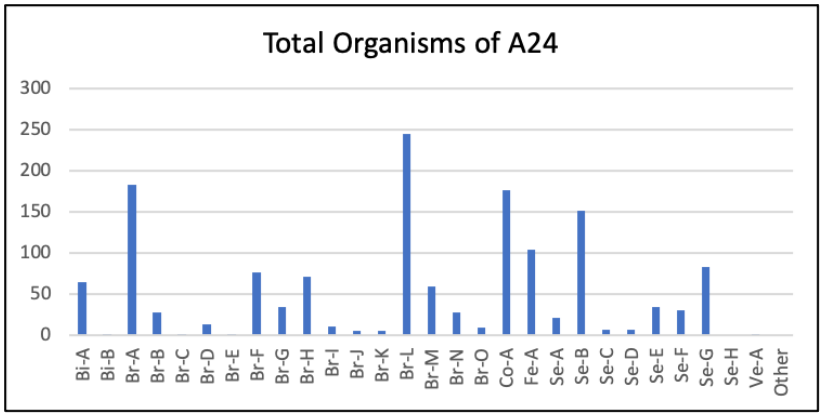

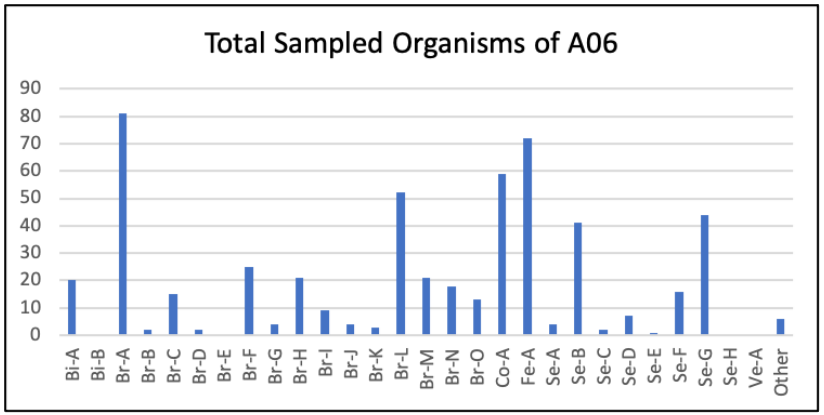

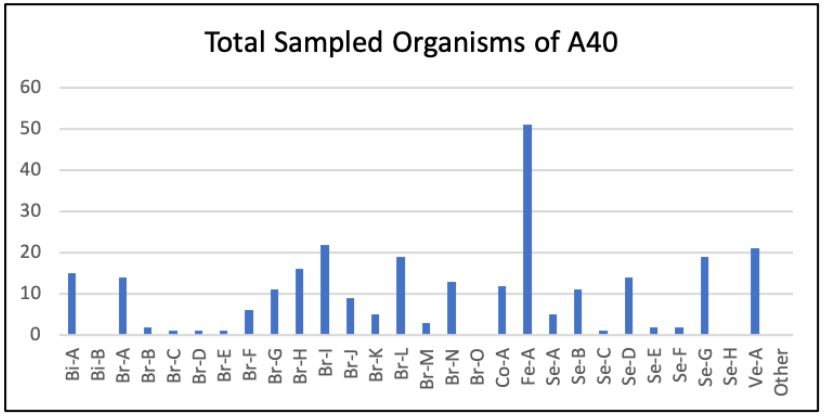

Figure 30 Total number of individuals identified from each unique species per amphora. (Author)

individuals) by Fe-A. There is over twice the amount of Fe-A than the next most populous species (Br-I). This is unique for the artifacts included in this research and shows that A40 is not biologically consistent with the other objects.

5.2.2 Organisms of Each Artifact Separated into Growth Phases

The organisms associated with each artifact can be further sub-divided into distinct growth phases. These are visually distinct shifts in the appearance, composition, colour, and/or organization of organisms encrusted to the artifacts. The contrast between two phases is often sharp but can also, at times, be blended together and less obvious. This is most likely the difference between sudden and gradual changes in the sedimentation of the site. In the following sections, the growth phases identified on amphorae A18, A24, A06, and A40 will be outlined and characterized. Results will show the variation in the biological composition of these different phases.

5.2.3 The Distinct Growth Phases of A18

Five different growth phases were identified on amphora A18. They were designated “A” (almost entirely covered by coralline algae and white in appearance), “B” (a thin phase distinguished by its colour), “C” (uniformly dense with overlapping organisms), “D” (sparser distribution of organisms and prominent bivalves), and “X” (mostly void of organisms and some signs of abrasion). The composition of each of these phases was investigated in order to quantify the differences between these visually distinct phases. The results of this are visually summarized in fig. 31. They reveal that there are three main compositionally distinct phases. Phase “A” (composed of 1% bivalves, 25% bryozoans, 13% corals, 32% foraminifera, 30% serpulids), phase “C” (composed of 3% bivalves, 54% bryozoans, 7% corals, 7% foraminifera, 29% serpulids), and phase “D” (composed of 30% bivalves, 27% bryozoans, 3% corals, 4% foraminifera, 34% serpulids,

1% other). Both phases “B” and “X” are compositionally consistent with phase “C” despite being visually distinct and varying drastically in individual organism counts (i.e.; phase “X” numbers only 185 individuals compared to the 755 in phase “C” but both are essentially identical in terms of how the organisms present can be grouped).

Each of the thirty-nine test squares recorded in association with A18 were assigned to one of the five visually distinct growth phases. In cases where a test square spanned multiple growth phases, a new split category was created (e.g.: a test square that included both “A” and “B” would be designated “A/B”).

The data in fig. 32 shows the biological data for A18 organized by unique species and phase. The values are the total number of individuals associated with each phase divided by the number of corresponding test squares associated with that phase. Performing this transformation on the data facilitates the comparison of values across phases with unequal representation. Each column is then effectively a single representative test square that distills the data of many. The highest value for each unique species is highlighted in yellow (e.g.: phase “B” has the greatest amount of Br-D so that corresponding square is yellow). The top three highest values for each phase are highlighted in green (e.g.: the three greatest values in phase “A” are Co-A, Fe-A, and Se-G so they are green). And when a value meets the criteria for both yellow and green highlighting, it appears as yellow/green striped. This colour scheme serves as an interpretive aid and works to highlight trends in the data.

The values of fig. 32 that are in green mirror the data from fig. 30 in that they highlight the same species which dominate the overall composition of A18 (Br-A, Br-L, Co-A, Fe-A, Se-B, and Se-G). This new table works to show how these species are distributed across the different growth phases. It shows, for example, that Co-A, Fe-A, and Se-G dominate phase “A” while Br-A, Br-L, and Se-B instead dominate phase “C”. Values in yellow work to highlight concentrations of unique organisms other than those which dominate across the amphora. For example, Br-E represents a very small percentage of the total organisms and is only found in phase “A”. Highlighting these organisms can potentially shed light on shifts in the immediate environment of these artifacts. They can serve as key indicator species if found to have different habitat requirements than those in earlier phases.

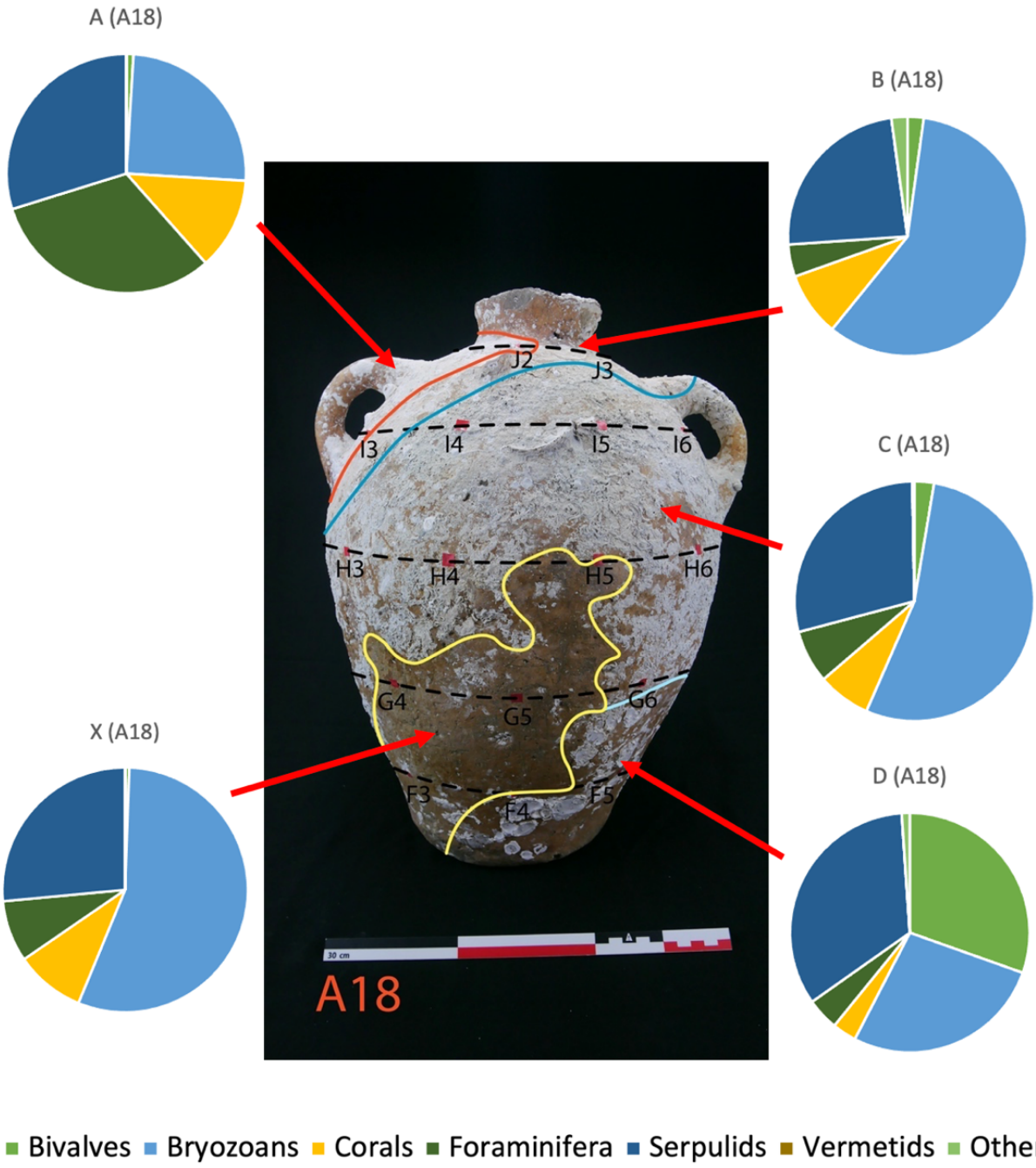

Figure 31 The composition (by major animal groups) for each identified growth phase on A18 (Author).

	Sum/# of Squares (A18)										
	D	C/D	C	B/C	B	A/B/C	A/B	A	D/X	X	C/X
Bi-A	9.33	6	2	2.5	1	0.5	0	0.25	3.5	0	0.83
Bi-B	0	0	0	0	0	0	0	0	0	0	0
Br-A	0	6	13.4	5	5	6.5	2.33	0.5	5	4.25	9.67
Br-B	0.33	0	0.5	0.5	5	0	0.67	0.75	0.5	0.75	0.33
Br-C	0.33	1	2	0.5	2	1	0	0	0	0.75	2.5
Br-D	0.67	0.5	0	0	1	0	0	0	0	0.5	0.33
Br-E	0	0	0	0	0	0	0.33	0.75	0	0	0
Br-F	0.33	1.5	2.3	3	2	2.5	2	1.5	0	0.25	1.83
Br-G	0.33	1.5	1.1	0	0	0.5	1.67	0	0	0	0.5
Br-H	0.33	1	2.2	1	4	0	2.67	1.25	0.5	0.5	0.83
Br-I	1.33	0	0.1	0	2	0.5	1.33	0.75	0	0	0
Br-J	0	2.5	0	0	0	0.5	0.67	0	0	0	0.17
Br-K	0	0	0.4	0	0	1	0	0	0	0	0.17
Br-L	3.33	9.5	9.2	3.5	5	4	0.67	0.75	3.5	4.5	8.67
Br-M	0.67	3	5.3	0	1	2.5	0.33	0	1	1.5	3
Br-N	0.33	1	1.6	0	0	2	0.67	0.25	0.5	0.25	0.33
Br-O	0.33	2	2.6	0.5	0	0	0	0	0	0	1.5
Co-A	1	3.5	5.4	3.5	4	5.5	6.33	3.25	0	1.5	3.5
Fe-A	1.33	5.5	5.4	2.5	2	6.5	10.67	8.25	1	1	4.33
Se-A	0	0.5	0.5	0.5	2	1	0	1.25	0	0	0.17
Se-B	4.33	7.5	9.6	1	3	4	2	1.5	2	3	5.83
Se-C	2	1.5	0.7	0	0	0	0	0	1.5	0	1
Se-D	0	0	0.1	1	0	1.5	1.67	1.5	0	0	0.17
Se-E	0.33	0.5	0.4	0.5	0	0	0.33	0.75	0	0	0.17
Se-F	0.33	1	3.3	0	0	0	0	0	1.5	0.5	2.33
Se-G	3.33	9.5	7.1	3.5	4	4	5	2.75	0.5	2.25	5
Se-H	0	0	0.1	0.5	2	0	0	0	0	0	0
Ve-A	0	0	0	0	0	0	1.33	0	0	0	0
Other	0.33	0	0.2	0.5	1	0	0	0	0	0.5	0

Figure 32 Biological composition of squares from each growth phase (A18). Highlighting the most abundant species of each square (green) and the phase with the highest count of each species (yellow) (Author).

	Largest Bryozoans of Each Phase (A18)										
	D	C/D	C	B/C	B	A/B/C	A/B	A	D/X	X	C/X
Br-A	0	13.75	10.5	3.25	3.5	6	1.25	0.5	1	8	6
Br-B	0.25	0	1	0.25	4	0	0.5	1	0.375	1.5	0.0625
Br-C	0.1875	1.125	1	0.75	1.5	0.3125	0	0	0	1.125	2.5
Br-D	0.25	0.5	0	0	0.125	0	0	0	0	0.25	0.125
Br-E	0	0	0	0	0	0	0.375	27	0	0	0
Br-F	0.25	0.25	2.5	0.75	0.25	1.125	0.375	0.75	0	0.375	0.75
Br-G	1	0.5	2.625	0	0	0.25	2.8125	0	0	0	0.5
Br-H	0.125	0.25	6.25	0.5	1.5	0	1	5.6875	0.25	0.25	2.5
Br-I	0.25	0	1	0	1.25	0.0625	0.375	0.25	0	0	0
Br-J	0	0.25	0	0	0	0.0625	0.25	0	0	0	0.25
Br-K	0	0	2.25	0	0	0.75	0	0	0	0	0.0625
Br-L	1.5	2	7.5	0.375	0.125	1.125	0.125	0.0625	0.625	0.875	3
Br-M	1.5	1.25	5.5	0	0.0625	2	0.0625	0	0.25	1	3.75
Br-N	0.25	0.25	0.25	0	0	0.375	0.25	0.0625	0.25	0.25	0.25
Br-O	0.25	0.25	3	0.0625	0	0	0	0	0	0	0.5

Figure 33 Values (in cm^2) for the size of bryozoans across all identified growth phases (A18) (Author).

Another indicator that can be used to better understand biological processes is variability in organism size. For each test square, the dimensions of the largest individuals belonging to each unique species were recorded and a value for their area (cm^2) was calculated. Several species exhibited very little variation in size (notably corals, foraminifera, and most serpulids). Bryozoans, on the other hand, exhibited a significant degree of variability. Seeing as they also represent the majority of the biomass associated with the artifacts, their results are taken as the most informative. The sizes of the largest bryozoans in each growth phase of A18 can be found in fig. 33. The results show that phase "C" and those linked with it (i.e.: phase "C/D" and "C/X") represent the largest individuals for 10 of the 15 unique bryozoan species. On the contrary, phase "A" only hosts one of the largest unique bryozoan species (Br-E). Interestingly though, this individual covers roughly $27cm^2$ and is by far the biggest bryozoan recorded in association with A18.

5.2.4 The Distinct Growth Phases of A24

Six different growth phases were identified on amphora A24. They were designated "A" (almost entirely covered by coralline algae and white in appearance), "B" (dense vertical growth of organisms but covered and obscured by encrusting coralline algae), "B2" (follows the same contour as "B" but appears distinct and is not covered by encrusting coralline algae), "C" (uniformly dense with overlapping organisms), "D" (sparser distribution of organisms and prominent bivalves), and "X" (mostly void of organisms and some signs of abrasion). The composition of each of these phases was investigated in order to quantify the differences between these visually distinct phases. The results of this are visually summarized in fig. 34. They reveal that there are four main compositionally distinct phases. Phase "A" (composed of 33% bivalves, 17% bryozoans, 33% corals, 17% serpulids), phase "B" (composed of 29% bryozoans, 24% corals, 37% foraminifera, 11% serpulids), phase "C" (composed of 2% bivalves, 57% bryozoans, 8% corals, 8% foraminifera, 25% serpulids), and phase "D" (composed of 17% bivalves, 53% bryozoans, 19% corals, 12% serpulids). Phase "C/X" is almost compositionally identical to

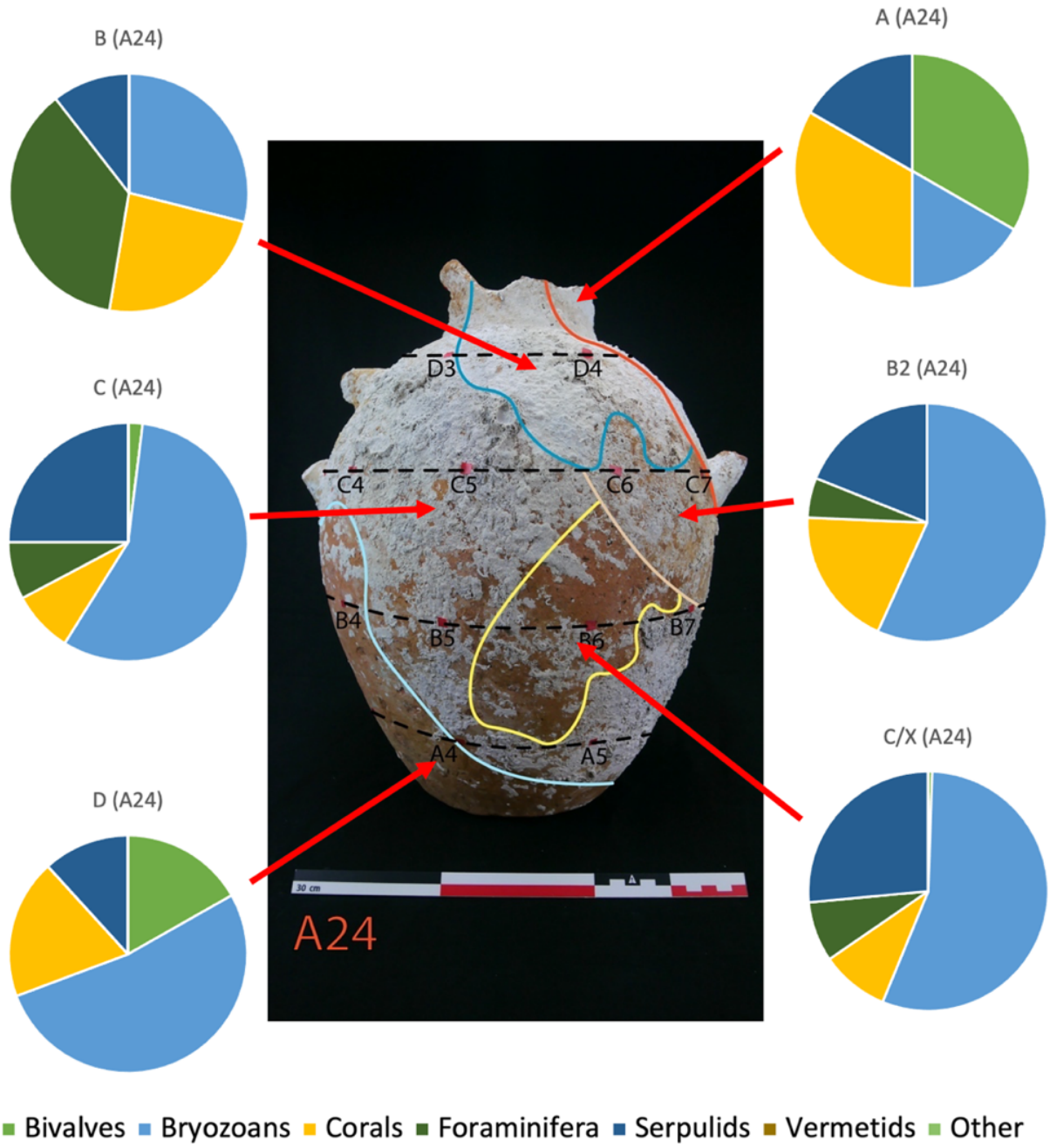

Figure 34 The composition (by major animal groups) for each identified growth phase on A24 (Author).

	Sum/# of Squares (A24)								
	D	C/D	C	B/C	B2	B	A/B	A	C/X
Bi-A	3	2.44	1.17	0.67	0	0	0.33	2	0.25
Bi-B	0	0.22	0	0	0	0	0	0	0
Br-A	0.7	7.22	8.33	6.33	7	2	1	0	7
Br-B	0.2	1.11	1.33	1	1	0	0.33	0	0.75
Br-C	0	0.11	0	0	0	0	0	0	0
Br-D	0.2	0.56	0.5	0	3	0	0	0	0
Br-E	0	0.11	0	0	1	0	0	0	0
Br-F	0.8	2.56	3.17	1.33	3	1.5	1	1	3
Br-G	1.7	0.22	1.83	0.33	0	0	0	0	1
Br-H	2.9	2.67	1.5	1	0	0	0.33	0	1.25
Br-I	0.5	0.33	0.17	0	0	0	0	0	0.5
Br-J	0.3	0	0.17	0.33	0	0	0	0	0
Br-K	0.1	0	0	1	0	0	0.67	0	0
Br-L	2	9.78	10.67	8.67	5	1	1.67	0	8.75
Br-M	0	1.89	3.83	2	1	0.5	0.33	0	2.75
Br-N	0	1.22	1.17	2	0	0.5	0	0	0.75
Br-O	0	0	1.5	0.33	0	0	0	0	0
Co-A	3.4	5.33	5	3	7	4.5	6.67	2	4.25
Fe-A	0	2.22	4.67	6.33	2	7	2	1	3.75
Se-A	0	1	0.5	0	3	2	0	0	0.5
Se-B	0.9	6.89	7.33	4	0	0	0.33	0	5.75
Se-C	0	0.56	0	0.33	0	0	0	0	0.25
Se-D	0.2	0.22	0.33	0	0	0	0.33	0	0
Se-E	0.9	2.33	0.5	0	0	0	0.67	0	0
Se-F	0.1	1.33	1.83	2	0	0	0	0	0.25
Se-G	0	2.11	4.5	3.33	4	0	0	1	5.5
Se-H	0	0	0	0	0	0	0	0	0
Ve-A	0	0.11	0	0	0	0	0	0	0
Other	0	0	0	0	0	0	0	0	0

Figure 35 Biological composition of squares from each growth phase (A24). Highlighting the most abundant species of each square (green) and the phase with the highest count of each species (yellow) (Author).

	Largest Bryozoans of Each Phase (A24)								
	D	C/D	C	B/C	B2	B	A/B	A	C/X
Br-A	2	8	14	10.5	1	0.25	2.25	0	24.5
Br-B	0.875	4.5	4.5	3	0.375	0	3.0625	0	2.625
Br-C	0	1.25	0	0	0	0	0	0	0
Br-D	2.25	1.5	0.75	0	0.25	0	0	0	0
Br-E	0	0.75	0	0	0.875	0	0	0	0
Br-F	0.75	6.125	1.5	0.75	2.625	0.25	0.375	0.75	1
Br-G	1.5	0.25	11	0.25	0	0	0	0	1.5
Br-H	12	3	12	0.375	0	0	0.25	0	0.75
Br-I	0.5	0.75	0.25	0	0	0	0	0	0.25
Br-J	0.25	0	0.25	0.25	0	0	0	0	0
Br-K	5	0	0	0.25	0	0	0.75	0	0
Br-L	3	12	9	0.25	0.75	0.375	1	0	5.25
Br-M	0	6	4.125	3.5	1.125	0.375	0.375	0	1.5
Br-N	0	0.25	0.375	1	0	0.25	0	0	0.25
Br-O	0	0	0.376	1.25	0	0	0	0	0

Figure 36 Values (in cm^2) for the size of bryozoans across all identified growth phases (A24) (Author).

phase “C” despite being visually distinct and comprising a lower density of organisms. Similarly, phase “B2” is consistent with phase “C” but also exhibits a transition towards phase “B” through an increased percentage of corals and a reduced percentage of serpulids.

Each of the thirty-nine test squares recorded in association with A24 were assigned to one of these six visually distinct phases. In cases where a test square spanned multiple growth phases, a new split category was created (e.g.: a test square that included both “A” and “B” would be designated “A/B”).

As with A18, fig. 35 shows the breakdown of unique species by phase and highlights the pervasiveness of Br-A, Br-L, Co-A, Fe-A, Se-B, and Se-G. Trends similar and different to A18 can be observed. Phase “C” for both A18 and A24 exhibit some of the highest numbers for Br-A, Br-L, and Se-B. Similarly, the data for both A18 and A24 shows how the composition of phase “A” is dominated by Co-A, Fe-A, and Se-G. Data for the two amphorae begins to diverge when looking at phase “D”. Both can be characterized by Bi-A but are otherwise compositionally different. Br-H and Co-A play an important role in the composition of “D” for A24 while it is instead Se-B and Se-G for amphora A18.

The sizes of the largest bryozoans in each growth phase of A24 can be found in fig. 36. The table highlights how almost all of the largest individuals for each unique species can be found in the lower phases. These are primarily phases “D” and “C” as well as those linked to them like “C/D”, “B/C”, and “C/X”. All the bryozoans identified in phases “A”, “A/B”, and “B” were significantly smaller than their counterparts in these lower phases. This distinction is clear in the data and marks a shift in conditions that were favourable to bryozoan growth to conditions that were not.

5.2.5 The Distinct Growth Phases of A06

Seven different growth phases were identified on amphora A06. They were designated “A” (almost entirely covered by coralline algae and white in appearance), “B” (a thin phase distinguished by its colour), “C” (uniformly dense with overlapping organisms and partially

covered by encrusting coralline algae), “C2” (uniformly dense with overlapping organisms), “C3” (occupying a similar contour as C but notably sparse by comparison), “D” (very sparse with almost no organisms), and “X” (mostly void of organisms and some signs of abrasion). The composition of each of these phases was investigated in order to quantify the differences between these visually distinct phases. The results of this are visually summarized in fig. 37. They reveal that there are three main compositionally distinct phases. Phase “A” (composed of 9% bivalves, 7% bryozoans, 11% corals, 49% foraminifera, 16% serpulids, 9% other), phase “C” (composed of 6% bivalves, 33% bryozoans, 18% corals, 23% foraminifera, 20% serpulids), and phase “C2” (composed of 2% bivalves, 63% bryozoans, 7% corals, 6% foraminifera, 22% serpulids). Phases “B” and “X” represent a small percentage of the amphora’s surface area and could not be entirely isolated by a test square. Phases “C3” and “D” are compositionally consistent with phase “C2” despite being visually distinct and comprising a lower density of organisms.

Each of the nine test squares recorded in association with A06 were assigned to one of these seven visually distinct phases. In cases where a test square spanned multiple growth phases, a new split category was created (e.g.: a test square that included both “A” and “B” would be designated “A/B”).

As with A18 and A24, fig. 38 shows the breakdown of unique species by phase and highlights the pervasiveness of Br-A, Br-L, Co-A, Fe-A, Se-B, and Se-G. The highest counts of individuals again mostly appear in the “C” phases and phase “A” is similarly characterized by Co-A and Fe-A. The biggest difference between A06 and the others is how Bi-A is distributed across the artifact. For A18 and A24, the highest counts for Bi-A were both in phase “D”. In the case of A06, there were no Bi-A recorded in phase “D” at all and the highest counts were instead clustered around phases “A”, “A/B”, and “C”.

The sizes of the largest bryozoans in each growth phase of A06 can be found in fig. 39. The table highlights again that the “C” phases house the vast majority of the largest bryozoans found on the artifact. The distinction between upper and lower phases, however, is not as clear cut as with A24. In this case, phases “A” and “A/B” contain the largest individuals for four different unique species. Particularly noteworthy is the largest individual of the Br-A species. It covers roughly 10cm^2, is located in “A/B”, and is the largest bryozoan recorded of any test square.

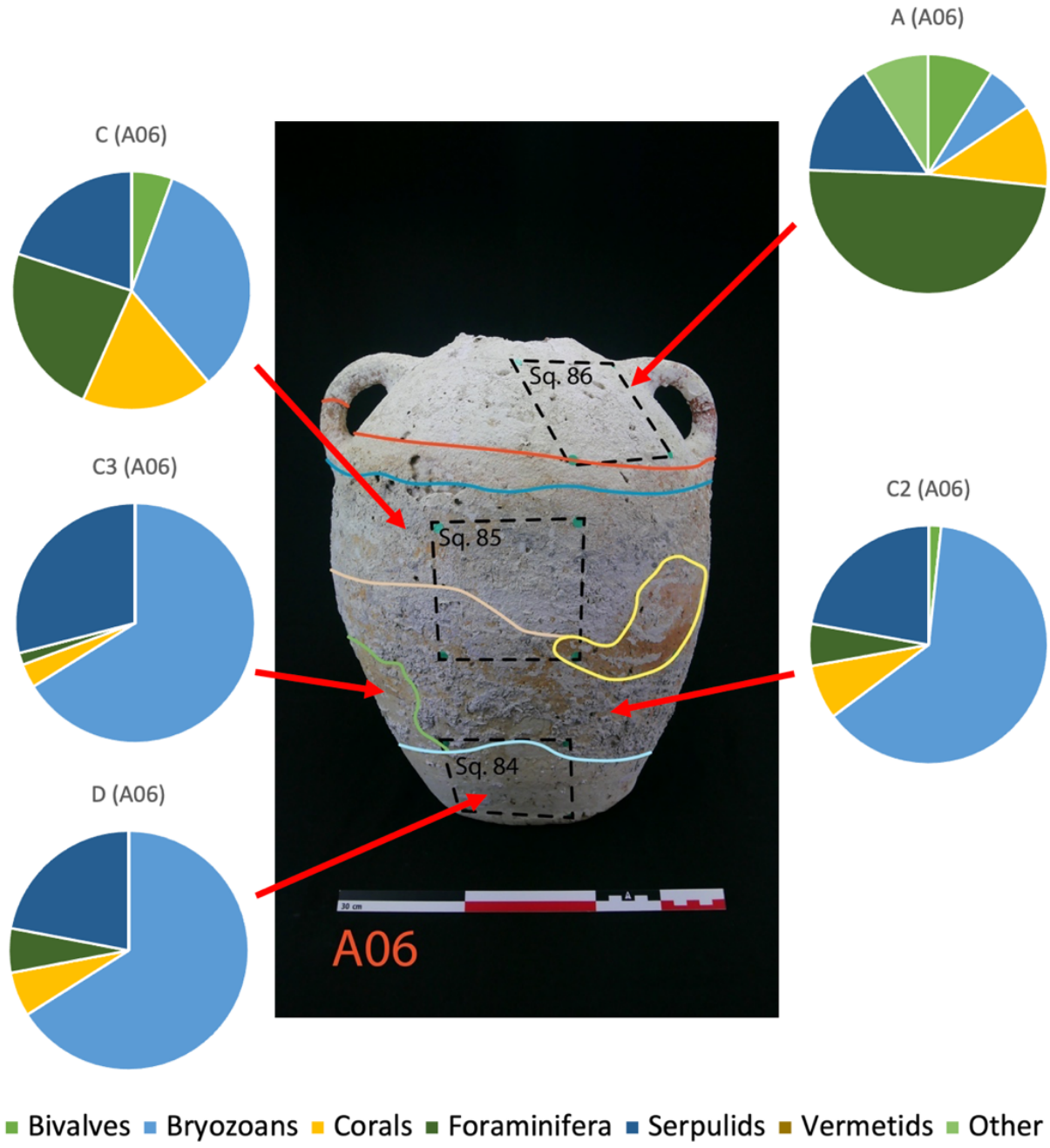

Figure 37 The composition (by major animal groups) for each identified growth phase on A06 (Author).

	Sum/# of Squares (A06)						
	D	C3	C2	C/C2	C	A/B	A
Bi-A	0	0	1.5	3	5	5	4
Bi-B	0	0	0	0	0	0	0
Br-A	4	13	18	12	7	5	0
Br-B	0	0	0	0	0	2	0
Br-C	0.5	3	2.5	4	2	0	0
Br-D	0	0	0.5	1	0	0	0
Br-E	0	0	0	0	0	0	0
Br-F	1.5	3	6	4	2	1	0
Br-G	0	0	1	1	1	0	0
Br-H	4	4	2.5	3	1	0	0
Br-I	0.5	2	1.5	0	2	1	0
Br-J	0	0	0.5	1	2	0	0
Br-K	0	1	1	0	0	0	0
Br-L	4	4	8	14	10	0	0
Br-M	1	3	6	1	1	1	1
Br-N	1	1	5	1	2	0	2
Br-O	0	7	3	0	0	0	0
Co-A	1.5	2	6.5	7	16	13	5
Fe-A	1.5	1	5	7	21	8	22
Se-A	0.5	2	0	1	0	0	0
Se-B	1.5	7	9.5	4	6	2	0
Se-C	0	0	1	0	0	0	0
Se-D	0	0	0	0	1	2	4
Se-E	0	0	0	0	1	0	0
Se-F	0.5	5	2.5	2	3	0	0
Se-G	3	4	6.5	11	7	0	3
Se-H	0	0	0	0	0	0	0
Ve-A	0	0	0	0	0	0	0
Other	0	0	0	0	0	2	4

Figure 38 Biological composition of squares from each growth phase (A06). Highlighting the most abundant species of each square (green) and the phase with the highest count of each species (yellow) (Author).

	Largest Bryozoans of Each Phase (A06)						
	D	C3	C2	C/C2	C	A/B	A
Br-A	5.25	4.125	9	6	0.125	10	0
Br-B	0	0	0	0	0	0.875	0
Br-C	0.125	0.75	0.5	0.625	0.125	0	0
Br-D	0	0	0.125	0.25	0	0	0
Br-E	0	0	0	0	0	0	0
Br-F	0.375	0.25	0.375	0.375	0.5	0.0625	0
Br-G	0	0	0.125	0.25	0.0625	0	0
Br-H	1.3125	1.5	1.5	0.25	4	0	0
Br-I	0.125	0.25	0.25	0	0.125	0.25	0
Br-J	0	0	0.0625	0.25	0.0625	0	0
Br-K	0	0.0625	0.125	0	0	0	0
Br-L	1	0.625	2	2.5	0.75	0	0
Br-M	0.125	0.375	6	0.0625	0.0625	0.125	0.0625
Br-N	0.0625	0.0625	0.125	0.0625	0.125	0	0.5625
Br-O	0	0.75	0.75	0	0	0	0

Figure 39 Values (in cm^2) for the size of bryozoans across all identified growth phases (A06) (Author).

5.2.6 The Distinct Growth Phases of A40

Three different growth phases were identified on amphora A40. They were designated “A” (almost entirely covered by coralline algae and white in appearance), “B” (a thin phase distinguished by its colour), and “C” (uniformly dense with overlapping organisms). The composition of each of these phases was investigated in order to quantify the differences between these visually distinct phases. The results of this are visually summarized in fig. 40. They reveal that there are two main compositionally distinct phases. Phase “A” (composed of 8% bivalves, 33% bryozoans, 4% corals, 24% foraminifera, 18% serpulids, 13% vermetids) and phase “C” (composed of 64% bryozoans, 9% foraminifera, 27% serpulids). Phase “B” represents a small percentage of the amphora’s surface area and could not be entirely isolated by a test square.

Each of the five test squares recorded in association with A40 were assigned to one of these three visually distinct phases. In cases where a test square spanned multiple growth phases, a new split category was created (e.g.: a test square that included both “B” and “C” would be designated “B/C”). Since “B” was a very thin band, no test square was solely within phase “B” for A40.

The overall composition of A40 is different than the other three amphorae. This can be seen in fig. 40 and is broken down by unique species and growth phase in fig. 41. Unlike the other amphorae, the unique species with the highest overall count (by a significant margin) is Fe-A. This species is most abundant in phase “A” but also appears in relatively high numbers in phases “B/C” and “C”. Amphora A40 also differs from the others in that it has higher rates of Br-H, Br-I, and Ve-A. Both Br-H and Ve-A are more prominent in the composition of phase “A” while Br-I is instead more prominent in phase “C”. This amphora also represents an interesting case because there are multiple unique species which only appear in one phase. Unique to phase “A” is Br-E, Se-D, Se-E, and Ve-A. Unique to phase “B/C” is Br-K, Se-C, and essentially Br-N. Unique to phase “C” is Br-C, Br-D, and Se-F.

The sizes of the largest bryozoans in each growth phase of A06 can be found in fig. 42. The table shows that A06 is consistent with the other artifacts in that phase “C” houses the majority of the largest bryozoans. Phase “A” for this artifact differs from other amphorae in that it

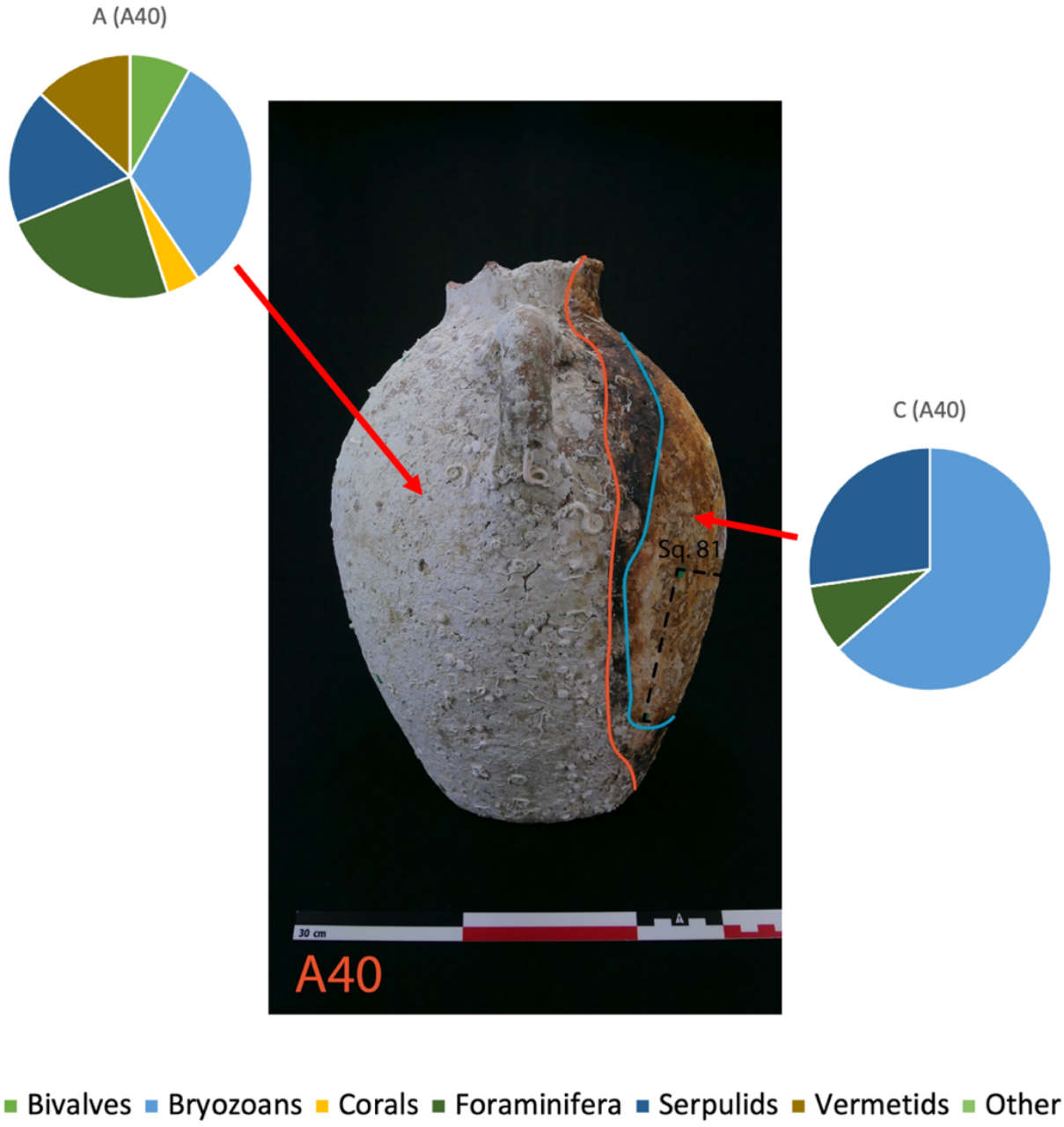

Figure 40 The composition (by major animal groups) for each identified growth phase on A40 (Author).

	Sum/# of Squares (A40)		
	C	B/C	A
Bi-A	0	2	4.33
Bi-B	0	0	0
Br-A	8	4	0.67
Br-B	1	0	0.33
Br-C	1	0	0
Br-D	1	0	0
Br-E	0	0	0.33
Br-F	3	1	0.67
Br-G	4	2	1.67
Br-H	2	1	4.33
Br-I	8	2	4
Br-J	1	0	2.67
Br-K	0	5	0
Br-L	11	0	2.67
Br-M	1	2	0
Br-N	1	12	0
Br-O	0	0	0
Co-A	0	5	2.3
Fe-A	6	7	12.67
Se-A	1	1	1
Se-B	8	2	0.33
Se-C	0	1	0
Se-D	0	0	4.67
Se-E	0	0	0.67
Se-F	2	0	0
Se-G	7	3	3
Se-H	0	0	0
Ve-A	0	0	7
Other	0	0	0

Figure 41 Biological composition of squares from each growth phase (A40). Highlighting the most abundant species of each square (green) and the phase with the highest count of each species (yellow) (Author).

	Largest Bryozoans of Each Phase (A40)		
	C	B/C	A
Br-A	4	0.125	3.125
Br-B	0.25	0	0.1875
Br-C	0.5	0	0
Br-D	1.5	0	0
Br-E	0	0	8.25
Br-F	1.125	0.25	0.75
Br-G	1.5	0.125	0.75
Br-H	1.875	1.5625	6
Br-I	0.25	0.0625	1
Br-J	0.0625	0	0.375
Br-K	0	0.0625	0
Br-L	6.375	0	0.125
Br-M	3	0.25	0
Br-N	0.125	0.0625	0
Br-O	0	0	0

Figure 42 Values (in cm^2) for the size of bryozoans across all identified growth phases (A40) (Author).

comprises the largest examples of four unique species. This is compared to only one for A06, one for A18, and zero for A24. Just as was the case for A18, Br-E was only found in phase “A” and is the largest recorded bryozoan on the artifact.

In addition to its different biological signature, A40 is also differentiated from the other artifacts by the organization of its growth phases. The visually distinct phases separate the amphora vertically as opposed to horizontally. This is indicative of different post-depositional processes and compounds the artifact’s status as an anomaly.

5.3 How the Artifacts and Organisms are Distributed Across the Site

5.3.1 Comparing Biological Data Across Artifacts

Two non-metric multidimensional scaling (NMDS) plots integrate the biological data collected from each amphora. Each point corresponds to a different test square and its proximity to others is an indication of greater biological similarity. In the first plot (fig. 43), the test squares are grouped by amphora. The amphora A18 displays the greatest internal variation and the majority of the other test squares can be situated within its bounds. Amphorae A06 and A40, however, only occupy a fraction of these bounds. In this way, they do not exhibit as much internal variation and can only be associated with certain squares from A18 and A24. In general, there is enough overlap between all the different amphorae to indicate a level of cohesiveness among the samples. No one artifact is entirely dissimilar from the others.

The second NMDS plot (fig. 44) organizes the same test squares by phase instead of by amphora. In this visualization, there is significantly less overlap between groups. Phases “A” and “D” are distinct but internally varied. This shows that they can be distinguished from other phases even though their compositions are diverse. Phase “C” shows a much tighter grouping indicative of less internal variation and a higher degree of similarity between artifacts. Phase “B” is less

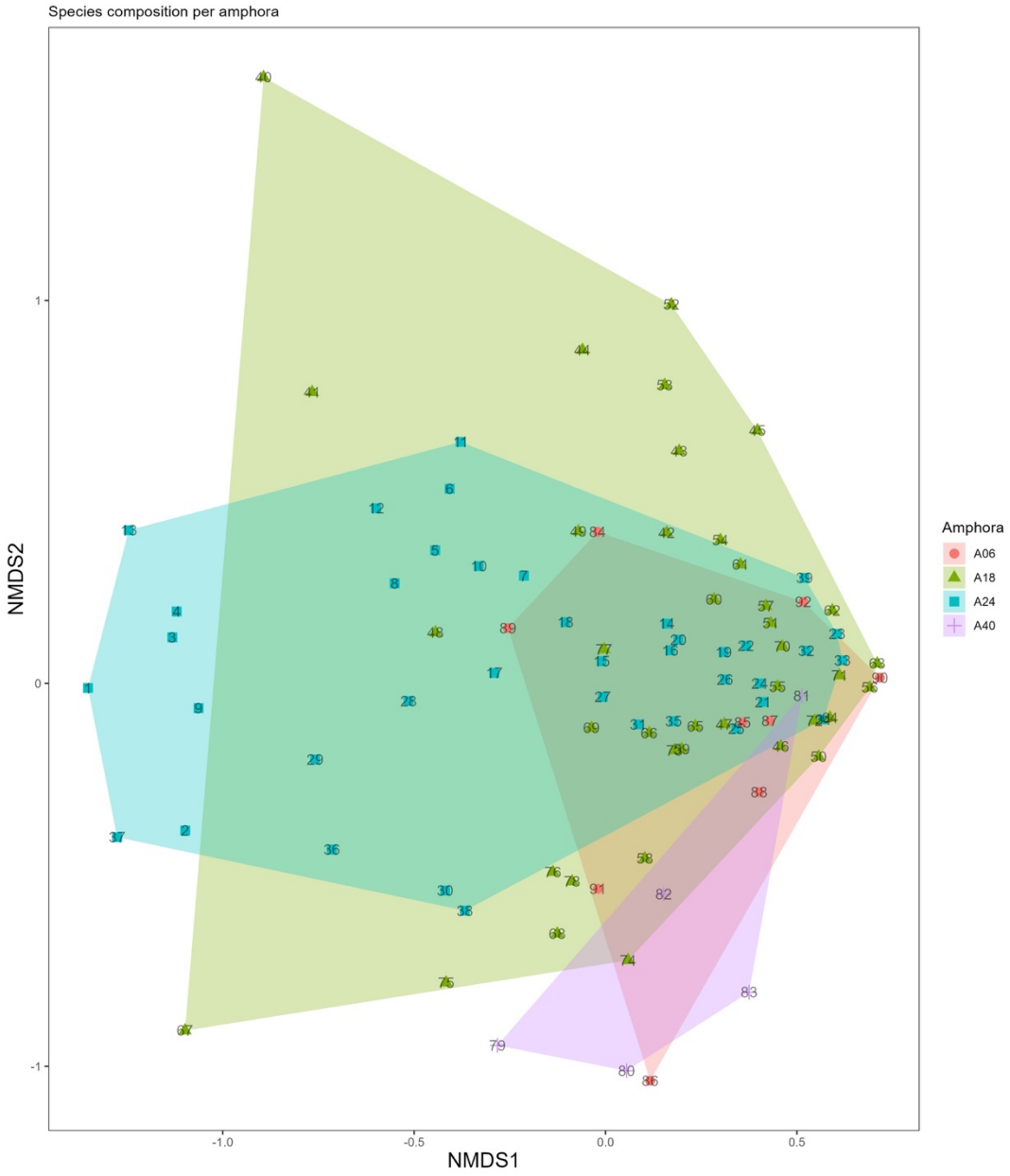

Figure 43 Sample squares grouped by amphora (E. Motivans and author).

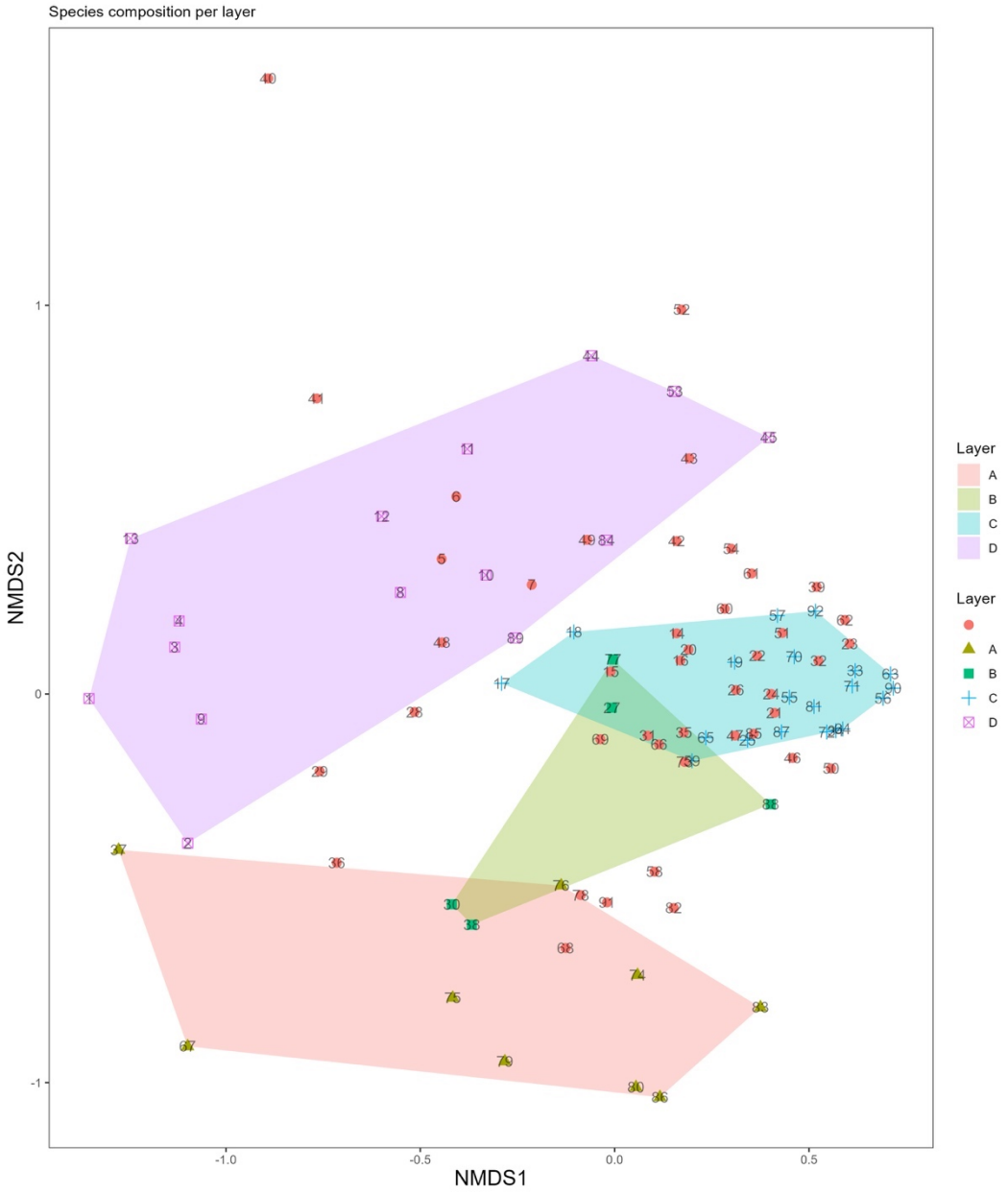

Figure 44 Sample squares grouped by growth phase (E. Motivans and author).

unique. The squares associated with phase “B” show a greater similarity to phases “A” or “C” than they do to their own distinct grouping.

These two NMDS plots contextualize the biological data and show how test squares from various artifacts recovered from around the site relate to each other. Importantly, they show that similar compositions can be observed in the various locations around the site and that the visually distinct phases identified on each amphora form their own clusters (with the exception of phase “B”). For the NMDS where sample squares are grouped by phase, only samples that represented a single phase were grouped. Samples that appear ungrouped are the ones that represent multiple phases (e.g.: “B/C” or “C/D”).

5.3.2 Biological Data Integrated into a 3D Model of the Site

The location, orientation, and relation of the artifacts to each other and the site plays a major role in interpreting the biological data. This spatial context was established through the use of photogrammetric models and 3D artifact renderings. The results of which can be seen in fig. 45 and 46. Since the artifacts A18, A24, A06, and A40 were 3D scanned while the test square stickers were still in place, the precise location of each test square is accurately linked to its real and original position at the site. This also means that the organisms mapped on the different artifacts can be used to understand not only the individual artifacts themselves, but how they relate to each other and the site as a whole.

5.3.3 A18 in Context

The biological growth of A18 is contextualized by the artifact’s integration into the 3D model. When viewed in the position it was recovered from, the visually distinct growth phases appear horizontal rather than diagonal (fig. 47). This indicates consistency in relation to the horizontal plane of the seabed. Although it was resting at an angle that could suggest post-

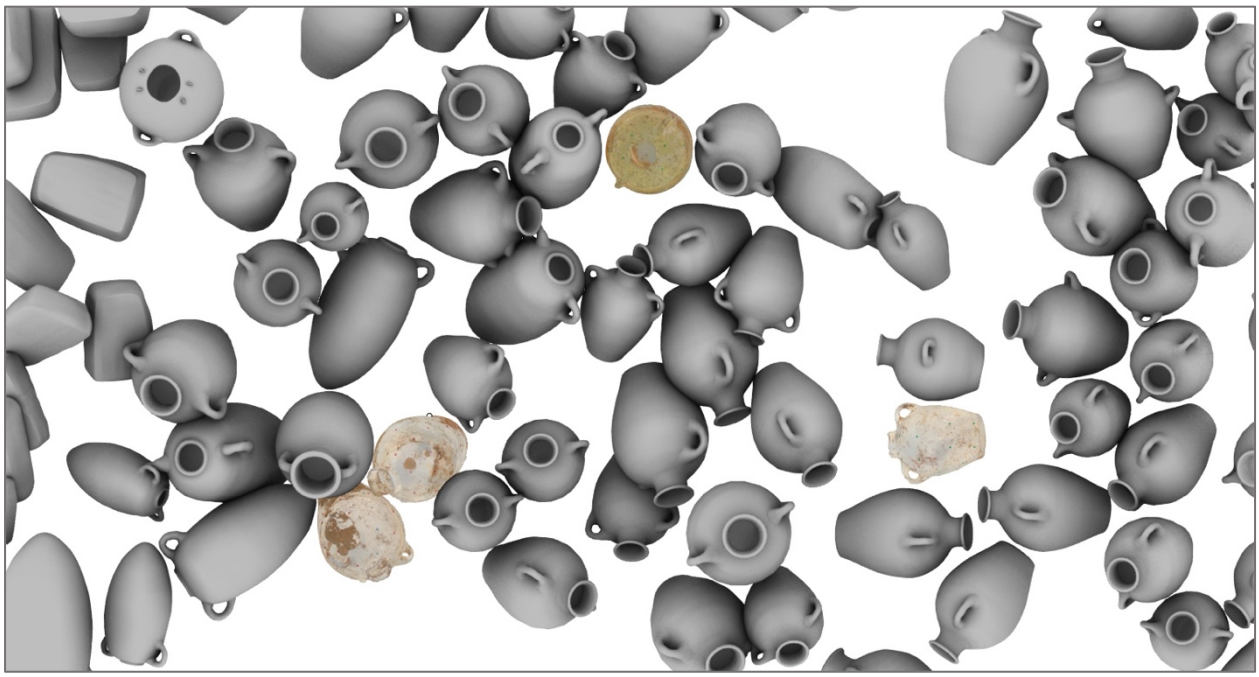

Figure 45 Scanned amphorae integrated into the composite 3D model. Seen from above (A. Bravo-Morata Rodríguez and author).

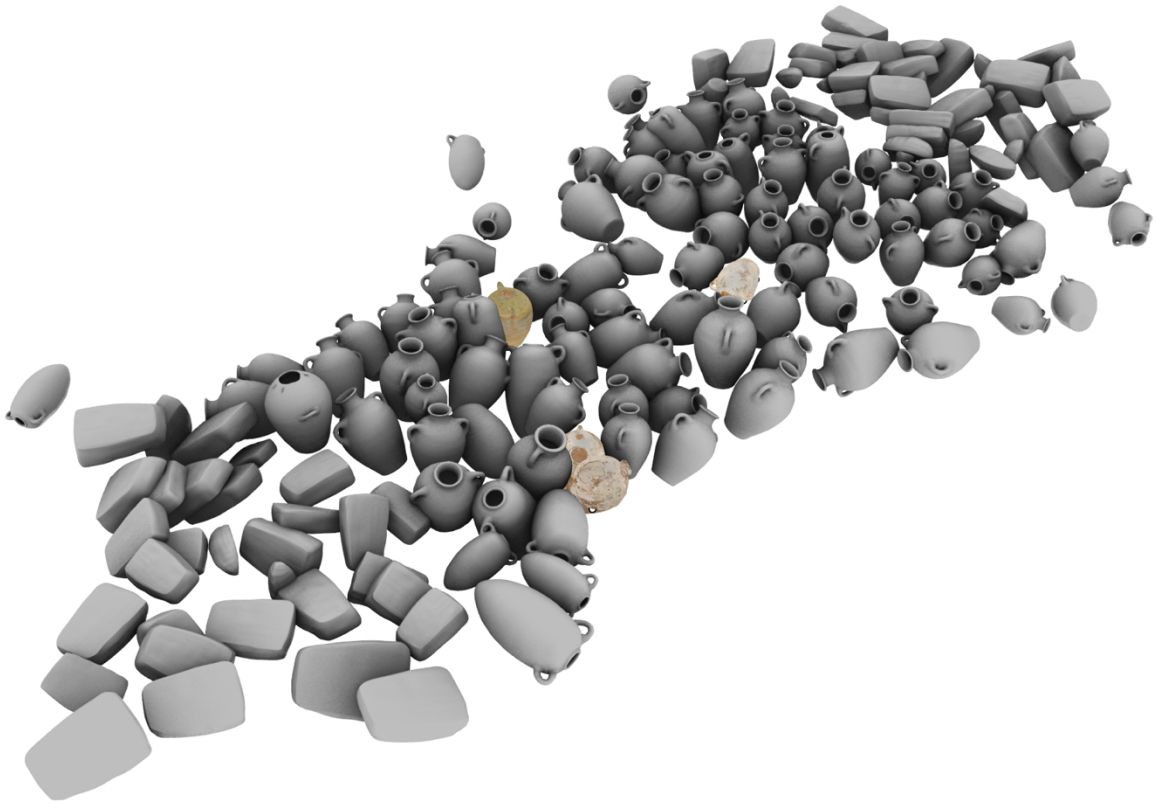

Figure 46 Scanned amphorae integrated into the composite 3D model. Wreck in its entirety seen from an angle (A. Bravo-Morata Rodríguez and author).

depositional movement, the organization of the organisms serve here as evidence for long-term stability. It can then be said that the amphora was in roughly this position when it first came to rest on the seabed or was moved into this position relatively quickly after its initial deposition. There are, however, significant signs of abrasion on the artifact. These two localized patches (delineated by phase "X") are located where A18 makes contact with A17 and on the corresponding underside of A18. The absence of growth and signs of abrasion found in these areas show that the artifact was indeed, for a period, moving slightly in a 'rocking' fashion. The reduced organism counts are likely not solely the result of abrasion, but also the hindrance of even initial colonization due to contact between amphorae.

5.3.4 A24 in Context

When contextualized as a result of its integration into the 3D model, A24 shows very similar patterning to A18. The artifact was recovered from a slanted position, but in this position, its distinct growth phases are neatly stacked horizontally and consistently with the seabed (fig. 48). Just as with A18, this is indicative of long-term stability. It is likely that this amphora had been in this position for the vast majority of, if not all, its time at the site. While not having undergone any major re-organization, there are still signs of movement on a smaller scale. Patches with fewer organisms and signs of abrasion (delineated by phase "X" and "B2") show that there was contact and some movement between A24 and A22/A17 on its sides. This can be seen clearer in fig. 49. Both artifacts are pictured isolated and in their original orientations. The growth phase lines reveal long-term consistency for both artifacts relative to each other (fig. 50).

5.3.5 A06 in Context

A24 is different from A18 and A24 because its growth phases appear horizontal rather than diagonal. This difference was explained when the artifact was integrated into a 3D model of

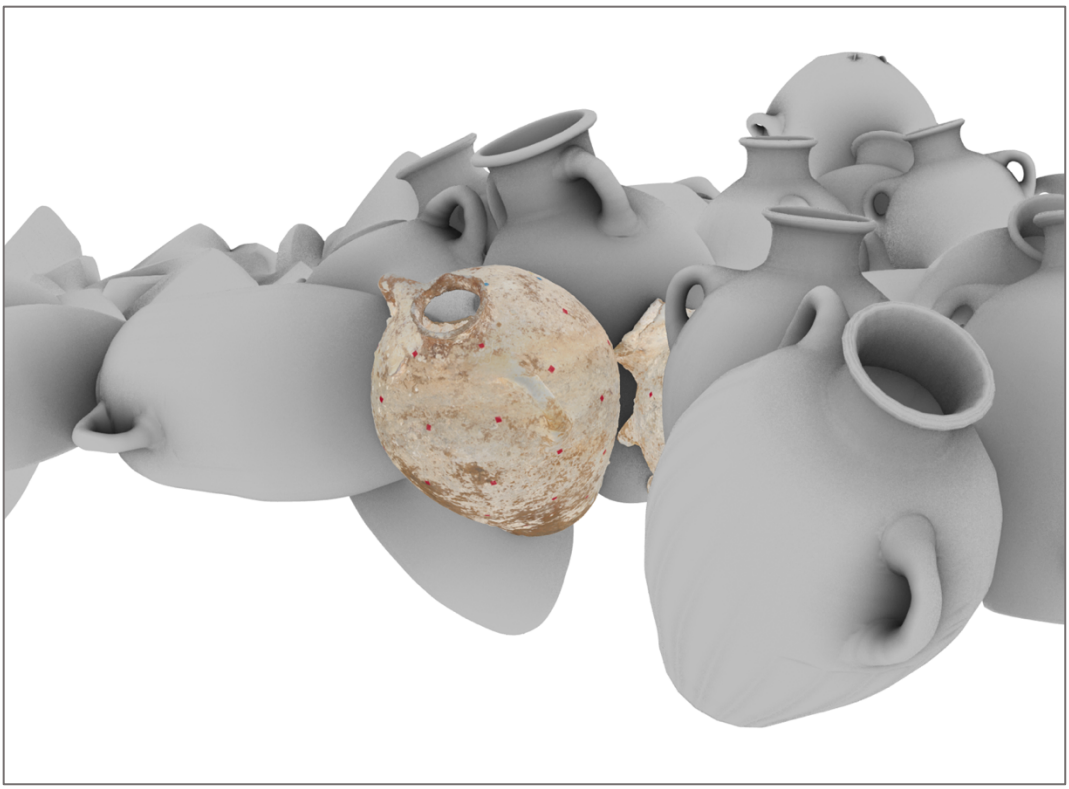

Figure 47 View of A18 and its surrounding spatial context (A. Bravo-Morata Rodríguez and author).

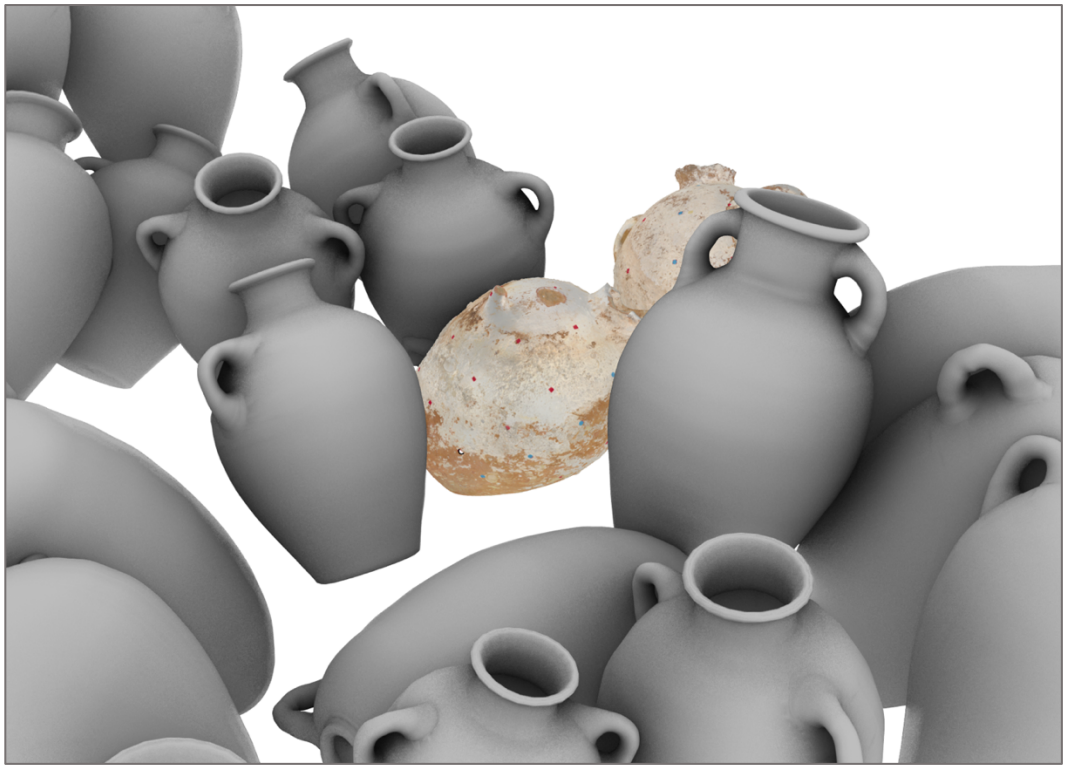

Figure 48 View of A24 and its surrounding spatial context (A. Bravo-Morata Rodríguez and author).

Figure 49 Images highlighting the abrasion that appears on A18 and A24. Shown isolated (top left), in context (bottom left), and in detail (right) (A. Bravo-Morata Rodríguez and author).

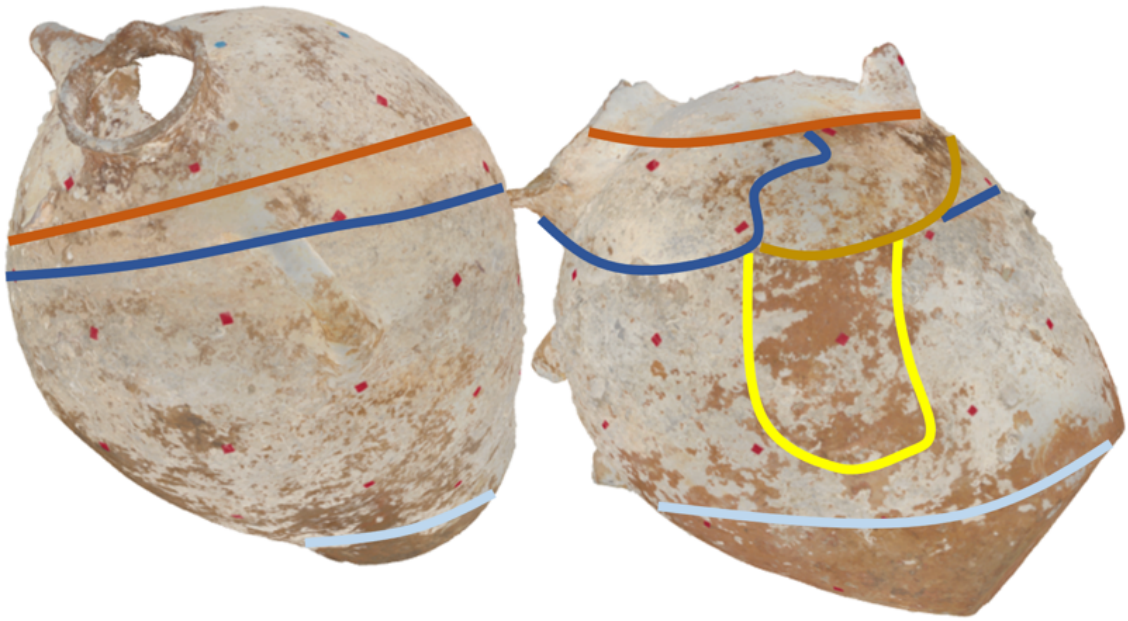

Figure 50 Isolated view of A18 and A24 in the positions they were recovered. Growth phases appear generally consistent across the surfaces of both artifacts (A. Bravo-Morata Rodríguez and author).

the site (fig. 51). Unlike the others, A06 was recovered from an upright position. The consistent horizontal growth phases preserved on its exterior also show that it has remained in this position for most of, if not all, its time at the site. Like A18 and A24, this amphora also has patches with fewer organisms and signs of abrasion. These areas, however, are distributed across the artifact differently and with greater irregularity. Neighbouring A05 and A31 can be linked with the most significant patches but it would appear another different process is acting on the artifact as well.

5.3.6 A40 in Context

Out of the four artifacts that are the focus of this research, A40 stands out as the clear outlier. Its growth phases are fewer, more distinct, and run vertically up the amphora when it is sat upright. When integrated into the 3D site model, the artifact can be seen on its side in the position from which it was recovered (fig. 52). The portion of the amphora that was buried appears fully and uniformly encrusted with no signs of abrasion. This means that it had to have been fully exposed at one point in order for these organisms to grow. It also means that it could not have been fully exposed in the position it was found. The artifact was supported only by sediment and shows none of the signs of abrasion that comes with contact from another amphora (as can be seen with A18, A24, and A06). This means that A40 underwent significant post-depositional movement. It is difficult to determine how it was positioned prior to this event because evidence for this is likely covered by what is now phase “A”. What can be said is that it was in a different position for long enough that growth comparable to phase “C” in A18 and A24 could develop. At which point, it came to rest in a new position where it was instantly partially buried in sediment that was already present.

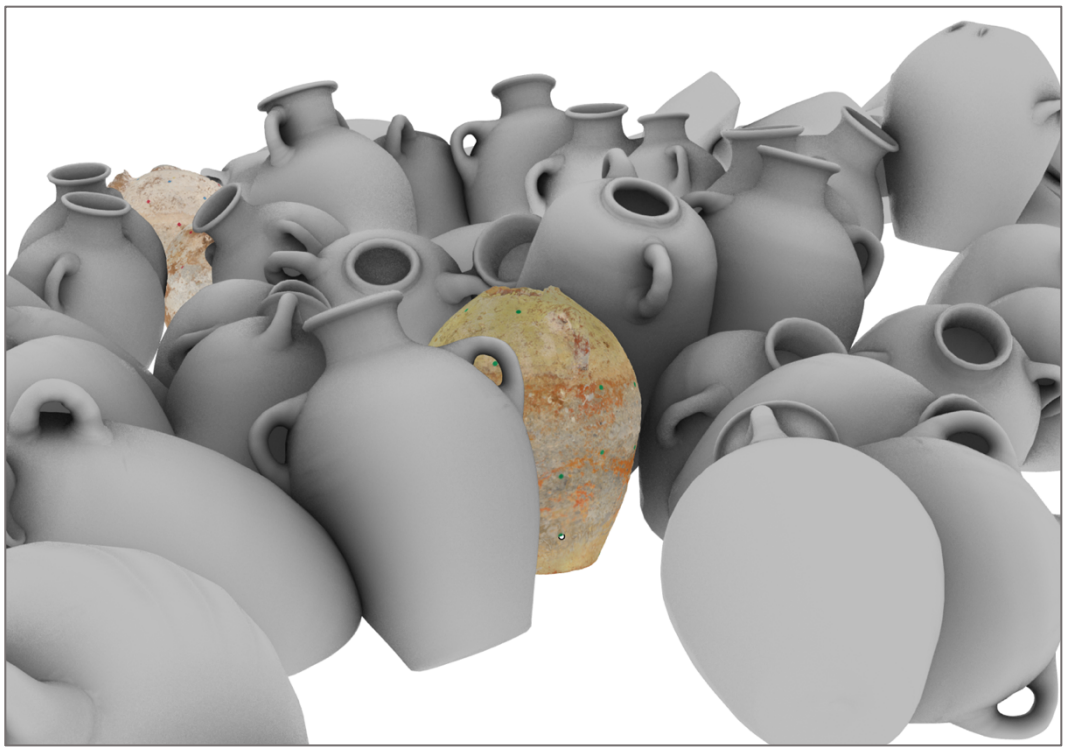

Figure 51 View of A06 and its surrounding spatial context (A. Bravo-Morata Rodríguez and author).

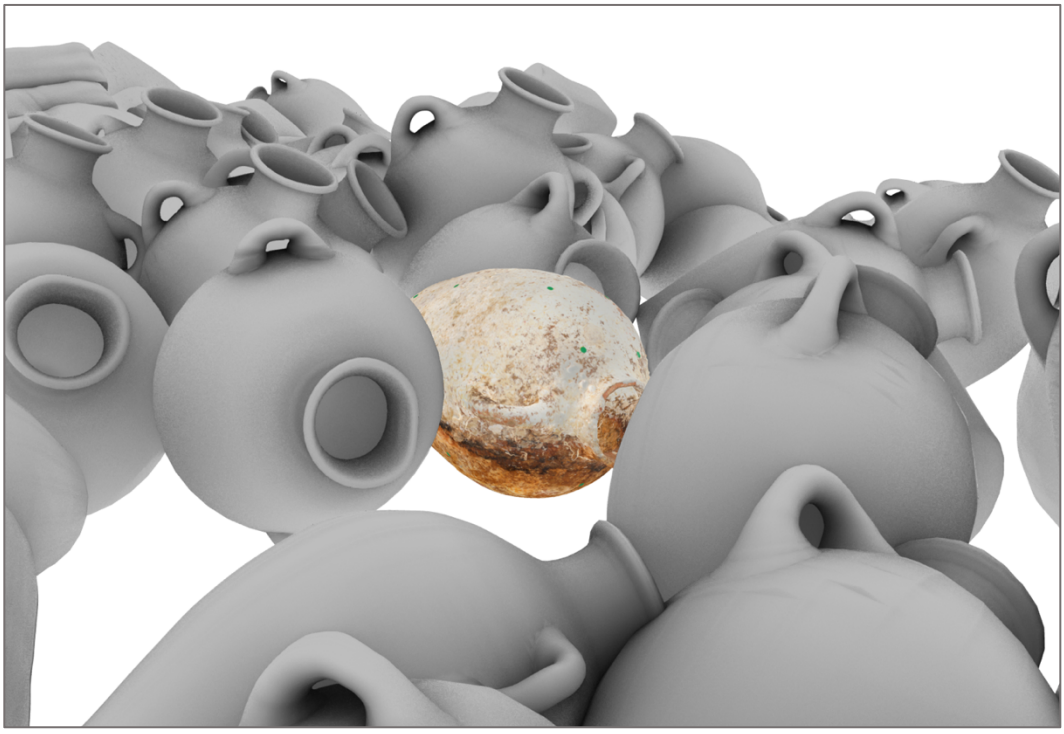

Figure 52 View of A40 and its surrounding spatial context (A. Bravo-Morata Rodríguez and author).

5.3.7 A18, A24, A06, and A40 as Proxies for Understanding the Site

One of the factors that influenced artifact selection was their dispersal across the site. This was to investigate the variability of biological processes in different parts of the wreck. A18, A24, A06, and A40 were selected, in part, because they could shed light on both port-starboard and fore-aft relationships. The similarities in the overall biological composition of A18, A24, and A06 point to comparable formation processes in their respective locations on either side of the wreck. The different biological signature and growth phase orientations of A40 instead suggest different processes acting on sections of the wreck lying further aft. This conclusion is compounded by the 3D examination of the amphorae in their recovered contexts. The gradual development of parallel phases of biological growth paired with consistent abrasion from
localized contact with neighbouring artifacts all reinforces interpretations of long-term stability. The absence of these indicators, paired with inconsistent biological growth, instead reinforce interpretations of major post-depositional re-organization.

While interpretations can only be made confidently about the four artifacts targeted by this research, the findings can nevertheless be extrapolated in order to speculate about processes affecting the wreck as a whole. For example, there are a number of other amphorae around A40 that are similarly resting on their side. The majority of these have not been raised and therefore could not be examined biologically. It is very likely, however, that they have similarly undergone significant post-depositional movement. These amphorae form a column (highlighted in fig. 53) which spans the width of the wreck. Such significant re-organization of the site could either represent a major event in the deterioration of the wooden structure of the ship, a later anthropogenic impact in the form of net fishing or a dragged anchor, or a major natural event like the powerful earthquake of 1693 (Azzopardi, 2013, p. 293).

The amphora A97 is an example of another artifact that had been recovered from around this impacted section of the site. Although not subjected to a complete biological analysis, comparing it superficially with A18, A24, A06, and A40 still provides a number of insights. What makes A97 interesting is that it exhibits both horizontal and vertical growth phases. The vertical growth phases exhibit at least a superficial likeness to phases “A”, “C”, and “D”. This shows that

the artifact was laying on its side for long enough that three distinct phases developed before it shifted and came to rest upright. When aligned with its orientation in the 3D model, it can be interpreted to have fallen in the direction of the disturbance. Likely into a void that was created as a result of the disturbance itself. This conclusion is reinforced by the mirroring of these phases on the inside of the amphora (fig. 54). Since the same perpendicular phases can be observed there, it is known that the differences in composition on the outside of the amphora were not the result of other processes like abrasion. Understanding the object's post-depositional re-organization in this way is made entirely possible by the prior characterizations of A18, A24, A06, and A40 and their integration into the 3D model.

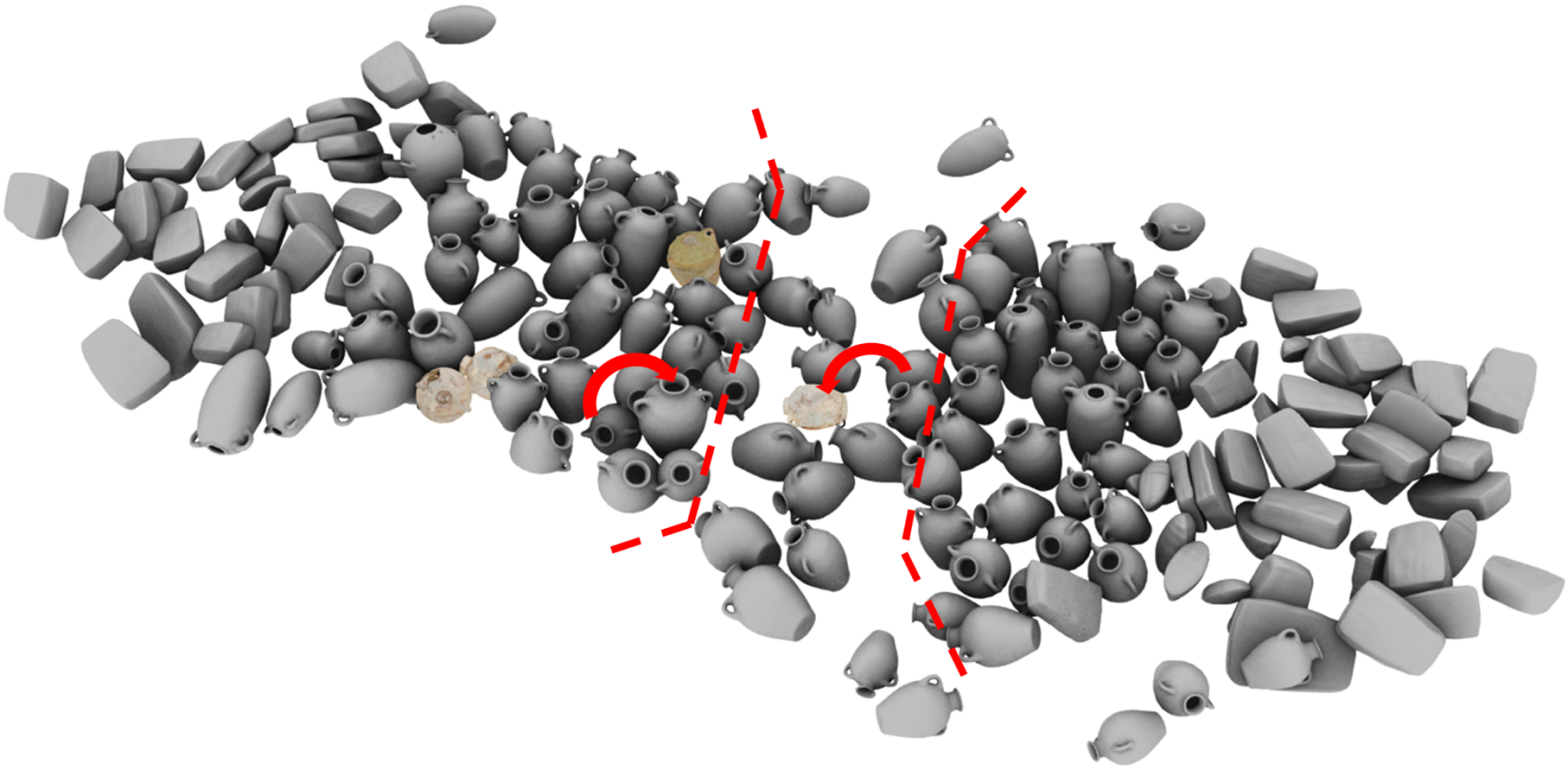

Figure 53 View of entire model. Highlighting the identified channel bisecting the wreck and the movement of A40 and A97 (A. Bravo-Morata Rodríguez and author)

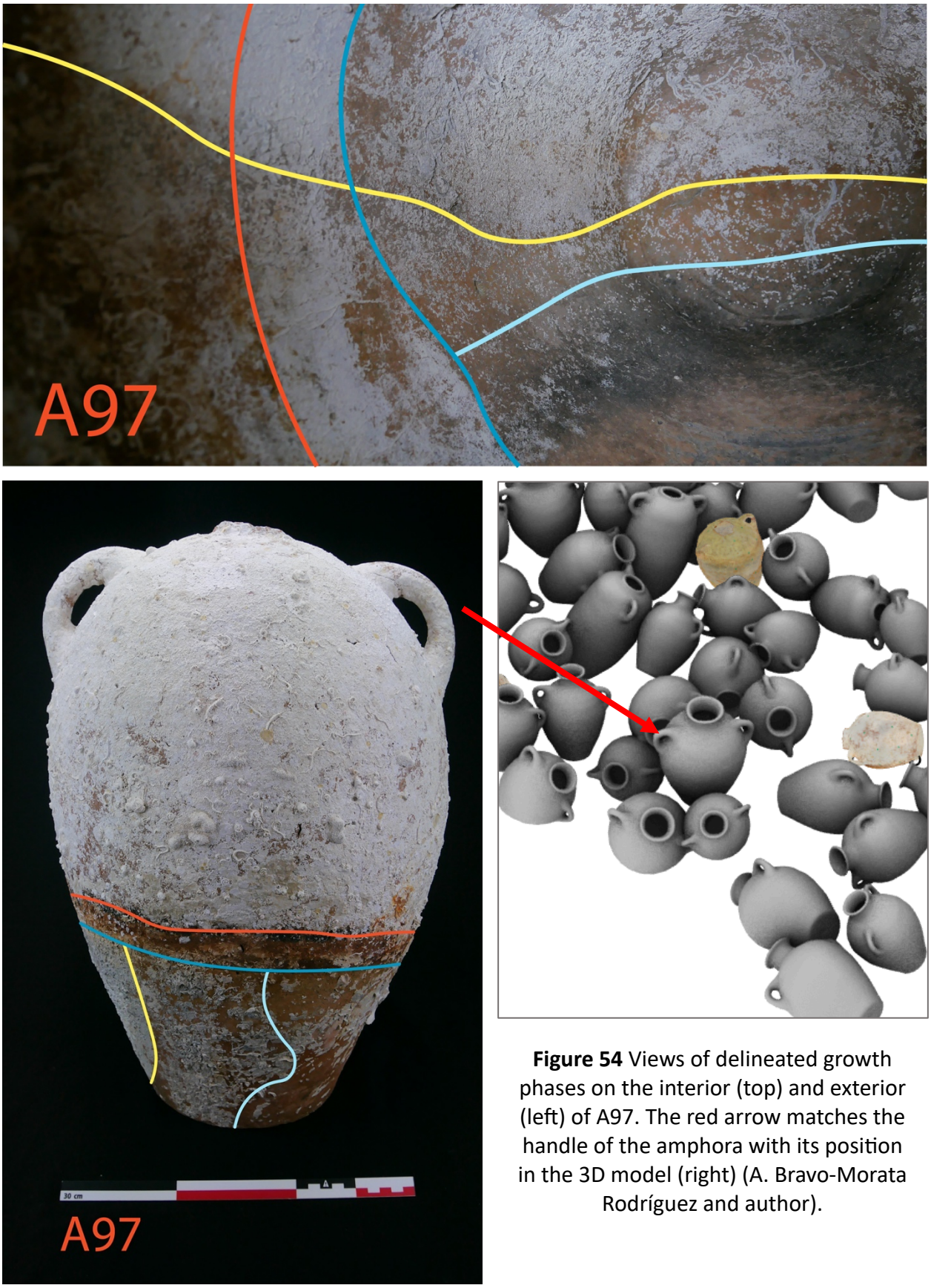

Figure 54 Views of delineated growth phases on the interior (top) and exterior (left) of A97. The red arrow matches the handle of the amphora with its position in the 3D model (right) (A. Bravo-Morata Rodríguez and author).

6. Discussion

6.1 Summary of Key Findings

As a result of this research, 4,121 individual marine organisms encrusting four amphorae and their spatial contexts along the archaeological artifacts were recorded. They were found to include Anthozoa (1 species), Bryozoa (15 species), Foraminifera (1 species), Mollusca – Bivalvia (2 species), and Mollusca – Vermetidae (1 species). The composition, size, and abundance of these organisms varied across the four selected artifacts but could be grouped into visually distinct 'growth phases'. These phases were characterized and quantitatively compared. Differences in the composition, orientation, and spatial context of these phases serve as a record of biological processes acting on the wreck and can be used to interpret site formation processes more broadly.

The presence of five visually and biologically distinct growth phases was confirmed. They were labelled alphabetically as "A", "B", "C", "D" and "X". Phase "A" represents the most recent living layer with the longest exposure while phase "D" represents the area that was buried first. Phase "X" is different because it is characterized primarily not by its biological growth but by the abrasion its growth has undergone.

Phase "A" is biologically and visually distinct from the other phases but also exhibits a high degree of internal variation. It is characterized primarily by higher counts of foraminifera and corals, coralline algae, and the unique species Br-E and Se-D. Phase "B" appears as a thinner transitional phase and displays a degree of overlap with both phase "A" and "C". Out of all the phases, "C" is the most consistent both internally and across the artifacts. Its composition is typically close to 2% bivalves, 57% bryozoans, 8% corals, 8% foraminifera, 25% serpulids. The top unique species in phase "C" are Br-A, Br-L, and Se-B and the phase is also home to the majority of the largest bryozoans. Phase "D" is visually and biologically distinct but internally varied. It is characterized primarily by bivalves, fewer individuals overall, and areas of bare ceramic. Lastly,

phase “X” is biologically consistent with its surrounding phase but is represented by far fewer individual organisms and signs of abrasion. The organization of these growth phases (“A”, “B”, “C”, “D”, and “X”) vary depending on amphora. They appear diagonally across A18 and A24, horizontally on A06, and vertically for A40.

The amphorae A18, A24, and A06 are all biologically consistent. They exhibit visually and compositionally similar growth phases and contain comparable proportions of the same top six most abundant unique species (Br-A, Br-L, Co-A, Fe-A, Se-B, and Se-G). A40, on the other hand, shows compositional similarity only to phases “A”, “B”, and “C” (not “D”) and has inconsistent proportions of a different set of dominant unique species (Br-H, Br-I, Br-L, Fe-A, Se-G, and Ve-A).

This biological data was contextualized when laser scans of the artifacts were integrated into a composite 3D model of the site. The resulting spatial context facilitated the interpretation of site formation processes acting on the wreck. It was determined that the abrasion characteristic of “X” phases (found on A18, A24, and A06 but not on A40) is the result of contact with neighboring artifacts. It was also determined that the successive growth phases on the artifacts ran mostly parallel to the seabed. In the case of A18 and A24 which were originally located adjacent to each other within the site, these phases exhibited a high level of uniformity and the same parallel lines ran across both amphorae. Because A06 and A40 are more isolated in the context of this research, their similarity to immediately neighboring artifacts could not be assessed. However, results indicated that A40 represented an anomaly and warranted further investigation.

Among the recovered artifacts was amphora A97. It was not a direct neighbor to A40 but was in relatively close proximity to it. A97 presents an interesting case because it has both vertical and horizontal growth phases. Its three vertical phases appear visually consistent with “A”, “C”, and “D” phases recorded on artifacts A18, A24, and A06 while its horizontal phases display a likeness to A40. When A97 was lined up with its position in the 3D model and these phases were interpreted, it was found that A97 was resting on its side for some time before undergoing movement in the direction of A40. By the end of this movement, the amphora was left resting in an upright position.

The encrusted organisms of A97 and A40, as well as an observable channel cutting across that section of the 3D model, compound the conclusion that this area of the wreck underwent significant post-depositional re-arrangement. The biological and spatial data collected for A18, A24, and A06 instead indicate overall long-term stability with the exception of consistent minor shifting and abrasion where the amphorae make contact with one another over a long period of time.

6.2 How the Findings Relate to the Aims

The first aim of this research is to identify and characterize the benthic organisms encrusted to amphorae recovered from the *Phoenician* shipwreck. This would contribute to a broader understanding of the site itself and its relationship to the marine environment. Many of the initial findings met the objectives set for satisfying this aim. As part of this research, the benthic organisms associated with the wreck's ceramic cargo were identified, described, counted, and measured. They were divided into five visually and biologically distinct growth phases that were in turn analyzed and compared against each other. As a result, the four amphorae serve as proxies for understanding which benthic organisms are present and how they are distributed across the ceramic cargo of the wreck. Ultimately satisfying the first aim of this research.

The second aim of this research is to develop and evaluate the effectiveness of a new method for interpreting the movement of underwater archaeological objects. This method is based on the idea that the different positions (i.e.: orientations and burial depths) of artifacts at a site are recorded by the marine organisms encrusted to them. Changes in these positions will be reflected and characterized by new biological growth that differs compositionally and/or visually. By examining these different growth phases, the life-history of artifacts on a site can be re-created and major events of post-depositional movement can be identified. Ultimately working towards a greater understanding of what the site looked like before the substantial loss of organic data (wooden ship structure, ropes, organic cargo, etc.) and before other potential natural or anthropogenic impacts.

The characterization of the five visually and biologically distinct growth phases plays an important role in satisfying the second aim of this research. These phases serve as a record of past growth on the objects and offer a snapshot of what organisms were present before sections were buried. When integrated into a 3D model of the site, the added spatial context furthered what interpretations could be made. This method proved successful in identifying the different movements of artifacts across the site. Further, it was able to distinguish between two different kinds of movement. The consistent and localized abrasion of neighboring artifacts that were otherwise stable (A18, A24, and A06) and the major re-organization of artifacts resulting in entirely new positions (A40 and A97).

6.3 Interpretation of Results

The concept of 'growth phases' is central to understanding what the results mean and how they confirm the two aims. This is because reading these phases informs both how the organisms are distributed across the artifacts and how different artifacts experienced movement. Changes in environmental conditions, sedimentation, and movement are recorded by these distinct phases and their different locations, orientations, and compositions.

It is important to recognize that growth does not occur uniformly and that there can be considerable variation even within the same phase. Certain organisms may favor one area within a phase based on, among other things, the availability of light, access to nutrients, and competition with other organisms. This type of variability was found to be greater in phases "A" and "D" and is highlighted by the NMDS plot showing dissimilarity (fig. 44). This also means that individual phases cannot be extrapolated to other areas of an artifact. For example, it cannot be assumed that an artifact would have been entirely covered by growth consistent with phase "D" before the development of other phases. At the time that phase "D" was forming, different growth could have been occurring at the top sections of the amphora. In this way, each phase serves only as a record of what was occurring in the area it now occupies. This also means that phase "A", as it occupies the area with the longest exposure, was developing since the site's initial

deposition. While much of this growth could now be covered by more recent organisms, it is important to not make the mistake of thinking that "A" only represents the most recent growth.

The amphora A18 serves as a good model for examining how factors like time and exposure determine biological composition. This is because a broken section of this artifact offers a view of what is happening on its inner walls (fig. 55). On the inside, a distinct line separates encrusted organisms from a bare surface. This inner growth phase lines up near perfectly with the exterior "A" phase and indicates uniformity in sedimentation. Despite both of these areas being exposed at the same time, their biological growth is strikingly different. The outside is entirely encrusted (as is typical for "A" phases across artifacts) but the inside is much sparser and visually dominated by larger and more abundant serpulids. This can be explained as the result of two main factors; 1. The inside has not been exposed for as long as "A". Biological growth could only begin encrusting the inside of the artifact after the stopper had deteriorated or been dislodged and the contents had been emptied. 2. The environment inside the amphora is covered, darker, and less exposed than the outside surface of the artifact. In this way, A18 serves as proof that time and environment can produce different compositions or growth phases on equivalent surfaces. It also serves as a model for their interpretation.

When interpreting the different phases that have been recorded and characterized as part of this research, it is important to do so through the lens of time and environment. When the ship first came to rest on the seabed, the amphorae would have most likely still been in the dark and covered environment of the ship's hold. This would have determined what kind of growth could occur and is probably represented by phase "D". While it is uncertain how long this environment would have persisted, the experimental sinking of a replica of the *Uluburun* offers some clues. The ship, dubbed the *Uluburun III*, was deliberately sunk in 20-30m of water near Kaş, Turkey on the 27th of October 2006. Just five years later, by the 16th of October 2011, the structure had completely collapsed and very little wood remained (fig. 56) (Varinlioğlu, 2020, p. 6-8). Its deterioration would have been accelerated due to the higher wave energy and increased biological activity that typically comes with a much shallower depth. These results should then be extrapolated to the *Phoenician* with a degree of hesitancy. Nevertheless, it suggests that the

Figure 55 Exterior and interior of A18 (Author).

Figure 56 Images showing the deterioration of *Uluburun III* (Varinlioğlu, 2020, p. 8).

period during which the wooden structure existed was short compared to the entire life-history of the site.

As the ship's structure collapsed, the once sheltered cargo would have undergone a rapid initial sedimentation. It is probably at this point that "D" became buried. After this had occurred, the site would have been more stable and sedimentation more gradual. The artifacts would now be exposed to light and the water column and this altered level of exposure would have subsequently resulted in biological growth of a different composition. Changes in biological communities in response to the physical changes of a site were also recorded by Mires & Meyer-Kaiser (2023) and works to support this interpretation.

Light is important for the growth of coralline algae which are photosynthetically active. These organisms essentially cover all of phase "A" and have a very slow growth rate (measured in μm) that is heavily influenced by temperature, light, and salinity (Gould & Ries, 2024; Lewis & Diaz-Pulido, 2017). It is then most likely that "A" and "C" both began to develop after the structure's collapse. With the coralline algae that defines "A" taking root at the highest points of the artifacts, where they benefited from the greatest light exposure, and slowly expanding downward to form the interface "B" where the two phases overlapped. Under such a model, "A" and "C" are distinct because of differences in light and sediment effects while "B" represents the ecotone/transitional zone that is intermediate between the two. Sedimentation on the site would gradually continue and ultimately bury portions of this interface to define the upper limit of phase "B". With such an understanding of how these growth phases came to form, variability in their location, orientation, or composition can be examined to determine object movement.

If the growth phases of an amphora all run parallel to each other along similar contours, it can be concluded that the object remained much in the same position throughout their formation. This was found to be the case for A18, A24, and A06. These artifacts did still exhibit signs of movement through abrasion (delineated by phase "X"). But the repeated abrasion of the same areas works to reinforce the conclusion that the artifacts were stable. The slight movements that are captured by "X" are the likely result of non-encrusting marine organisms interacting with the site (in addition to the possible effects of bottom currents that are not strong enough to displace the amphorae but still cause minor motion). This interpretation is supported by photos

that show an eel sheltering in one of the amphorae (fig. 57) and a collection of shells indicative of octopus activity around the opening of A18 (fig. 58). The impact of burrowing organisms is also highlighted by Ferrari & Adams (1990) and is not to be underestimated. The resin-casting of burrows was used to show how individual invertebrates, fish, and crustaceans can be responsible for turning over kilograms worth of sediment every year (Ferrari & Adams, 1990, p, 140-142). This subsidence and sediment transport would, in addition to the direct interaction of animals such as eels and octopi, lead to the shifting of artifacts and result in abrasion.

In other cases, the movement of artifacts can be much more extreme. Major events of post-depositional movement are evidenced by inconsistent and perpendicularly intersecting growth phases. These were observed when examining amphorae A40 and A97. Both artifacts also lacked visible signs of abrasion. This means that they were either not in contact with other artifacts or these “X” phases were encrusted over after the artifacts were re-positioned. A40 is biologically inconsistent with artifacts associated with long-term stability and does not have a visible “D” phase. The lack of a “D” phase can be explained if the artifact was stacked higher among the cargo and did not undergo any initial sedimentation when the ship structure broke apart. However, when integrated into the 3D model, the artifact was found resting on its side and occupying the same plane as artifacts with “D” phases. This, and the absence of abrasion, suggests that the artifact fell from a higher level and came to rest in an area that was already sedimented to the point where no contact with other artifacts was possible. A97 similarly shows evidence for two different positions. It has parallel “A”, “C”, and “D” phases that indicate it was on its side for a substantial amount of time before shifting to an upright position and developing new “A” and “B” phases. When examined in the context of the 3D model, both A40 and A97 were found to have fallen in the direction of an apparent channel bisecting the wreck. This channel is itself an anomaly and the research done on A40 and A97 can be used to interpret it.

The channel was identified around midship and is characterized by a lower density of artifacts in a variety of different positions. A40 and A97 were both found to have fallen in into this channel from opposite directions. Because of their biological growth, it is known that their movement did not occur as part of the initial deposition of the site but rather a good while after. Long enough for three distinct growth phases to form on A97. This suggests at least two

Figure 57 An eel pictured inside one of the amphorae from the *Phoenician* (Courtesy of the Department of Classics & Archaeology, University of Malta).

Figure 58 Shells indicative of octopus activity pictured outside the mouth of A18 (Courtesy of the Department of Classics & Archaeology, University of Malta).

possibilities; 1. That this void existed from the beginning and was maintained by parts of the ship's structure (e.g., bulkheads or other lateral elements perhaps strengthening the area around a mast). When these elements finally deteriorated, at a slower pace than other parts of the ship, the artifacts on either side would have no longer been supported and would have fallen into the channel or 2. This void did not exist as part of the original organization of the ship and was the result of a later foreign impact. This could have been of an anthropogenic or natural origin and would include things like a dragged anchor, fishing gear, or the earthquake of 1693. At this point it is impossible to definitively endorse one possibility or the other. It is interesting to note, however, that the ongoing study of two other Phoenician wrecks has identified similar features (Bravo-Morata Rodríguez, n.d.). This would support the argument that the observable channel existed as a feature of the ship's construction and is characteristic of Phoenician shipbuilding traditions.

6.4 Comparison with Theory/Previous Research

Biological processes are the focus of only a fraction of the studies which examine the varied site formation processes of underwater archaeological sites. Of these, a significant number assess the role of shipwrecks as artificial reefs. These studies tend to align more with the first aim of this dissertation as their intention is to identify and characterize the marine organisms associated with underwater cultural heritage sites. Some papers examine the relationship of broader groups of organisms (Paxton et al. 2022; Paxton et al. 2024), while others may have a narrower focus, such as considering only fish (Davis, Carlson, and Caselle 2018; Simon, Joyeux, and Pinheiro 2013), sessile and sedentary macrofauna (Lira et al. 2010), sponges (Olinger et al. 2019), corals (Burns et al. 2023), fouling communities (Jimenez et al. 2017), or microbiomes (Hamdan et al. 2021, Hampel et al. 2022).

This dissertation has a narrower focus as well because it centers on the benthic encrusting organisms present at the site. In this case, the most pertinent study is that of Gravina et al. (2021). Its focus is the benthic invertebrate community associated with a bronze naval ram from the First

Punic War (264-241 BCE). As the ram was recovered off the Aegadian Islands from a depth of 75-95m, it also represents the closest study geographically. The authors identified a total of 114 species. Of these, 58 were mollusks (33 gastropods and 25 bivalves), 33 were polychaetes, and 23 were bryozoans (Gravina et al., 2021, p. 4). These results differ from the results of this dissertation because Gravina et al. (2021) also sampled sediment trapped within the ram. As a result, their study includes not only encrusted species but also motile ones, all of which were mollusks. Sediments from the *Phoenician* were similarly sieved and 54 mollusk species were identified. They represent a range of substrate preferences (soft silts to sands, hard, sea grass, and coral) but all are consistent with the continental shelf and depths to around 200m (Giaime, 2023). These mollusks, however, were not included in the scope of this dissertation and the focus is instead on the organisms that were encrusted to the objects' surface.

In the study by Gravina et al. (2021), the encrusting organisms were identified to a species level and their life traits and ecological affinities were examined. Despite the relative geographical proximity, comparable time spent on the seabed, and similar depths of the two sites, there appears to be no overlap in bryozoan species. This was determined based on comparison with a list of identified species included in their publication (Gravina et al. 2021, p. 7-8). Differences in benthic composition were expected between the ram and the *Phoenician*, but not to this extent. Although it is possible that a common species will be identified through further study, the significant dissimilarity of the two sites will not change. This is the result of differences in both the surrounding environments and in the nature of the archaeological material itself (bronze and ceramic). A study by Bethencourt et al. (2018) supports this conclusion as it determined that mollusks, bryozoans, annelids, and barnacles contributed to the differentiation of communities settled on various artificial substrates (copper, brass, cast, iron, pine, and oak) and that these communities also differed between two sites only 9NM apart (Bethencourt et al., 2018, p. 102-108).

While the first aim of this dissertation overlaps with that of the study of Gravina et al. (2021), the second aim and overall focus of the research differs meaningfully. A wreck site represents a sampling tool for Gravina et al. (2021). It is a proxy for studying marine biodiversity and ecosystem responses to the intrusion of a human-built structure. As such, archaeology was

used by the researchers to answer biological questions. This dissertation is different in that it instead uses biology to answer archaeological questions.

Research that draws on marine biology to inform archaeology-led questions can functionally be separated into two categories. There are studies that examine marine organisms for what they take away from archaeological sites. These will typically focus on quantifying the deterioration caused by marine borers (Palma and Santhakumaran, 2014; Björdal et al., 2012; Pournou, 2018). And there are studies that instead explore marine organisms for what they add to a site. These will use marine organisms as records of spatial and environmental data (Ricci et al., 2019; Secci et al., 2021). One of the aims of this dissertation is to develop and evaluate the effectiveness of a new method for interpreting the movement of underwater archaeological objects using the organisms encrusted to them. As such, it fits into the second group.

The study by Ricci et al. (2019) focuses on marble statues recovered from the *Antikythera* shipwreck (Greece). Since artifacts were being lifted from the site as early as 1901, the excavation was not recorded with as much detail as it would have been today. This means that little is actually known about the statues' original positions on the site. The work of Ricci et al. (2019) was then to examine what bio-erosion and benthic organisms were left on the statues to hypothesize their depositional conditions and examine ecological successions. The work of Secci et al. (2021), on the other hand, focuses on the *Mazatos* shipwreck (Cyprus) whose excavation has been thoroughly documented using modern technology and methods. Their focus is instead to capitalize on three-dimensional recording and modelling techniques to highlight sediment and biogenic horizons across the site. Ultimately creating a model that can be used to interpret the natural site formation processes that have interacted with the wreck.

This dissertation went about collecting data differently than both of these studies because the goal was to differentiate the composition of growth phases. In order to facilitate the comparison of these data sets, standardized 10x10 cm test squares were employed. This is an accepted method for the study of marine benthos and would be more suited to the aims of this research than the use of transects or photography alone (Eleftheriou, 2013, p. 11-15). It also ensures that variation across an artifact is accounted for. Depending on its placement, a vertical transect would miss other growth phases that were vertically oriented. This high-resolution data

also lent itself to statistical analysis using Bray-Curtis Dissimilarity. Meaning that differences in composition could be analyzed across phases and artifacts. This was not something required by the aims of Ricci et al. (2019) or Secci et al. (2021).

The method used by this dissertation for the production of a 3D model drew heavily on those employed by Secci et al. (2021). Much in the same way, 3D models of the amphorae were made (albeit using a laser scanner instead of photogrammetry) and aligned with their relative positions in photogrammetric models of the site as a whole. The main difference is that, for this dissertation, the scans were made after desalination and with the test square markers in place. This meant that the biological data could be linked precisely with their positions across the site. It also meant that the coloration of the objects, reflective of their state at the time of recovery, would not bias the interpretation or identification of past phases. This coloration, visible in fig. 59, has the potential to visually obscure the distinction between phases "C" and "D" as they would both appear uniformly blackened. By examining the artifacts after these colours had faded, the organisms themselves guided the delineation of phases.

Calcareous algae, Foraminifera, Porifera, Anthozoa, Serpulidae, Bryozoa, and Brachiopoda were all identified on the marble cargo of *Antikythera* (Ricci et al., 2019, p. 86-91). Unlike the bronze ram, the marble statues exhibit a higher level of overlap with organisms identified on the *Phoenician*. Although not all are confirmed, there appears to be bryozoans of the genera *Smittoidae*, *Turbicellepora*, *Schizoporella*, *Tubuliporina*, and *Lichenopora* present at both sites. This raises interesting questions because it runs counter to what one might hypothesize. It is unexpected that the ceramic cargo of the *Phoenician* would display a greater similarity to marble objects from a shallower and further away site than it would to a bronze object from a similar depth and closer location. This likely has something to do with the material of the artifacts (i.e., stone/ceramic vs. metal). Unfortunately, it is impossible to compare these results to those from the *Mazatos* wreck. For that study, the organisms were only sorted into seven broader categories. These categories were; "coral, macro algae, calcareous algae, sponges, bryozoans, other organisms (e.g., polychaetes, foraminifera, bivalves), as well as […] free or uncolonized substrate (e.g. clay, marine aggregates)" (Secci et al., 2021, p. 7). However, research is still ongoing and the

Figure 59 Photogrammetric model made of the *Phoenician* during excavation in 2019. Of note is the discoloration and redox staining that is visible on the exterior of the amphorae (Courtesy of the Department of Classics & Archaeology, University of Malta).

publishing of additional biological data from the site is anticipated. When this occurs, more fruitful comparisons may be possible.

As a result of studying the identified organisms, Ricci et al. (2019), were able to confirm which parts of the statues were exposed and which parts would have been buried. The possibility that earthquakes or a small landslide could have re-arranged the objects and exposed different surfaces was also discussed (Ricci et al., 2019, p. 103). For their part, Secci et al. (2021) used the 3D model to reconstruct two seafloors and illustrate changes in the sedimentation of the site. This allowed for the investigation of natural processes affecting the wreck and emphasizes the importance of new digital applications in archaeology (Secci et al., 2021, p. 9-10).

The present work engages with and synthesizes the work of, among others, Gravina et al. (2021), Ricci et al. (2019), and Secci et al. (2021). It draws on the approaches and methods of each while, at the same time, experimenting with a new innovative approach to address questions that had been left unanswered.

7. Conclusion

7.1 Significance

This dissertation puts forward a new method for the collection and interpretation of stratified underwater biological data preserved on moveable objects. It outlines how biological processes, specifically the growth of benthic encrusting organisms, can serve as a record of past spatial/environmental relationships and can be used to inform site formation processes. This new method has been proven effective at identifying and interpreting the movement of artifacts in an underwater archaeological context. It is the first to integrate biological data into a 3D site model to prove which areas of a site represent the most and least amount of disturbance. By using standardized test squares instead of transects, it also offers an alternate approach to data collection that is capable of better capturing the diversity of growth phases belonging to an artifact. These standardized units facilitate the comparison of biological data between the test squares of different phases and between the objects themselves.

This research has not only identified and characterized the encrusted benthic community associated with the *Phoenician* wreck but has used this data to provide multiple lines of evidence that differentiates between relative stability and movement in objects. Further, it has proven effective at identifying two types of movement. One that is characterized by the continuous shifting and abrasion of neighboring artifacts and another that represents major events of post-depositional re-organization. This was done through the identification of patterns in ecological succession and the discovery of objects that deviated from this pattern.

One example of this, A97, is significant because it highlights the importance of this type of research. The object was recovered from an upright position that could easily be mistaken as stable and consistent with other upright artifacts. The interpretation of its growth phases, however, revealed that it has undergone significant movement. This finding challenges the

assumptions made about the stability of ceramic cargoes and reinforces the importance of examining benthic organisms as records of spatial data when interpreting a site.

This dissertation has provided new insights into the site formation processes of the *Phoenician* wreck and has entered it into an emerging academic dialogue with other sites in the Mediterranean. It has produced a new method of biological/archaeological interpretation that is essentially universal in application. A replicate study can be carried out on any archaeological site where marine benthos are observed. It is hoped that this method will continue to be used and adapted for the future study of formation processes acting on underwater archaeological sites.

7.2 Limitations/Future Directions

This research was successful in its aims; 1. to identify and characterize the benthic organisms encrusted to amphorae recovered from the *Phoenician* shipwreck and 2. to develop and evaluate the effectiveness of a new method for interpreting the movement of underwater archaeological objects. Nevertheless, this research would have benefited from larger datasets. While a respectable 4 121 individual organisms were recorded, not all phases were represented equally. This is mainly the result of the unequal distribution of phases across artifact surfaces. A24, for example, could only accommodate a single test square for its “A” phase but had ten squares for its “D” phase. It would have then benefitted the research to have data for additional artifacts but, due to time limitations, this was not feasible.

There are a number of interesting future directions that warrant the investment of more time. Firstly, the site of the *Phoenician* would benefit from additional study. It is still uncertain exactly what the identified channel represents. While it is hypothesized that a void in the ship’s structure resulted in the major re-organization of that area, it cannot as of yet be confirmed. The biological evaluation of other artifacts from that area may still hold the key to resolving this.

Currently, the majority of the species that make up this research have not been identified to a species or even genus level. A better understanding of these species and their ecological affinities would inform succession between phases and add depth to their interpretation. For

example, a higher percentage of organisms suited to cave environments in phase “D” would support the hypothesis that this phase formed while the objects were still enclosed within the shadows of the hull. Identifying these organisms to a species or genus level would also enrich comparisons with other sites (notably those of Ricci et al. 2019 and Gravina et al. 2021).

It is also important that this new method be used on other sites. Testing on different kinds of artifacts and in different environments would help in evaluating the effectiveness of the method and in refining it. An ideal site for this would be the *Tower* wreck. It is very close to the site of the *Phoenician* and at a similar depth but is a multi-component and very disorganized site. With different deposition events and mixed chronologies, it would serve as a good testing ground for the new method. The application of this approach to the *Tower* wreck would likely result in new answers for a site where many questions relating to site formation processes still persist.

Comparing the encrusted benthic communities of the *Phoenician* and *Tower* wreck is also likely to yield interesting results in its own right. How different are the biological signatures of two sites in very close proximity to each other? Is it possible to differentiate between the sites based on benthic data alone? If yes, then other new potential research avenues open up. It may well be possible to link looted artifacts with their original sites using this method.

In achieving its two aims, this dissertation has opened up the possibility of many new and exciting research avenues.

LIST OF SOURCES

Anastasi, M., Capelli, C., Gambin T., and Sourisseau, J. C. (2021) 'The Xlendi Bay shipwreck (Gozo, Malta): a petrographic and typological study of an archaic ceramic cargo', *Libyan Studies*, 52, pp. 166-172.

Antonelli, F., Ricci, S., Petriaggi, B. D., and Ortuño, M. B. (2019) 'Study of the bioerosion of Phoenician elephant tusks from the shipwreck of Bajo de la Campana: lots of hypotheses, few certainties', *Facies*, 65(2), pp. 1–12.

Aubet, M. E. (2001) *The Phoenicians and the West; Politics, Colonies, and Trade*. 2nd ed. Cambridge: Cambridge University Press.

Avshalom-Gorni, D., Frankel, R. and Getzov, N. (2004) 'Grooved Upper Grinding Stones of Saddle Querns in Israel', *Tel Aviv (1974)*, 31(2), pp. 262–267.

Azzopardi, E. (2013) 'The Shipwrecks of Xlendi Bay, Gozo, Malta', *International Journal of Nautical Archaeology*, 42(2), pp. 286-295, DOI: 10.1111/1095-9270.12020

Bethencourt, M., Fernández-Montblanc, T., Izquierdo, A., González-Duarte, M. M., and Muñoz-Mas, C. (2018) 'Study of the influence of physical, chemical and biological conditions that influence the deterioration and protection of Underwater Cultural Heritage', *The Science of the total environment*, 613-614, pp. 98–114. DOI: 10.1016/j.scitotenv.2017.09.007

Bieler, R., Collins, T. M., Golding, R., Granados-Cifuentes, C., Healy, J. M., Rawlings, T. A., and Sierwald, P. (2023) 'Replacing mechanical protection with colorful faces–twice: parallel evolution of the non-operculate marine worm-snail genera Thylacodes (Guettard, 1770) and Cayo n. gen. (Gastropoda: Vermetidae)', *PeerJ (San Francisco, CA)*, 11, pp. 1-64. DOI: 10.7717/peerj.15854.

Björdal, C., Gregory, D., Manders, M., Al-Hamdani, Z., Appelqvist, C., Havenhand, J., and Dencker, J. (2012) 'Strategies for Protection of Wooden Underwater Cultural Heritage in the Baltic Sea Against Marine Borers. The EU Project 'WreckProtect'', *Conservation and management of archaeological sites*, 14(1-4), pp. 201–214. DOI: 10.1179/1350503312Z.00000000017

Bonanno, A. (2005) *Malta: Phoenician, Punic, and Roman*. Malta: Midsea Books.

Bravo-Morata Rodríguez, A., (forthcoming) 'Hypothetical reconstruction and comparative study of the ships of Xlendi (Gozo, Malta), Tanit and Elissa (Ashkelon, Israel). Contribution to the study of Phoenician marine trade in the Mediterranean in the 8th and 7th centuries BC', UNPUBLISHED.

Brennan, M. L., Davis, D., Ballard, R. D., Trembanis, A. C., Vaughn, J. I., Krumholz, J. S., Delgado, J. P., Roman, C. N., Smart, C., Bell, K. L. C., Duman, M., and DuVal, C. (2016) 'Quantification of bottom trawl fishing damage to ancient shipwreck sites', *Marine geology*, 371, pp. 82–88.

Burns, J. H. R., Pascoe, K. H., Ferreira, S. B., Kane, H., Kapono, C., Carrell, T. L., Reyes, A. and Fukunaga, A. (2023) 'How Do Underwater Cultural Heritage Sites Affect Coral Assemblages?', *Remote sensing (Basel, Switzerland)*, 15(8), pp. 1-15. DOI: 10.3389/fclim.2022.1011194

Calcinai, B., Perasso, C. S., Petriaggi, B. D., and Ricci, S. (2019) 'Endolithic and epilithic sponges of archaeological marble statues recovered in the Blue Grotto, Capri (Italy) and in the Antikythera shipwreck (Greece)', *Facies*, 65(2), pp. 1–18.

Cassar, C. (2000) *A concise history of Malta*. Malta: Mireva.

Davis, K., Carlson, P. M., and Caselle, J. E. (2018) 'Herbivorous fish populations respond positively to a shipwreck removal and associated alteration of Benthic Habitat', *Frontiers in Marine Science*, 9, pp. 1-11. DOI: 10.3389/fclim.2022.1011194

Delaporta, K., Jasinski, M.E., and Søreide, F. (2006) 'The Greek-Norwegian Deep-Water Archaeological Survey', *International Journal of Nautical Archaeology*, 35(1), pp. 79-87, DOI: 10.1111/j.1095-9270.2006.00090.x

Demesticha, S. (2011) 'The 4th-Century-BC Mazotos Shipwreck, Cyprus: a preliminary report', *International journal of nautical archaeology*, 40(1), pp. 39–59.

Drap, P., Merad, D., Hijazi, B., Gaoua, L., Nawaf, M. M., Saccone, M., Chemisky, B., Seinturier, J., Sourisseau, J. C., Gambin, T., and Castro, F. (2015) 'Underwater Photogrammetry and Object Modeling: A Case Study of Xlendi Wreck in Malta', *Sensors (Basel, Switzerland)*, 15(12), pp. 30351–30384.

Dumas, F. (1962) *Deep-water archaeology.* London: Routledge and Kegan Paul.

Eleftheriou, A. (2013) *Methods for Study of Marine Benthos*. 4th Edition. Newark: Wiley-Blackwell. DOI: 10.1002/9781118542392

Fernández-Montblanc, T., Izquierdo, A., Quinn, R., and Bethencourt, M. (2018) 'Waves and wrecks: A computational fluid dynamic study in an underwater archaeological site', *Ocean engineering*, 163, pp. 232–250.

Ferrari, B. and Adams, J. (1990) 'Biogenic modifications of marine sediments and their influence on archaeological material', *International Journal of Nautical Archaeology*, 19(2), pp. 139-151, DOI: 10.1111/j.1095-9270.1990.tb00247.x

Foecke, T., Ma, L., Russell, M. A., Conlin, D. L., and Murphy, L. E. (2010) 'Investigating archaeological site formation processes on the battleship USS Arizona using finite element analysis', *Journal of archaeological science*, 37(5), pp. 1090-1101.

Foglini, F., Prampolini, M., Micallef, A., Angeletti, L., Vandelli, V., Deidun, A., Soldati, M., and Taviani, M. (2016) 'Late quaternary coastal landscape morphology and evolution of the Maltese Islands (Mediterranean Sea) reconstructed from high-resolution seafloor data', *Geological Society, London*, Special Publications, 411(1), pp. 77-95.

Fronteau, G., Boyer, F., Jaccottey, L., Le Quellec, V., Lepareux-Couturier, S., Milleville, A., Monchablon, C., Robin, B., and Picavet, P. (2020) 'Limestone millstones: Facies, provenance and use of sandy to pure limestones in France', *Journal of lithic studies*, 7(3), pp. 1–20.

Gambin, T. (2005) 'The harbours of ancient Gozo', *Malta Archaeological Review*, 6, pp. 20-26.

Gambin, T., Chemisky, B., and Drap, P. (2018) 'Exploring the Phoenician shipwreck off Xlendi bay, Gozo. A report on methodologies used for the study of a deep-water site', *Underwater Technology*, 35(3), pp. 71–86.

Gambin, T. (2020) ‘Malta: Submerged landscapes and early navigation’, In Bailey, G., Galanidous, N., Jöns, H.P. and Mennenga, M. (ed.) *The archaeology of Europe’s drowned landscapes*. Springer, pp. 341-346.

Gambin, T., Sourisseau, J. C., and Anastasi, M. (2021) ‘The cargo of the Phoenician shipwreck off Xlendi Bay, Gozo: analysis of the objects recovered between 2014–2017 and their historical contexts’, *International Journal of Nautical Archaeology*, 50(1), pp. 3-18.

Gambin, T. (2024) Email to Anton Motivans, 28 March.

Giaime, M. (2023). Email to Anton Motivans, 15 April.

Gibbs, M. (2006) ‘Cultural Site Formation Processes in Maritime Archaeology: Disaster Response, Salvage and Muckelroy 30 Years on’, *International journal of nautical archaeology*, 35(1), pp. 4–19.

González-Duarte, M. M., Fernández-Montblanc, T., Bethencourt, M., and Izquierdo, A. (2018) ‘Effects of substrata and environmental conditions on ecological succession on historic shipwrecks’, *Estuarine, coastal and shelf science*, 200, pp. 301–310.

Gordó-Vilaseca, C., Templado, J., and Coll, M. (2022) ‘The Need for Protection of Mediterranean Vermetid Reefs’, In DellaSala, D.A. and Goldstein, M.I. (ed.) *Imperiled: The Encyclopedia of Conservation*. Elsevier, pp. 644-651,

Gould, J. and Ries, J.B. (2024) ‘Linear extension and calcification rates in a cold-water, crustose coralline alga are modulated by temperature, light, and salinity’, *Limnology and Oceanography*, 69(1), pp. 158-172. DOI: 10.1002/lno.12474

Gravina, M. F., Casoli, E., Donnarumma, L., Giampaoletti, J., Antonelli, F., Perasso, C. S., and Ricci, S. (2021) 'First Report on the Benthic Invertebrate Community Associated With a Bronze Naval Ram From the First Punic War: A Proxy of Marine Biodiversity', *Frontiers in Marine Science*, 8(772499), pp. 1-17.

Greene, E.S., Leidwanger, J. and Özdaş, H.A. (2011) 'Two Early Archaic Shipwrecks at Kekova Adası and Kepçe Burnu, Turkey', *International journal of nautical archaeology*, 40(1), pp. 60–68.

Guy-Haim, T., Hyams-Kaphzan, O., Yeruham, E., Almogi-Labin, A., and Carlton, J. T. (2017) 'A novel marine bioinvasion vector: Ichthyochory, live passage through fish', *Limnology and oceanography letters*, 2(3), pp. 81–90. DOI: 10.1002/lol2.10039.

Hamdan, L. J., Hampel, J. J., Moseley, R. D., Mugge, R. L., Ray, A., Salerno, J. L., and Damour, M. (2021) 'Deep-sea shipwrecks represent island-like ecosystems for marine microbiomes', *The ISME Journal Multidisciplinary Journal of Microbial Ecology*, 15(10), pp. 2883–2891. DOI: 10.1038/s41396-021-00978-y.

Hampel, J. J., Moseley, R. D., Mugge, R. L., Ray, A., Damour, M., Jones, D., and Hamdan, L. J. (2022) 'Deep-sea wooden shipwrecks influence sediment microbiome diversity', *Limnology and oceanography*, 67(2), pp. 482–497. DOI: .1002/lno.12008.

Horn, T.W. (2014) *Determining seasonal corrosion rates in ferrous-hulled shipwrecks: A case study of the USS Huron*. East Carolina University: ProQuest Dissertations Publishing.

Jimenez, C., Andreou, V., Evriviadou, M., Munkes, B., Hadjioannou, L., Petrou, A., and Abu Alhaija, R. (2017) 'Epibenthic communities associated with unintentional artificial reefs (modern shipwrecks) under contrasting regimes of nutrients in the Levantine Sea (Cyprus and Lebanon)', *PloS one*, 12(8), pp. 1-16.

Jimenez, C., Hadjioannou, L., Petrou, A., Andreou, V., and Georgiou, A. (2017) 'Fouling communities of two accidental artificial reefs (modern shipwrecks) in Cyprus (levantine sea)', *Water (Basel)*, 9(1), pp. 1-9. DOI: 10.3390/w9010011.

Kazianes, D., Simossi, A., and Demetrios Haniotes, F. K. (1990) 'Three amphora wrecks from the Greek world', *International Journal of Nautical Archaeology*, 19(3), pp. 225-232, DOI: 10.1111/j.1095-9270.1990.tb00260.x

Lewis, B., and Diaz-Pulido, G. (2017) 'Suitability of three fluorochrome markers for obtaining in situ growth rates of coralline algae', *Journal of Experimental Marine Biology and Ecology*, 490, pp. 64-73, DOI: 10.1016/j.jembe.2017.02.004.

Lira, S. M. de A., Farrapeira, C. M. R., Amaral, F. M. D., and Ramos, C. A. C. (2010) 'Sessile and sedentary macrofauna from the Pirapama Shipwreck, Pernambuco, Brazil', *Biota neotropica*, 10(4), pp. 155–165. DOI: 10.1590/S1676-06032010000400021.

MacLeod, I. D. and Steyne, H. (2011) 'Managing a Monitor - the Case of HMVS Cerberus in Port Phillip Bay: Integration of Corrosion Measurements with Site Management Strategies', *Conservation and management of archaeological sites*, 13(4), pp. 334–361.

Marriner, N., Gambin, T., Djamali, M., Morhange, C., and Spiteri, M. (2012) 'Geoarchaeology of the Burmarrad ria and early Holocene human impacts in western Malta', *Palaeogeography, palaeoclimatology, palaeoecology*, 339(341), pp. 52–65.

Mifsud, J. (2019) *Phoenician shipwreck amphorae: A palynological study*. Malta: University of Malta.

Mires, C. H. and Meyer-Kaiser, K. S. (2023) 'A Case Study in Maritime Heritage Ecology: Understanding How Structural Changes to the 1898 Shipwreck Portland Affect Biological Diversity and Colonization', *Journal of maritime archaeology*, 18(2), pp. 197–218. DOI: 10.1007/s11457-023-09359-2.

Montefalcone, M. (2022) 'Serpulid reefs and their role in aquatic ecosystems: A global review', In Sheppard, C. (ed.) *Advances in Marine Biology*. Academic Press, 92, pp. 1-54.

Moore, J. D. (2015) 'Long-Term Corrosion Processes of Iron and Steel Shipwrecks in the Marine Environment: A Review of Current Knowledge', *Journal of maritime archaeology*, 10(3), pp. 191–204.

Morton, B. (2024) 'Bivalve', In: *Britannica*, [Online]. Available from: https://www.britannica.com/animal/bivalve (Accessed: 28 February 2024)

Muckelroy, K. (1976) 'The Integration of historical and archaeological data concerning an historic wreck site: The 'Kennemerland', *World Archaeology* 7(3), pp. 280–89.

Muckelroy, K. (1978) *Maritime Archaeology*. Cambridge: Cambridge University Press.

n.a. (2024) 'coral', In: Britannica, [Online]. Available from: https://www.britannica.com/animal/coral (Accessed: 4 March 2024)

n.a. (n.d.) 'foraminiferan', In: Britannica, [Online]. Available from: https://www.britannica.com/science/foraminiferan (Accessed: 4 March 2024)

Olinger, L. K., Scott, A. R., McMurray, S. E., and Pawlik, J. R. (2019) 'Growth estimates of Caribbean reef sponges on a shipwreck using 3D photogrammetry', *Scientific reports*, 9(1), pp. 1-12. DOI: 10.3389/fclim.2022.1011194

Palma, P. and Santhakumaran, L. N. (2014) *Shipwrecks and global 'worming'.* Oxford, England: Archaeopress.

Paxton, A. B., Ebert, E. F., Casserley, T. R., and Taylor, J. C. (2022) 'Intuitively visualizing spatial data from biogeographic assessments: A 3-dimensional case study on remotely sensing historic shipwrecks and associated marine life', *Frontiers in climate*, 4, pp. 1-6. DOI: 10.3389/fclim.2022.1011194

Paxton, A. B., McGonigle, C., Damour, M. Holly, G., Caporaso, A., Campbell, P. B., Meyer-Kaiser, K. S., Hamdan, L. J., Mires, C. H., and Taylor, J. C. (2024) 'Shipwreck ecology: Understanding the function and processes from microbes to megafauna', *Bioscience*, 74(1), pp. 12–24. DOI: 10.1093/biosci/biad084.

Pournou, A. (2018) 'Assessing the Long-Term Efficacy of Geotextiles in Preserving Archaeological Wooden Shipwrecks in the Marine Environment', *Journal of maritime archaeology*, 13(1), pp. 1–14. DOI: 10.1007/s11457-017-9176-9.

Quinn, R. (2007) 'The Assimilation of Marine Geophysical Data into the Maritime Sites and Monuments Record, Northern Ireland', *Historical archaeology*, 41(3), pp. 9–24.

Quinn, R., Forsythe, W., Breen, C., Boland, D., Lane, P. and Omar, A. L. (2007) 'Process-based models for port evolution and wreck site formation at Mombasa, Kenya', *Journal of archaeological science*, 34(9), pp. 1449–1460.

Quinn, R. and Boland, D. (2010) 'The role of time-lapse bathymetric surveys in assessing morphological change at shipwreck sites', *Journal of archaeological science*, 37(11), pp. 2938–2946.

Quinn, R. and Smyth, T. A. G. (2018) 'Processes and patterns of flow, erosion, and deposition at shipwreck sites: a computational fluid dynamic simulation', *Archaeological and anthropological sciences*, 10(6), pp. 1429–1442.

Renzulli, A., Santi, P., Gambin, T., and Serrano, P. B. (2019) 'Pantelleria Island as a centre of production for the Archaic Phoenician trade in basaltic millstones: new evidence recovered and sampled from a shipwreck off Gozo (Malta) and a terrestrial site at Cádiz (Spain)', *Journal of Archaeological Science: Reports*, 24, p. 338-349.

Ricci, S., Sanfilippo, R., Basso, D., Perasso, C. S., Antonelli, F., and Rosso, A. (2019) 'Benthic Community Formation Processes of the Antikythera Shipwreck Statues Preserved in the National Archaeological Museum of Athens (Greece)', *Journal of maritime archaeology*, 14(1), pp. 81–106.

Royal, J. G. (2006) 'The 2005 Remote-Sensing Survey of the South-Eastern Bozburun Peninsula, Turkey: Shipwreck Discoveries and their Analyses', *International Journal of Nautical Archaeology*, 35(2), pp. 195-217, DOI: 10.1111/j.1095-9270.2006.00112.x

Ryland, J. S. (n.d.) 'Moss Animal', In: *Britannica*, [Online]. Available from: https://www.britannica.com/animal/moss-animal (Accessed: 28 February 2024)

Sakellariou, D., Georgiou, P., Mallios, A., Kapsimalis, V. Kourkoumelis, D. Micha, P. Theodoulou, T., and Dellaporta, K. (2007) 'Searching for Ancient Shipwrecks in the Aegean Sea: the Discovery of Chios and Kythnos Hellenistic Wrecks with the Use of Marine Geological-Geophysical Methods', *International Journal of Nautical Archaeology*, 36(2), pp. 365-381, DOI: 10.1111/j.1095-9270.2006.00133.x

Schiffer, M. (1987) *Formation Processes of the Archaeological Record*. Albuquerque: University of New Mexico Press.

Secci, M., Demesticha, S., Jimenez, C., Papadopoulou, C., and Katsouri, I. (2021) 'A Living Shipwreck; An integrated three-dimensional analysis for the understanding of site formation processes in archaeological shipwreck sites', *Journal of Archaeological Science*: Reports, 35, pp. 1-11.

Short, E. C. (2000) *Malta: Strategic Impact During World War II*. United States of America: Defence Technical Information Center.

Simon, T., Joyeux, J. C. and Pinheiro, H. T. (2013) 'Fish assemblages on shipwrecks and natural rocky reefs strongly differ in trophic structure', *Marine environmental research*, 90, pp. 55–65. DOI: 10.1016/j.marenvres.2013.05.012.

Sisma-Ventura, G., Antonioli, F., Silenzi, S., Devoti, S., Montagna, P., Chemello, R., Shemesh, A., Yam, R.m Gehrels, R., Dean, S., Rilov, G., and Sivan D. (2020) 'Assessing vermetid reefs as indicators of past sea levels in the Mediterranean', *Marine geology*, 429. DOI: 10.1016/j.margeo.2020.106313.

Smyth, T. A. G. and Quinn, R. (2014) 'The role of computational fluid dynamics in understanding shipwreck site formation processes', *Journal of archaeological science*, 45(1), pp. 220–225.

Varinlioğlu, G. (2020) 'Assessing a Decade of Kaş Underwater Archaeopark', *International journal of nautical archaeology*, 49(1), pp. 74–86. DOI: 10.1111/1095-9270.12389

Vella, N. C. (2005) 'Phoenician and Punic Malta', *Journal of Roman Archaeology*, 18, pp. 436 – 450. DOI: 10.1017/S1047759400007479.

Vidal Gonzalez, P. (1999) 'Malta in Phoenician and Punic times', *Malta Archaeological Review*, 3, pp. 26-30.

Yatoo, M. A. (2016) ‘Significance of Stone Bowls and Saddle Querns: A Case Study of Archaeological Sites in North-west Kashmir’, *Journal of Central Asian Studies (Srinagar)*, 23(1), pp. 195-200.

Zhang, Y., Hartemink, A. E. and Huang, J. (2021) ‘Spectral signatures of soil horizons and soil orders – An exploratory study of 270 soil profiles’, *Geoderma*, 389(114961), pp. 1-14.

APPENDIX

Species	Image	Description
Bi-A		Oyster sp.?
Bi-B		Very small example Ridges radiating out from hinge
Br-A		The shape of the colony is uniform and the zooid well defined. Wide quadrangular opening Mostly flat structure with ridges between each zooecium

Br-B		Could belong to more than one genus. Pitted appearance Non-linear arrangement (more diamond-like pattern) Zooecia oval and clearly distinct (easy to draw an outline around each one)
Br-C	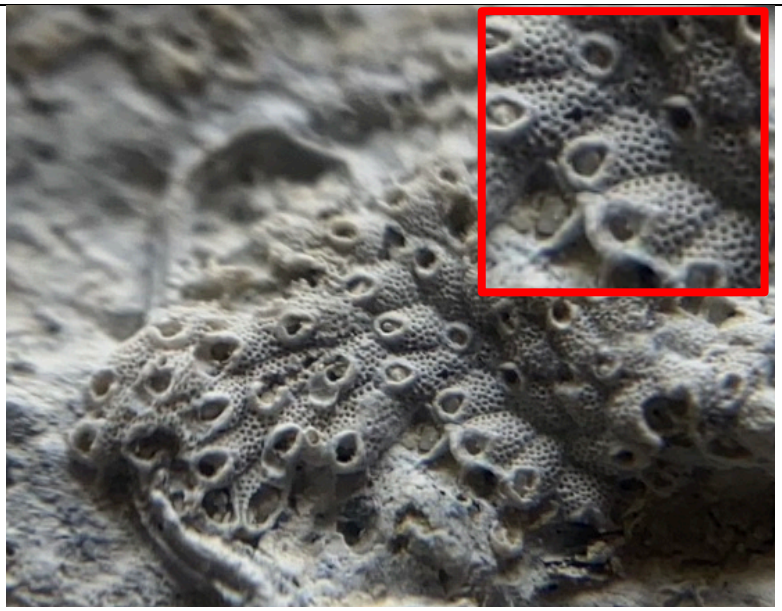	Pitted appearance Relatively individually defined zooecia Prominent areolae
Br-D		Smittoidea sp.? Some pitting Very evident linear organization Adjacent zooecia in a given row are not so clearly separated

Br-E		Maybe same as D, but no big areolae around the zooid. Clear linear organization Individual zooecia not clearly defined, almost like a linear arrangement of openings Small circular openings that appear in pairs
Br-F		Could belong to more than one genus. Clear linear organization, rows radiating out from centre point Individual zooecia clearly defined Small openings, somewhat triangular in shape
Br-G		Turbicellepora sp.? Disorganized and vertically oriented zooecia Circular openings Individual zooecia somewhat spherical (plump, not flat)

Br-H		Schizoporella unicornis? two triangular avicularia on top of the orifice zooecia organized in diamond-like pattern Spherical/plump individual zooecia Spines present next to orifice -
Br-I	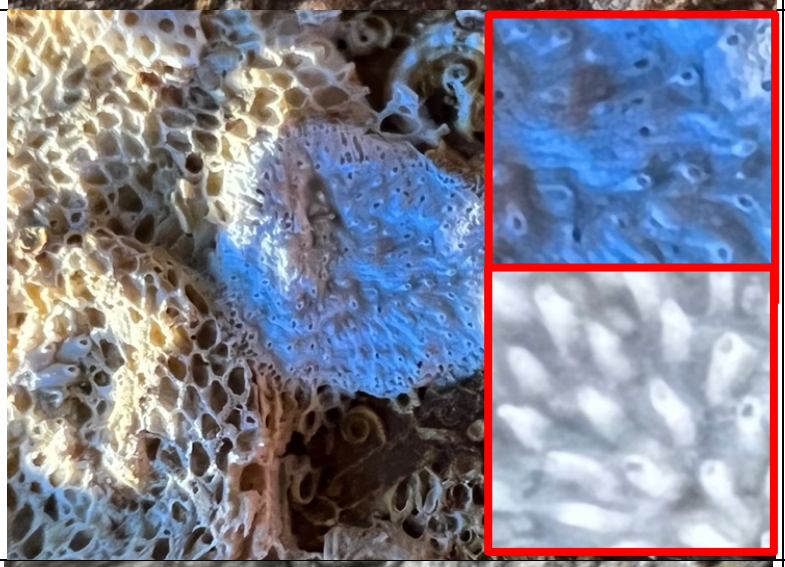	suborder Tubuliporina Flat and loosely organized individuals Individual zooecia not clearly defined but appear more as tubular openings in one uniform underlying base
Br-J		Lichenopora? Mound shaped, circular colony Many openings grouped very closely together

Br-K	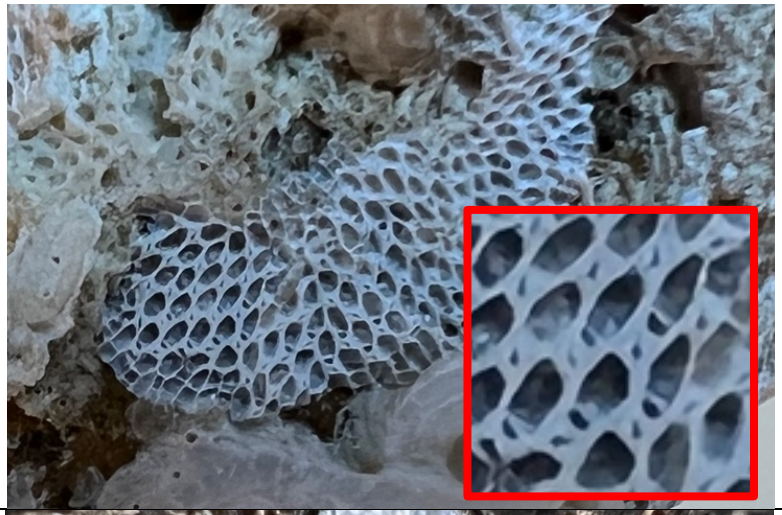	Conopeum reticulum? Open structure with pairings of larger and smaller openings.
Br-L	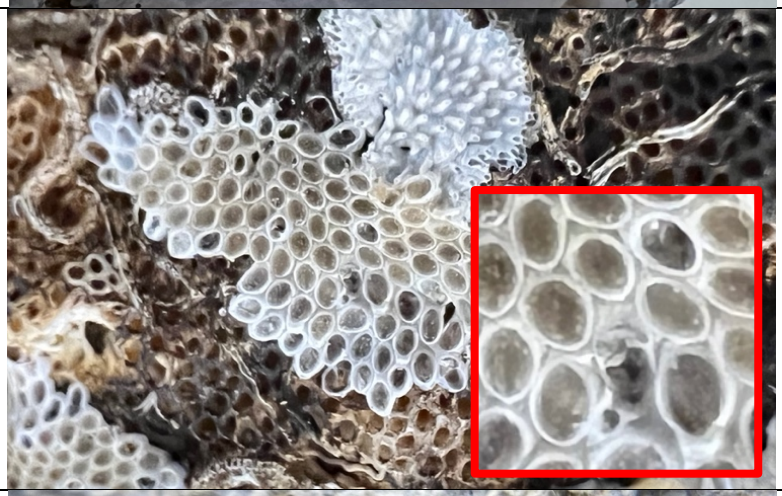	Conopeum seurati? Open structure with large oval holes
Br-M	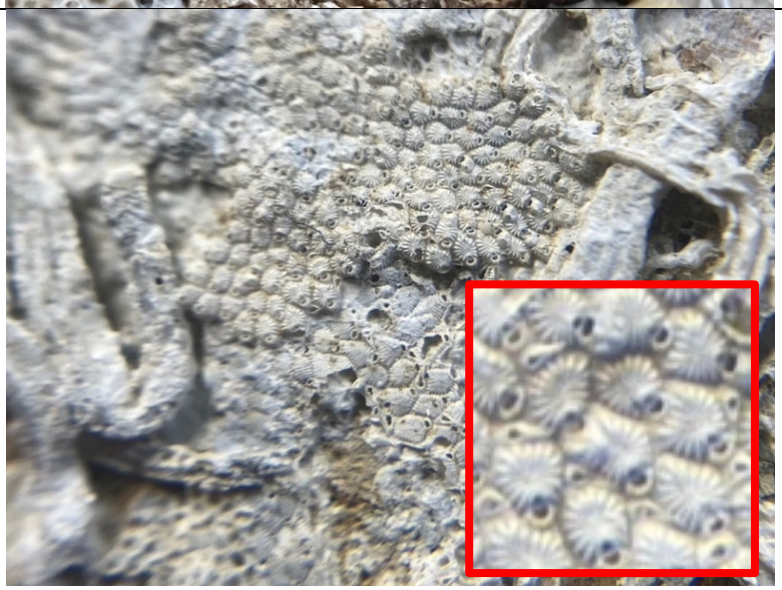	Individually defined zooids with ridges radiating out from center Slightly recessed opening

Br-N	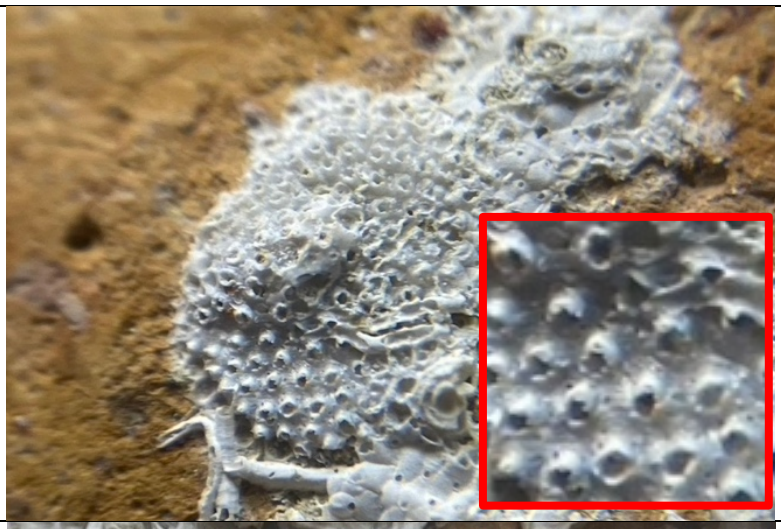	Individual zooids not clearly defined. Appear more as slightly protruding tubular openings from a single fabric
Br-O	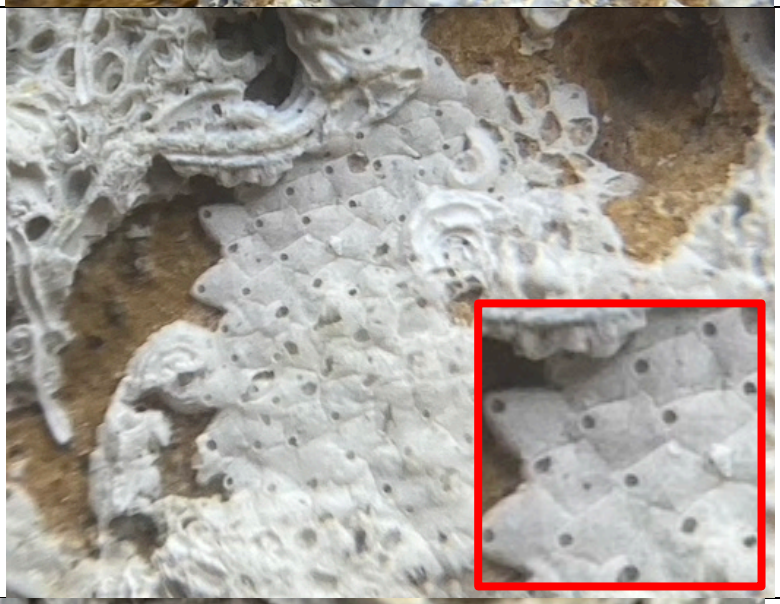	Individual zooids relatively well defined. Angular and almost triangular in shape Fairly uniform and organized orientation Small opening
Co-A		Anthozoa (stone coral) Mostly individual polyps Some examples of budding Rarely larger than 1cm in diameter

Fe-A		Foraminifera Pink hue of test
Se-A		Tightly coiled along one flat plane
Se-B		Open coiled Ridged series (three prominent) Small opening <1mm

Se-C		Open coiled Transverse ridges Relatively thick
Se-D		Relatively larger opening Triangular cross-section Single prominent “spikey” ridge on top
Se-E		Longitudinal ribs Relatively larger opening ~4mm Circular cross-section Growth lines

Se-F		Very pronounced latitudinal ribbing
Se-G		Characterized by the smooth appearance of its exterior (no ribs or spines)
Se-H		Conical and coiled sideways Relatively large upward opening Potentially vermetid?

Sp-A	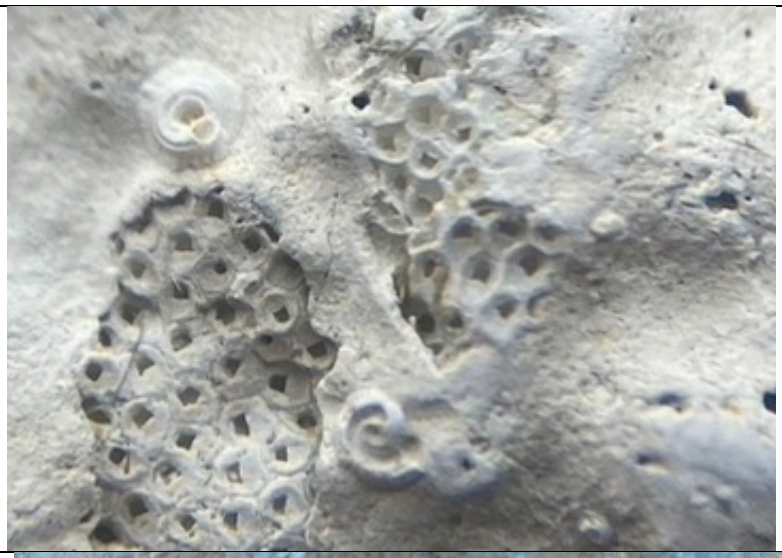	Very small and coiled usually no more than once
Ve-A		Vertically coiled with upward-facing openings
Other		Pictured to the left is one example of an organism that would be classified as “other” in this research. Not bivalve, bryozoan, coral, foraminifera, serpulid, or vermetid